UNIVERSITY OF CALIFORNIA,
IRVINE

Investigating the role of a plant extract, *Corydalis Yanhusuo*, in morphine tolerance and dependence

DISSERTATION

submitted in partial satisfaction of the requirements
for the degree of

DOCTOR OF PHILOSOPHY

in Pharmacological Sciences

by

Lamees Alhassen

Dissertation Committee:
Professor Olivier Civelli, Chair
Professor Geoffrey Abbott
Professor Shahrdad Lotfipour

2024

Dedication

To my dad

Table of Contents

List of Figures

Acknowledgements

I wish to convey my profound gratitude to the countless individuals whose unwavering support and guidance have illuminated my path on this demanding odyssey leading to the culmination of my Ph.D. thesis. Their relentless encouragement, invaluable insights, and steadfast backing have been pivotal in this momentous achievement.

First and foremost, my heartfelt appreciation goes to my dissertation advisor, Olivier Civelli. His profound wisdom, unwavering patience, and tireless dedication have been a constant wellspring of inspiration. His mentorship and guidance have proven indispensable in shaping the trajectory of my research, and for that, my gratitude knows no bounds.

I extend my sincere thanks to the esteemed members of my dissertation committee, Dr. Geoff Abbott and Dr. Shahrdad Lotfipour, whose expertise and discerning feedback at various stages of this project have markedly enhanced the quality of this work. Their constructive critiques and thoughtful suggestions have been invaluable.

I'm indebted to my colleagues and peers at the University of California, Irvine, whose camaraderie, thought-provoking discussions, and shared experiences have enriched my academic expedition in myriad ways. I owe special gratitude to Dr Amal Alachkar, Dr. Ryan Yoshimura and Dr. Khawla Nuseir for their early guidance at the inception of my Ph.D. journey, as well as

Dr. Hung Anh Nguyen, Dr. Derk Hogenkamp, Dr. Rainer Reinschield, and the dedicated members of the Civelli and Alachkar lab for their collaborative spirit, support, and assistance.

My family deserves profound appreciation for their unwavering faith in me and the constant encouragement that sustained me through the rigors of this endeavor, specifically Wedad and Sammy Alhassen; their love, understanding, and unwavering support have been my steadfast pillars.

To my friends, both longstanding and newfound, who offered not only academic support but also unwavering emotional solace, I am genuinely thankful. Your friendship has not only lightened the burdens of this academic quest but also enriched its significance.

Lastly, I extend my gratitude to the myriad individuals and resources at UC Irvine whose support and access to invaluable resources were pivotal. Their contributions, often behind the scenes, have been instrumental in making this dissertation possible.

To all those who have played a part in this academic journey, whether explicitly mentioned here or not, your collective efforts have not gone unnoticed. This dissertation stands as a testament to our shared commitment and support.

I express my sincere thanks for your invaluable role in shaping this significant chapter of my life.

The text of this dissertation is a reprint of the materials as it appears in:

Alhassen, Lamees, Khawla Nuseir, Allyssa Ha, Warren Phan, Ilias Marmouzi, Shalini Shah, and Olivier Civelli. 2021. The Extract of *Corydalis yanhusuo* Prevents Morphine Tolerance and Dependence. *Pharmaceuticals* 14, no. 10: 1034.

used with permission from Pharmaceuticals.

Vita

Lamees Alhassen

EDUCATION

University of California, Irvine

Doctor of Philosophy in Pharmacological Sciences, GPA 4.0 Fall 2019- 2024

Thesis Committee: Olivier Civelli, Geoff Abbot, Shahrdad Lotfipour,

University of California, Irvine

Masters of Science in Pharmacology, GPA 3.9 Fall 2017-2019

University of California, Riverside Fall 2012- Fall 2014

Bachelor of Science in Bioengineering, GPA 3.0

Publications

[1] Alhassen L, Alhassen W, Wong C, Sun Y, Xia Z, Civelli O, Hoshi N. Dehydroepiandrosterone Sulfate (DHEAS) Is an Endogenous Kv7 Channel Modulator That Reduces Kv7/M-Current Suppression and Inflammatory Pain. J Neurosci. 2023 Oct 25;43(43):7073-7083.

[2] Alhassen L, Dabbous T, Ha A, Dang LHL, Civelli O. The Analgesic Properties of *Corydalis yanhusuo*. Molecules. 2021 Dec 10;26(24):7498.

[3] Alhassen L, Nuseir K, Ha A, Phan W, Marmouzi I, Shah S, Civelli O. The Extract of *Corydalis yanhusuo* Prevents Morphine Tolerance and Dependence. Pharmaceuticals (Basel). 2021 Oct 12;14(10):1034.

[4] Alhassen, S., Chen, S., Alhassen, L. *et al.* Intergenerational trauma transmission is associated with brain metabotranscriptome remodeling and mitochondrial dysfunction. *Commun Biol* 4, 783 2021.

[5] Sanathara N, Alhassen L, Marmouzi I, Khoudari M, Phan J, Alhassen W, Civelli O, Alachkar A. Oxytocin-MCH circuit regulates monosynaptic inputs to MCH neurons and modulates social recognition memory. Neuropharmacology. 2021 Feb 15;184:108423.

[6] Alhassen, L., Phan, J., Argelagos, A. *et al.* Mating and parenting experiences sculpture mood-modulating effects of oxytocin-MCH signaling. *Sci Rep* 2020, 10, 13611.

[7] Vawter MP, Schulmann A, Alhassen L, Alhassen W, Hamzeh AR, Sakr J, Pauluk L, Yoshimura R, Wang X, Dai Q, Sanathara N, Civelli O, Alachkar A. Melanin Concentrating Hormone Signaling Deficits in Schizophrenia: Association With Memory and Social Impairments and Abnormal Sensorimotor Gating. Int J Neuropsychopharmacol. 2020 Mar 10;23(1):53-65.

[8] Alhassen L, Phan A, Alhassen W, Nguyen P, Lo A, Shaharuddin H, Sanathara N, Civelli O, Alachkar A. The role of Olfaction in MCH-regulated spontaneous maternal responses. Brain Res. 2019 Sep 15;1719:71-76.

[9] Alachkar A, Alhassen L, Wang Z, Wang L, Onouye K, Sanathara N, Civelli O. Inactivation of the melanin concentrating hormone system impairs maternal behavior. Eur Neuropsychopharmacol. 2016 Nov;26(11):1826-1835.

Abstract of the Dissertation

Investigating the role of a plant extract, *Corydalis Yanhusuo*, in morphine tolerance and dependence

By

Lamees Alhassen

Doctor of Philosophy in Pharmacological Sciences

University of California, Irvine, 2024

Professor Olivier Civelli, Chair

The opioid epidemic, fueled by the over prescription of opioid analgesics, necessitates innovative strategies to enhance the efficacy of opioid therapy while mitigating its adverse effects. This dissertation investigates the potential of Corydalis yanhusuo extract (YHS) and GPR 139 in addressing opioid-related challenges. Chapter 1 provides a comprehensive overview of the opioid epidemic, emphasizing the need for alternative approaches to opioid therapy. In Chapter 2, we delve into the multifaceted impact of YHS on morphine antinociception, showcasing its potential to enhance the efficacy of morphine and consequently reduce opioid dependence. Our findings reveal that the coadministration of YHS with morphine not only hinders the development of morphine tolerance, dependence, and addiction but also demonstrates a remarkable capacity to reverse morphine dependence and addiction in animals subjected to extended morphine treatments. These results collectively suggest the potential utility of YHS as a co-medication in morphine therapies, offering a promising avenue to mitigate adverse morphine effects. Chapter 3 delves into the molecular mechanisms underlying YHS's ability to reduce morphine tolerance. By exploring

the modulation of mu opioid receptor (MOR) expression in various brain regions, including the lateral septal nucleus, primary and secondary motor cortex, anterior cingulate cortex, and thalamus, the study aims to elucidate the potential of YHS in preventing tolerance development.

Chapter 4 explores the bioactive constituents of YHS, focusing on those with the capability to inhibit the development of morphine tolerance. Using reverse phase high-performance liquid chromatography (HPLC) and tolerance assays, the study aims to identify the active compounds responsible for YHS's mitigating effects on morphine tolerance, laying the groundwork for targeted interventions in pain management.

Chapter 5 explores the multifaceted role of GPR 139, a receptor discreetly expressed in the medial habenula, in modulating neurobehavioral circuits. The study systematically evaluates the potential of the GPR 139 agonist, JNJ-63533054, as a versatile pharmacological agent. The focus lies on its multifaceted attributes, particularly its remarkable ability to inhibit morphine-induced analgesia and self-administration. This suggests a promising avenue for JNJ-63533054 as an analgesic, showcasing its potential in pain management and its potential to modulate opioid-related behaviors. The findings underscore the versatility of JNJ-63533054, positioning it as a candidate with dual implications, both in mitigating pain responses and potentially addressing concerns related to opioid misuse and addiction. In addition, this chapter investigates the interaction between YHS and GPR 139 in blocking morphine tolerance. By elucidating whether GPR 139 is involved in the mechanism by which YHS mitigates morphine tolerance, the study provides insights into alternative pathways for targeting pain medications.

In conclusion, this dissertation presents a comprehensive investigation into the potential of YHS and morphine as co-medications in opioid therapy. These findings offer promising avenues for developing alternative strategies to address the opioid epidemic and improve pain management.

Chapter 1: Introduction

1. Exploring the Spectrum of Pain: A Comprehensive Analysis of Types and Mechanisms for In Depth Understanding

Pain, a complex and multifaceted phenomenon, plays a pivotal role in human experience and health. This section delves into the intricate landscape of pain, aiming to provide a comprehensive understanding of its diverse manifestations, ranging from acute to chronic, nociceptive to neuropathic. By examining the intricate interplay of biological, psychological, and social factors contributing to pain perception, this section seeks to unravel the intricacies of the human pain experience. Through an exploration of the mechanisms governing the sensory and emotional aspects of pain, this section aims to offer insights that may pave the way for more effective approaches to pain management in the future.

1.1 Defining Pain

Pain is an instinct in human primates, defined as a distressing sensation and an emotional experience linked to actual or potential tissue damage [1]. Its primary purpose is to alert the body's defense mechanism, prompting a response to avoid further harm [1]. Pain sensation involves the activation of receptors in primary afferent fibers, including unmyelinated C-fibers and myelinated Aσ-fibers, which are dormant in the absence of pain and activated in the presence of a potential noxious stimulus [2].

The brain detects pain and responds to threats through a series of sensory events [2]. Pain perception occurs in three main stages: first, pain sensitivity; second, transmission of signals from the periphery to the dorsal horn (DH) in the spinal cord through the peripheral nervous system (PNS); and third, transmission of signals to the higher brain via the central nervous system (CNS)

[2]. Signal transmission occurs through two routes: the ascending pathway, carrying sensory information from the body to the brain via the spinal cord, and the descending pathway, where nerves travel downward from the brain to reflex organs via the spinal cord [2].

Pain is a broad topic that can arise from various sources, affecting different parts of the body. It can stem from conditions like cancer, fibromyalgia, neuropathic pain, persistent post-surgical pain, arthritis, childhood and adolescent pain, headache and migraine, orofacial pain, visceral pain, musculoskeletal pain, and pelvic pain [3]. The International Association for the Study of Pain (IASP) classifies pain based on factors such as the body region involved, the pattern of occurrence (acute or chronic), or the dysfunctional system causing the pain (e.g., gastrointestinal, nervous) [1]. However, a more simplified classification considers three characteristics: symptoms, mechanisms, and syndromes.

The mechanism and pathways of pain perception involve both the central nervous system (CNS) and peripheral nervous system (PNS) [2]. The PNS, comprising nerves and ganglia outside the brain and spinal cord, connects the CNS to organs and limbs, facilitating communication [2]. Meanwhile, the CNS, consisting of the spinal cord and brain, interprets information from the PNS and coordinates bodily activities before sending responses to effector organs [2].

1.2 Basic Mechanisms of Pain

Essentially, the fundamental mechanism of pain unfolds through three distinct events—transduction, transmission, and modulation—when confronted with noxious stimuli. To illustrate, transduction progresses along the nociceptive pathway in a sequential manner: (1) stimulus events transform into chemical tissue events; (2) these chemical tissue and synaptic cleft events then convert into electrical events within the neurons; and (3) the electrical events in the neurons are

transduced back into chemical events at the synapses [1]. Following the completion of transduction, the subsequent phase involves transmission, wherein electrical events propagate along neuronal pathways, with neurotransmitters in the synaptic cleft transmitting information from a post-synaptic terminal of one cell to a presynaptic terminal of another [4]. Simultaneously, the modulation event occurs across all levels of nociceptive pathways, involving up- or down-regulation through the primary afferent neuron, DH, and higher brain centers [4]. Collectively, these processes culminate in a singular outcome—the initiation and completion of the pain pathway, enabling the perception of the painful sensation triggered by the stimulus [5].

Neurons play a crucial role in connecting, receiving, and processing nociceptive information in both the CNS and PNS [5]. There are three main types of neurons in our body: sensory neurons (which transmit information to the CNS), interneurons (which relay signals between afferent and efferent neurons), and motor neurons (which carry signals away from the CNS). All neurons share common components—soma, axon (myelinated or unmyelinated), and dendrites—and form intricate networks in the body [6]. These neurons communicate through specialized connections called synapses, where chemical and electrical signals are transmitted. The signals, either inhibitory or excitatory, are sent from one neuron's dendrites and soma to another's (synaptic transmission) [6]. After receiving signals, neurons transmit them through axons as brief pulses called action potentials [6]. These action potentials travel along axons, activate synapses, and are sent to other neurons, forming pathways that carry signals from the source to the spinal cord or brain [7]. Sensory neurons in the dermis and epidermis react to stimuli like touch by sending signals, while motor neurons receive signals from the brain and spinal cord, producing responses such as muscle contractions and affecting glandular outputs. Neurons are essential for our body's ability to react to environmental stimuli, enabling us to respond to potential dangers

[7].

Axons, also called nerve fibers, are the primary part of a neuron responsible for carrying action potentials in one direction—from dendrites to axonal terminals and from one neuron to another [8]. Axons can be myelinated or unmyelinated. The myelin sheath, known as the node of Ranvier, enhances the speed of impulse propagation along myelinated fibers through saltatory conduction, generating action potentials at each node [8]. It also acts as an insulator to prevent electrical impulses from escaping during transmission. In unmyelinated fibers, impulses move continuously but at a slower pace. Aδ-fibers of primary afferent neurons are myelinated, while C-fibers are unmyelinated. Most preganglionic neurons of efferent neurons are myelinated [9]. Nodes of Ranvier have small gaps and contain K+ and Na+ channels, serving as an energy reserve during action potential transmission. Sensory neurons (afferent) are classified into three main groups—Group A, B, and C—based on impulse velocity, axon diameter, and function. Motor neurons (efferent) are grouped into Type Ia, Ib, II, III, and IV [9].

Essentially, pain transmission relies on maintaining a balance between excitatory and inhibitory influences acting on the neuron circuits within the somatosensory system. The CNS plays a pivotal role in pain transmission at various levels, including the spinal cord (supraspinal), the brainstem (midbrain, medulla oblongata, and pons), and the cortical regions (cerebral cortex) [10]. The dorsal horn (DH) of the spinal cord is crucial in integrating inputs from primary afferent neurons and local interneuron networks, as well as receiving descending signals from the supraspinal center [10]. In the ascending system, primary afferent nociceptors convey noxious information to projection neurons in the DH of the spinal cord. Subsequently, a subset of these projection neurons transmits sensory information to the thalamus, reaching the somatosensory cortex through the spinothalamic tract. This pathway provides details on the intensity and location

of the noxious stimulus [10]. The spinothalamic tract consists of two parts—the lateral spinothalamic and anterior spinothalamic tracts, each serving distinct functions [10]. The lateral spinothalamic tract focuses on pain and temperature sensation, while the anterior spinothalamic tract conveys information related to crude touch and firm pressure sensation to the thalamus [11]. Other projection neurons connect with the cingulate and insular cortices via the parabrachial nucleus and the amygdala, contributing to the overall pain experience [11]. The PAG integrates information from higher brain centers, including the hypothalamus, amygdala, and frontal lobe, as well as receiving ascending nociceptive input from the DH [12]. The PAG controls the processing of nociceptive information in the DH of the spinal cord through projection neurons to RVM and dorsolateral pontine tegmentum (DLPT) [12]. Various neurotransmitters, including endogenous opioids, cannabinoids, 5-hydroxytryptamine (5-HT), and norepinephrine (NE), are highly expressed through the PAG/RVM pathways [12].

1.3 Types of Pain

Consequently, pain is internationally categorized into three main classes—nociceptive pain, neuropathic pain, and inflammatory pain [13]. Nociceptive pain manifests as either acute or chronic, with acute pain characterized by sudden onset and short duration, while chronic pain persists or recurs for over three months [13]. Chronic pain significantly impacts both physical and psychological well-being, ranking as a primary reason for adults seeking medical attention and correlating with limitations in daily activities, anxiety, depression, reduced quality of life, and opioid dependence [13][14]. The economic burden of chronic pain is substantial, contributing to an estimated $560 billion annually in direct medical costs, lost productivity, and disability programs [15].

Acute nociceptive pain results from the activation of peripheral nociceptors by noxious stimuli, with afferent signals subject to modification by descending systems originating from various central nervous system regions, including the hypothalamus, lateral tegmental area, and somatosensory cortex [16]. Activation of these descending pathways induces analgesic effects modulated by neurotransmitters such as noradrenaline and serotonin [17]. Persistent acute pain leads to neuronal remodeling in both the spinal cord and the brain, resulting in reduced modulation of painful nerve impulses, increased excitability and sensitivity of pain signal-transmitting nerve cells, and an overall heightened connection between peripheral and central nervous system cells [18]. This peripheral and central sensitization contributes to hyperalgesia, an exaggerated response to painful stimuli, and allodynia, pain in response to normally non painful stimuli [19]. Dysfunction of descending serotonergic and noradrenergic modulatory pathways disrupts the balance between inhibitory and excitatory pain signaling pathways in the central nervous system [20]. Over time, pain hypersensitivity can develop, leading to changes in the brain that perpetuate chronic pain [20]. The complexity of chronic pain poses challenges for responding to analgesic and anti-inflammatory drugs alone, prompting the widespread prescription of opioids for this type of pain [20].

Neuropathic pain results from damage or dysfunction of the nervous system, leading to aberrant signaling and perception of pain [18]. It is often described as burning, tingling, or shooting pain and can be challenging to treat effectively [18]. Conditions such as diabetic neuropathy, postherpetic neuralgia, and nerve compression syndromes are common causes of neuropathic pain [21]. Neuropathic pain results from damage or disease in the somatosensory nervous system [21]. It arises from various pathological mechanisms and is categorized based on anatomy or cause. Common triggers include metabolic disorders (like peripheral diabetic neuropathy), viral

infection-related neuropathies (such as post-herpetic neuralgia, HIV, leprosy), autoimmune disorders affecting the central nervous system (like multiple sclerosis and Guillain–Barre syndrome), chemotherapy-induced peripheral neuropathies, traumatic nervous system damage (e.g., spinal cord injury and amputation), inflammatory disorders, hereditary neuropathies, and channelopathies [21].

Inflammatory pain is the feeling and emotional response to harmful stimuli during an immune or inflammatory reaction [22]. The inflammatory response is a well-coordinated set of processes that occur after injury or infection to address and resolve the issue [22]. It is marked by classic symptoms: redness, heat, swelling, pain or hypersensitivity, and loss of function. In normal circumstances, inflammation is crucial for healing wounds. However, acute inflammation causes noticeable pain by directly activating sensory neurons transmitting pain signals [23]. More commonly, inflammation lowers the threshold for sensory neuron activation (especially nociceptors) or increases their firing in response to a stimulus, known as peripheral sensitization [23]. This leads to heightened sensitivity to painful stimuli (hyperalgesia) or perceiving non-painful stimuli as painful (allodynia) [23]. Of greater concern in clinical settings is chronic inflammatory pain, which occurs in conditions like rheumatoid arthritis (an autoimmune disorder) and osteoarthritis. Chronic inflammatory pain can stem from a prolonged immune or inflammatory response and alterations in the expression of proteins affecting the excitability of sensory neurons [24].

2. Comprehensive Approaches to Mitigating the Opioid Epidemic: Integrating Opioid and Non-Opioid Treatments, Including Traditional Chinese Medicine and Non-Opioid Receptor-Based Therapies

The opioid epidemic, a pressing public health crisis, is marked by the widespread misuse and addiction to opioid substances. Opioids, despite their effectiveness in pain management, pose significant risks of dependence and overdose. Addressing this crisis requires a comprehensive approach, encompassing both opioid and non-opioid treatment options. Incorporating non-opioid receptor-based treatments and traditional Chinese medicine into the therapeutic landscape provides alternative perspectives on pain management, offering holistic approaches that extend beyond conventional pharmaceutical interventions. A well-rounded strategy, integrating these diverse treatment modalities, holds the potential to address the opioid epidemic while providing safer and more varied options for individuals navigating pain and addiction challenges.

2.1 The rise of the opioid epidemic

The origins of the opioid epidemic can be linked to the widespread prescription of opioid painkillers [25]. In the 1990s, pharmaceutical companies reassured the medical community that opioids were safe and non-addictive, leading to an increase in their prescription for chronic pain management [26]. The prescription rates for opioids, such as oxycodone and hydrocodone, surged during the early 2000s [26]. The well-intentioned goal of addressing pain management resulted in a substantial increase in the availability of prescription opioids, contributing to the subsequent epidemic [27]. As prescription opioids became more tightly regulated, individuals turned to illicit opioids, such as heroin, which was often more accessible and affordable [25]. This shift

exacerbated the epidemic, leading to a surge in heroin-related overdoses [28].

The significant increase in opioid misuse in the past 25 years has led to a serious public health crisis, marked by a sharp rise in drug overdose deaths [25]. In 2017, around 12 million Americans misused opioids, leading to over 47,000 deaths from opioid overdose [29]. This marked a 345% increase in overdose fatalities from 2001 to 2016, with a particularly steep rise since 2015 [30]. The U.S. Department of Health and Human Services declared the growing opioid misuse issue a national public health emergency in 2017 [31]. In recent years, scholars, researchers, health professionals, and politicians have focused on the opioid misuse problem. While there have been calls for a comprehensive public health approach, the full scope of such a strategy hasn't been clearly defined or put into action. Despite various interventions being implemented over time, they have generally failed to effectively reduce non-fatal and fatal overdoses on a national scale [32]. Approaches targeting only one aspect, like restricting opioid supply, are insufficient to address the opioid epidemic. The situation is further complicated by the rapidly changing nature of the epidemic, such as the widespread availability of fentanyl and its analogues since around 2013, leading to a sharp increase in overdose death rates despite improvements in other public health indicators, such as prescription opioid misuse [32].

Moreover, despite the recent attention drawn to the escalating fatalities, the issue of opioid misuse is not a new one. Opioid use disorder (OUD) has been a debilitating condition causing significant harm and mortality to individuals, families, and communities for many decades [32]. Although the introduction of agonist treatments in the 1970s provided crucial relief for some with this illness, only a few people received any treatment even before the current crisis [33]. The increasing criminalization of drug use further pushed a significant portion of this population into the criminal justice system [34]. Thus, the inadequate response to the harms of opioids, both from

public health and societal perspectives, has been a longstanding issue, and there is a pressing need for new and expanded responses [34].

The complexity of the crisis is evident in the various influences stemming from individual factors, interpersonal relationships, and community and societal impacts [29]. Addressing the opioid epidemic requires a multifaceted approach, encompassing policy changes, improved prescribing practices, enhanced addiction treatment, and increased public awareness [29]. Ongoing research aims to better understand the factors contributing to opioid misuse and develop innovative strategies for prevention and intervention [29].

2.2. Contemporary Challenges in Chronic Pain Management

Opioids, known for their analgesic properties, have a history of use spanning over 5,000 years [35]. The term "opiate" specifically refers to opioids derived from the opium poppy, such as morphine and codeine [35]. Opioids encompass semi-synthetic opiates (derived from natural opiates) and synthetic opioids like methadone or fentanyl [35]. This term broadly covers compounds binding to opiate receptors, including mu (μ), kappa (κ), delta (δ) receptors, and opioid-receptor-like-1 (ORL-1) [35]. Opioid peptides and receptors are found throughout nociceptive neural circuitry and critical areas of the central nervous system, including structures related to reward and emotion [36].

Although morphine has been the traditional gold standard for addressing severe pain, certain patients either do not attain sufficient pain relief or experience intolerable side effects from the use of this medication [37]. While opioids remain highly effective analgesics, they come with a range of side effects, such as dependence, tolerance, constipation, and respiratory depression [38]. Pain relief-induced addiction has become a significant crisis in medicine, associated with

high disease morbidity [39]. Opioid use, even for a short duration, may predispose certain individuals to opioid use disorder, a pressing public health crisis globally [39]. However, reducing opioid prescriptions may mitigate the risk of misuse. The rise in opioid misuse over the past 25 years has led to the opioid epidemic, with approximately 12 million Americans misusing opioids and over 47,000 dying from opioid overdoses in 2017 [40]. Elevated opioid doses are linked to increased toxicity and mortality [40].

2.4. Contemporary Challenges in Inflammatory Pain

Inflammation and pain are intricate bodily responses that can lead to persistent health issues. Managing them is a clinical challenge due to the complex network of molecules and receptors involved [22]. The discovery of natural and synthetic compounds with pain-relieving and anti-inflammatory properties has played a crucial role in addressing various painful and inflammatory diseases [41]. However, concerns about side effects, particularly in chronic conditions, have led to numerous studies evaluating the safety and effectiveness of new natural and synthetic products for pain and inflammation treatment [41].

Nonsteroidal anti-inflammatory drugs (NSAIDs) are extensively used in the USA due to their proven effectiveness in alleviating pain and inflammation [42]. In 2000 alone, over 111 million prescriptions for NSAIDs were issued in the country, and these medications are also prevalent over-the-counter, with more than 30 billion tablets sold annually [43]. Notably, more than one-third of older adults take NSAIDs daily, and 70% use them at least once a week [44].

Despite their widespread use, a significant drawback of traditional NSAIDs is their potential for gastrointestinal toxicity [45]. Studies have shown that 15–30% of regular NSAID users develop gastric or duodenal ulcers, and throughout the 1990s, these NSAID-related events

led to around 100,000 hospitalizations and 16,500 deaths annually [46]. Recent research indicates a 67% decline in the risk of serious NSAID-related stomach issues over the past decade [47]. This improvement is attributed to factors such as lower NSAID doses, the use of gastroprotective agents like proton pump inhibitors (PPIs), and the introduction of selective cyclo-oxygenase (COX)-2 inhibitors [48].

The cost of treating gastrointestinal side effects associated with NSAIDs ranges from US$0.66 to US$1.25 for every US$1 spent on NSAIDs [44]. Moreover, about one-third of the expenses related to managing arthritis are linked to treating adverse effects of NSAIDs [44]. Given the extensive use of these medications, the potential health problems associated with NSAID-related gastrointestinal issues are significant [49]. Alternatively, selective COX-2 NSAIDs may be considered for patients at high risk of gastrointestinal events, as they have roughly half the gastrointestinal risks compared to nonselective NSAIDs [50]. However, recent concerns have been raised about the potential cardiovascular toxicity of the entire NSAID class, including both selective and nonselective agents [50].

2.5 Mechanism of Opioid Tolerance

Morphine stands as the quintessential opioid analgesic, serving as the benchmark against which other pain relievers are evaluated [52] [51]. Its primary mechanism of action involves binding to the mu-opioid receptor (MOR) in both the CNS and PNS [52]. In exploring the intricacies of opioid tolerance, the traditional theory posits the downregulation of opioid receptors as a fundamental explanation [53]. Prolonged exposure to opioid agonists, such as morphine, precipitates a reduction in the number of available opioid receptors, thereby contributing to a diminished response to the drug over time [54].

Furthermore, opioid receptors, particularly MOR, undergo desensitization and uncoupling from downstream signaling pathways following agonist exposure [52]. This process renders the receptor less responsive to the drug, even in the continued presence of the agonist [52]. The complexity deepens with chronic exposure to morphine, where elevated levels of cyclic adenosine monophosphate (cAMP) are observed [55]. This surge is attributed to the upregulation of adenylyl cyclase, protein kinase A (PKA), and CREB [56]. The resulting dysregulation of cAMP signaling is postulated to contribute significantly to the development of tolerance [57].

Adding to this intricate web of mechanisms, β-arrestins, specifically β-arrestin 2, emerge as key players in the regulation of MOR internalization [58]. The concept of biased agonism introduces an additional layer of complexity, as different agonists exert distinct effects on MOR regulation, contributing to the multifaceted nature of opioid tolerance [59]. Studies exploring the modulation of acute analgesic tolerance reveal the significance of JNK inhibition, specifically c-Jun N-terminal kinase, in mitigating this phenomenon [60]. Notably, GRK-3 (G protein receptor kinase 3) does not influence this process, a distinction observed with certain μ agonists like fentanyl or oxycodone [61].In essence, the intricate interplay of downregulation, desensitization, cAMP dysregulation, biased agonism, and the differential impact of signaling pathways collectively shape the mechanisms underpinning opioid tolerance, presenting a nuanced and multifaceted landscape that contributes to the reduced efficacy of opioids over extended periods of use [54].

2.6 Traditional medicine & Corydalis yanhusuo plant extract

For over 7000 years, various plant extracts have served as analgesics [62]. Notably, morphine, considered the gold standard in analgesic therapy, is derived from a plant alkaloid [62].

The plant extract from Corydalis yanhusuo, known as YHS, comprises over 160 compounds, including alkaloids, organic acids, volatile oils, amino acids, alcohols, and sugars [63]. More than 80 alkaloids have been identified in YHS, encompassing tertiary amines, quaternary alkaloids, and numerous non-alkaloids [63]. One study investigated the effects of YHS in various pain animal models. In this study, YHS was evaluated for its antinociceptive activity using the tail flick, formalin paw licking, von Frey filament, and hot box assays after spinal nerve ligation [64]. YHS demonstrated an increase in tail flick latency without inducing tolerance [64]. Additionally, it reduced paw licking time in the formalin assay and elevated the paw withdrawal threshold latency in the von Frey and hot box assays [64]. These findings collectively suggest that YHS effectively mitigates acute, inflammatory, and neuropathic pain without causing tolerance [64].

To unravel its mechanism of action, YHS underwent screening against various G-protein coupled receptors, and its mechanism was studied using knock-out mice [64]. This investigation revealed that YHS acts, in part, through the dopamine D2 receptor [64]. Further delving into YHS and its alkaloids, Dehydrocorybulbine (DHCB) was isolated from YHS and found to exhibit antinociceptive activity [62]. It was demonstrated that DHCB's antinociceptive effect primarily stems from its interaction with D2 receptors [62]. DHCB proved effective against inflammatory and neuropathic pain without inducing antinociceptive tolerance [62]. Moreover, several studies advocate for pain treatment through non-opioid receptors to mitigate the negative side effects associated with opioids alone.

2.7. Treatment of pain through non-opioid receptors

GPR139, a Gq-coupled receptor, is activated by essential amino acids like L-tryptophan and L-phenylalanine [65]. Predominantly expressed in the brain and pituitary, GPR139's

physiological function remains elusive despite advanced pharmacological tools. Some studies hint at its involvement in addiction, Parkinson's disease, and schizophrenia [66]. In contrast to opioids, which target MOR to alleviate pain but pose addiction risks, one study identified the orphan receptor GPR139 with anti-opioid activity [67,68]. Deleting GPR139 in mice enhanced opioid-induced inhibition of neuronal firing, impacting morphine-induced analgesia, reward, and withdrawal [67]. A GPR139 agonist, JNJ-63533054, reduced morphine analgesia and suppressed morphine intake in the reward assay [67]. These in vivo results suggest that GPR139 negatively regulates responses to acute opioid exposure and potentiates withdrawal from chronic opioid administration. Additionally, GPR139 inhibits MOR signaling in vitro, impacting MOR trafficking and signaling properties [67-72]. Another study explored co-expression between the dopamine D2 receptor and GPR139, revealing a similar distribution pattern in the brain and pituitary across species [66]. Co-expression occurred in dopaminergic signaling pathways, indicating a functional interaction between GPR139 and D2 under physiological conditions. These findings propose GPR139 and D2 as potential targets to enhance opioid safety [66].

Chapter 2: The Extract of *Corydalis yanhusuo* Prevents Morphine Tolerance and Dependence

Alhassen, Lamees, Khawla Nuseir, Allyssa Ha, Warren Phan, Ilias Marmouzi, Shalini Shah, and Olivier Civelli. 2021. "The Extract of *Corydalis yanhusuo* Prevents Morphine Tolerance and Dependence" *Pharmaceuticals* 14, no. 10: 1034.

Author Contributions

Conceptualization, L.A., K.N. and O.C.; methodology, L.A. and K.N.; software, L.A., W.P., A.H. and I.M.; validation, A.H., W.P. and I.M.; formal analysis, L.A., A.H. and W.P.; investigation, L.A. and K.N.; resources, O.C.; data curation, L.A., K.N., A.H.; writing—original draft preparation, O.C.; writing—review and editing, L.A., S.S. and O.C.; visualization, L.A. and O.C.; supervision, O.C.; project administration, O.C.; funding acquisition, O.C. and S.S. All authors have read and agreed to the published version of the manuscript.

Funding

This work was supported by the Eric L. and Lila D. Nelson Chair in Neuropharmacology and by a grant from the UCI Research Growth Investment Fund to OC. IM was a recipient of an IBRO Research Fellowship.

Abstract

The opioid epidemic was triggered by an overprescription of opioid analgesics. In the treatment of chronic pain, repeated opioid administrations are required which ultimately lead to tolerance, physical dependence, and addiction. A possible way to overcome this conundrum consists of a co-medication that maintains the analgesic benefits of opioids while preventing their adverse liabilities. YHS, the extract of the plant *Corydalis yanhusuo*, has been used as analgesic in traditional Chinese medicine for centuries. More recently, it has been shown to promote analgesia in animal models of acute, inflammatory, and neuropathic pain. It acts, at least in part, by inhibiting the dopamine D2 receptor, suggesting that it may be advantageous to manage addiction. We first show that, in animals, YHS can increase the efficacy of morphine antinociceptive and, as such, decrease the need of the opioid. We then show that YHS, when coadministered with morphine, inhibits morphine tolerance, dependence, and addiction. Finally, we show that, in animals treated for several days with morphine, YHS can reverse morphine dependence and addiction. Together, these data indicate that YHS may be useful as a co-medication in morphine therapies to limit adverse morphine effects. Because YHS is readily available and safe, it may have an immediate positive impact to curb the opioid epidemic.

Institutional Review Board Statement

All animal experiments were carried out in accordance with the University of California, Irvine's Animal Institutional Animal Care and Use Committee (IACUC #2002–2343).

Introduction

Over the past two decades, dramatic increases in opioid overdose mortality have occurred in the United States and other nations. Recognized as a public health crisis, it is commonly referred to as the opioid epidemic [73]. The opioid epidemic started with an increase in opioid prescriptions to treat chronic pain. Chronic pain is a therapeutic challenge and its management by opioids is controversial [74]. Non-opioid treatments should be the preferred first step, but are often replaced by opioid medications as conditions worsen [75].

Opioids are administered for their superior analgesic effectiveness. However, associated with repetitive opioid administration is the development of tolerance, which represents a loss of efficacy upon time [76]. Pain-afflicted patients require higher doses of opioids to maintain a mostly pain-free state, which in turn increases the risk of dependence, addiction, and fatal overdose [77, 78]. In animals, tolerance is monitored by quantifying analgesic responses over repeated opioid administration [79]. Repeated administration of opioids also leads to physical dependence, i.e., the need for maintained administration. Dependence manifests itself with the emergence of withdrawal symptoms when the use of opioids is abruptly discontinued and can be precipitated by opioid antagonists [79, 80, 81]. It can be quantified by treating opioid-dependent animals with naloxone and monitoring withdrawal symptoms. Dependence is also associated with the desire to repeat the positive reinforcing effects of the opioids [82]. While it involves numerous neuronal systems, it is predominantly mediated by the dopaminergic mesocorticolimbic reward system [82, 83, 84, 85]. In experimental animals, addiction can be assessed by using assays monitoring drug-seeking behaviors, such as conditioned place preference (CPP) [86, 87, 88].

The US Centers for Disease Control and Prevention (CDC) has issued guidelines aiming at reducing the use of opioid drugs [73, 89]. Recommendations include prescribing over-the-counter

pain relievers, such as acetaminophen and ibuprofen in lieu of opioids. Nonsteroidal anti-inflammatory drugs (NSAIDs) are most effective against mild to moderate pain linked to inflammation. Indeed, the lack of efficacy of acetaminophen in chronic pain conditions has been documented [90, 91, 92].

The CDC guidelines also accept the use of opioids in combination with non-opioid therapy after careful assessment of pain control. We reflected that, ideally, the co-administration of a non-opioid drug should not only decrease the need of the opioid drug but also prevent its tolerance-inducing or addictive properties [75]. The extract of the plant *Corydalis yanhusuo* (YHS) may offer such an opportunity as a safe and readily available co-medication in the treatment of chronic or severe pain.

YHS has been used as an analgesic in traditional Chinese medicine (TCM) for centuries [93, 94]. We have reported that YHS effectively attenuates acute, inflammatory and chronic pain in animal models. It elicits these responses without causing tolerance. Its mode of action relies at least in part on its antagonistic activity at the dopamine D2 receptor [93]. This suggested to us that it may also have anti-addictive properties. Therefore, we evaluated the antinociceptive activity of YHS in combination with morphine as well as its role in decreasing morphine tolerance and dependence. We finally assess YHS abilities to reverse these responses.

Results

The antinociceptive activity of morphine in the presence of YHS.

Antinociceptive activities were measured using foot withdrawal latency (FWL) in the hot plate assay [23 95]. Mice were first tested before injection for their basal FWL response which was found to be similar in the range of 3–7 secs. Then, mice were injected intraperitoneally (i.p.) with saline or variable doses of morphine (M) or YHS (Y). FWL was measured at 30 min, 60 min, and 120 min after the injection. Figure 2.1A shows the FWL of mice injected with saline or morphine (2.5 mg/kg), YHS (250 mg/kg), or the combination of morphine and YHS (2.5 mg and 250 mg/kg, respectively) at different times after injection. At these doses, morphine induces a FWL response that is smaller than YHS but when both are combined the response is strongly increased. When variable doses of morphine, YHS, or YHS and morphine are compared (Figure 2.1B), dose responses show that YHS potentiates the antinociceptive activity of morphine. Indeed, co-administration of YHS at 250 mg/kg increases the morphine 2.5 mg/kg FWL response to that equivalent to morphine 10 mg/kg.

A.

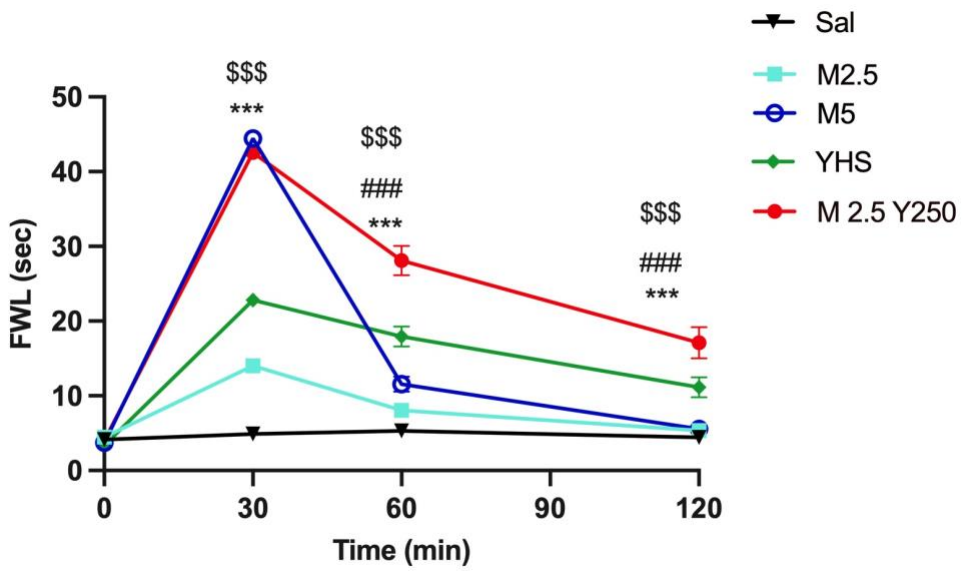

B.

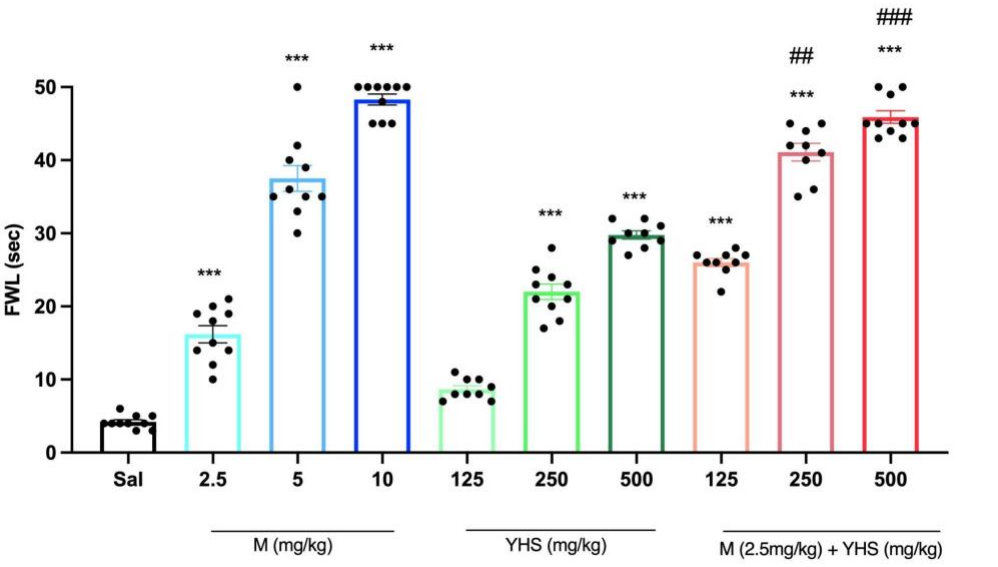

Figure 2.1 YHS increases morphine antinociception. **A.** Foot withdrawal latency (FWL) of mice injected with saline, morphine (2.5 mg/kg), YHS (250 mg/kg), or the combination of morphine and YHS (2.5 mg and 250 mg/kg, respectively) at 30, 60, and 120 min after i.p. administration (n = 10). The black dots correlate to the number of animals used in each experiment. Two-way

ANOVA revealed significant drug effects F (3, 288) = 332.8 $p < 0.0001$, time effect F (4, 288) = 217.5 $p < 0.0001$, and drug x interaction time F (12, 288) = 55.29 $p < 0.0001$, followed by Tukey's multiple comparison test *** $p < 0.001$ compared with M2.5 mg/kg, $$$ $p < 0.0001$ compared with saline, ### $p < 0.0001$ compared with M5 mg/kg. **B.** FWL at 30 min after morphine (2.5 mg/kg, 5 mg/kg, 10 mg/kg), YHS (125 mg/kg, 250 mg/kg, 500 mg/kg),or morphine + YHS (n = 9–10) i.p. administration. One-way ANOVA revealed significant drug effects F = 247.2, $p < 0.0001$, followed by Tukey's multiple comparison test *** $p < 0.001$ compared with saline, ## $p < 0.01$, ### $p < 0.001$ compared with M2.5 mg/kg. YHS prevents morphine tolerance.

Tolerance was assessed by injecting morphine, YHS, or a combination of both twice daily for 6 days. As shown in Figure 2.2A and Figure 2.7, morphine (2.5 mg/kg) lost its antinociceptive activity over the seven-day period while analgesic effects of YHS (250 mg/kg) were retained. Moreover, when combined, YHS was able to completely prevent tolerance development to any morphine dose tested, while retaining the additive antinociceptive effect of the combination (Figure 2.2B).

A.

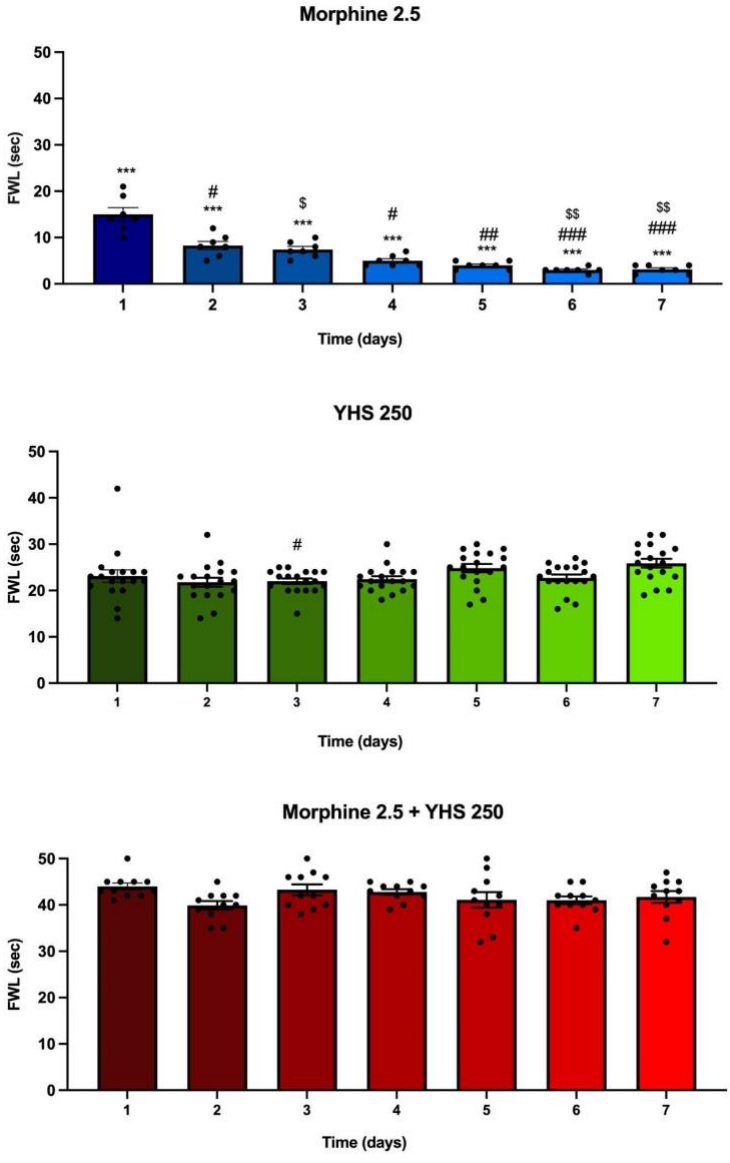
Morphine 2.5
FWL (sec)
Time (days)
YHS 250
FWL (sec)
Time (days)
Morphine 2.5 + YHS 250
FWL (sec)
Time (days)

B.

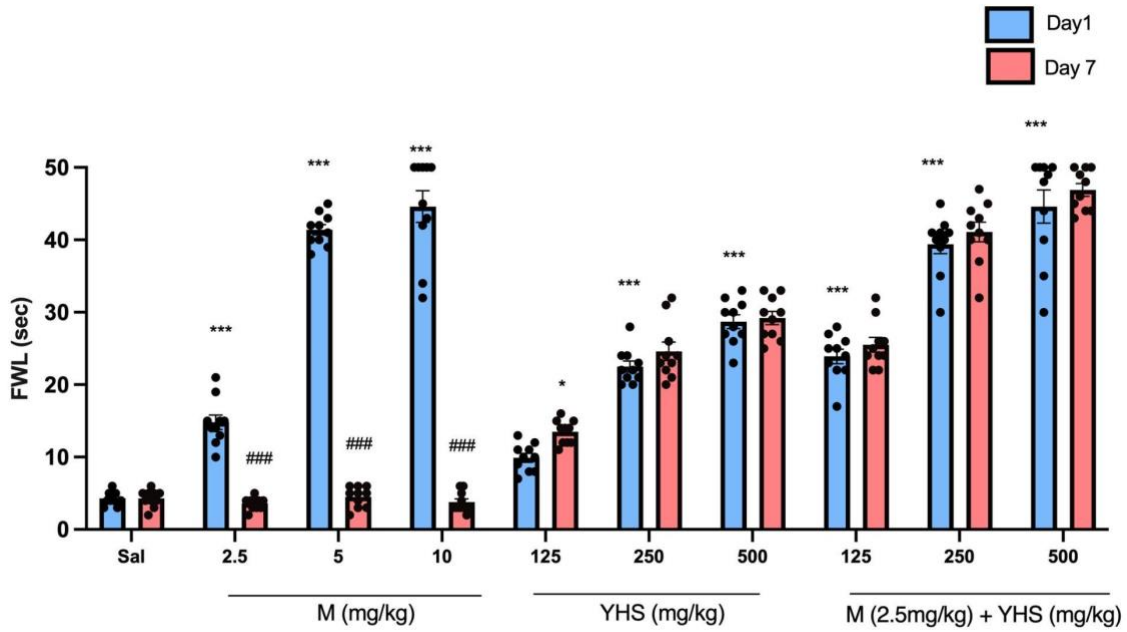

Figure 2.2 YHS inhibits morphine tolerance. **A.** FWL at 30 min after morphine 2.5 mg/kg (M2.5), YHS (250 mg/kg), and morphine +YHS (M2.5+YHS) (i.p. administration) over a period of 7 days (n = 7–11) to display tolerance. The black dots correlate to the number of animals used in each experiment. The gradient color for each figure shows the time-dependent change. One-way ANOVA followed by Tukey's test revealed significant drug tolerance over 7 days $F = 33.59$, $p < 0.0001$, D1 *** $p < 0.001$ compared with D2-D7, D2 ### $p < 0.0001$, ## $p < 0.01$ compared with D4-D7, D3 $$ $p < 0.01$, $ $p < 0.05$ compared with D6 and D7 in the morphine (2.5 mg/kg) group. One-way ANOVA followed by Tukey's test revealed no significant drug tolerance over 7 days for YHS (250 mg/kg) group, D3 # $p < 0.05$ compared with D7. One-way ANOVA followed by Tukey's test revealed no significant drug tolerance over 7 days for the combination group. **B.** Comparison of FWL at day 1 and day 7 30 min after i.p. administration of morphine, YHS, and morphine + YHS (n = 10). Two-way ANOVA revealed significant tolerance amongst all morphine

doses (2.5, 5, 10 mg/kg) $F(9, 180) = 291.3$ $p < 0.0001$, followed by Tukey's multiple comparison test, ### $p < 0.001$. Two-way ANOVA revealed significant analgesic effects between saline and all other groups on Day 1, $F(9, 180) = 291.3$ followed by Tukey's multiple comparison test *** $p < 0.001$ compared with saline, $p < 0.05$ compared with saline. YHS prevents morphine dependence.

To investigate the effects of YHS and morphine on withdrawal, we observed chronically treated animals after naloxone injection. Withdrawal behaviors, such as body grooming, jumping, writhing, head shakes, genital licking, face wiping, teeth chattering, dysphoria, rearing, chewing, and diarrhea, were scored over a 15-min time period. Figure 2.3 displays the various withdrawal behaviors observed in each group. While morphine-treated mice (2.5 and 5 mg/kg) showed significantly elevated signs of nalone-precipitated withdrawal, animals chronically treated with YHS (250 mg/kg) or a combination of morphine (2.5 mg/kg) + YHS displayed no withdrawal behaviors and were indistinguishable from saline-treated controls. It appears that co-administration of YHS (250 mg/kg) is sufficient to prevent establishment of typical morphine dependence. Sniffing was unchanged in all treatment groups and served as an internal control for natural behavior.

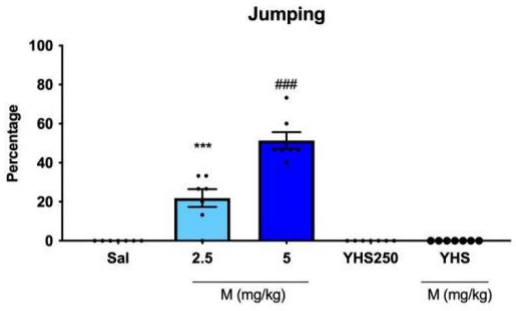
Jumping
Percentage
100
80
60
40
20
0
***
###
Sal
2.5
5
YHS250
YHS
M (mg/kg)
M (mg/kg)

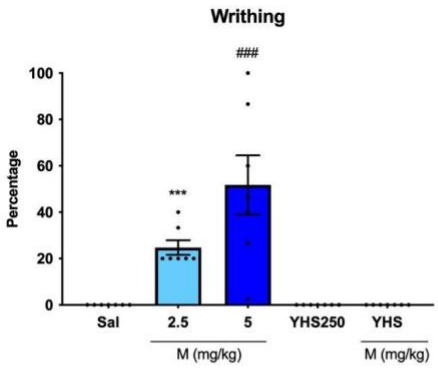
Writhing
Percentage
100
80
60
40
20
0
***
###
Sal
2.5
5
YHS250
YHS
M (mg/kg)
M (mg/kg)

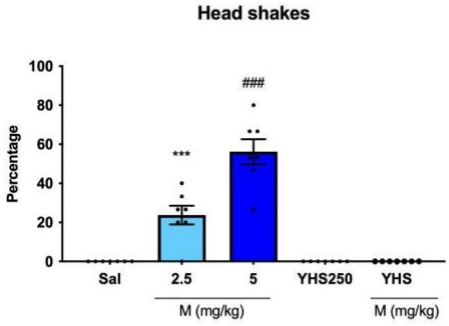
Head shakes
Percentage
100
80
60
40
20
0
***
###
Sal
2.5
5
YHS250
YHS
M (mg/kg)
M (mg/kg)

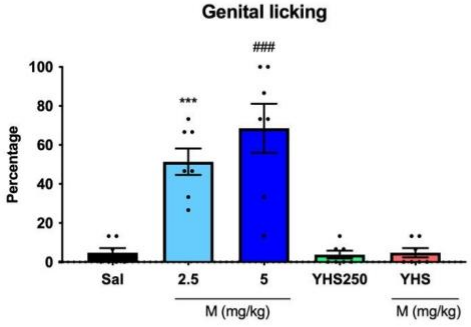
Genital licking
Percentage
100
80
60
40
20
0
***
###
Sal
2.5
5
YHS250
YHS
M (mg/kg)
M (mg/kg)

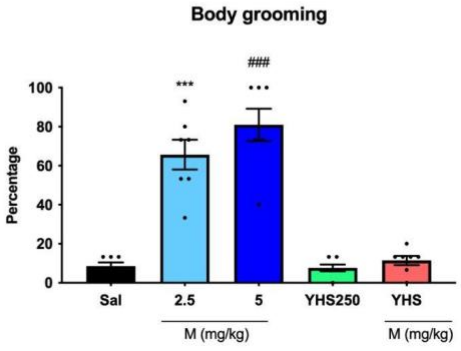
Body grooming
Percentage
100
80
60
40
20
0
***
###
Sal
2.5
5
YHS250
YHS
M (mg/kg)
M (mg/kg)

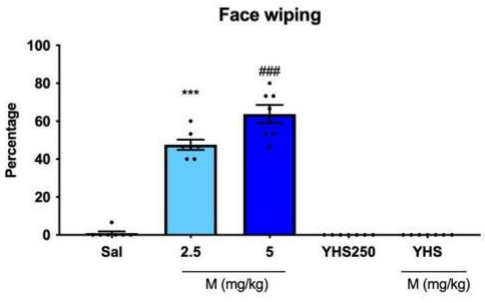
Face wiping
Percentage
100
80
60
40
20
0
***
###
Sal
2.5
5
YHS250
YHS
M (mg/kg)
M (mg/kg)

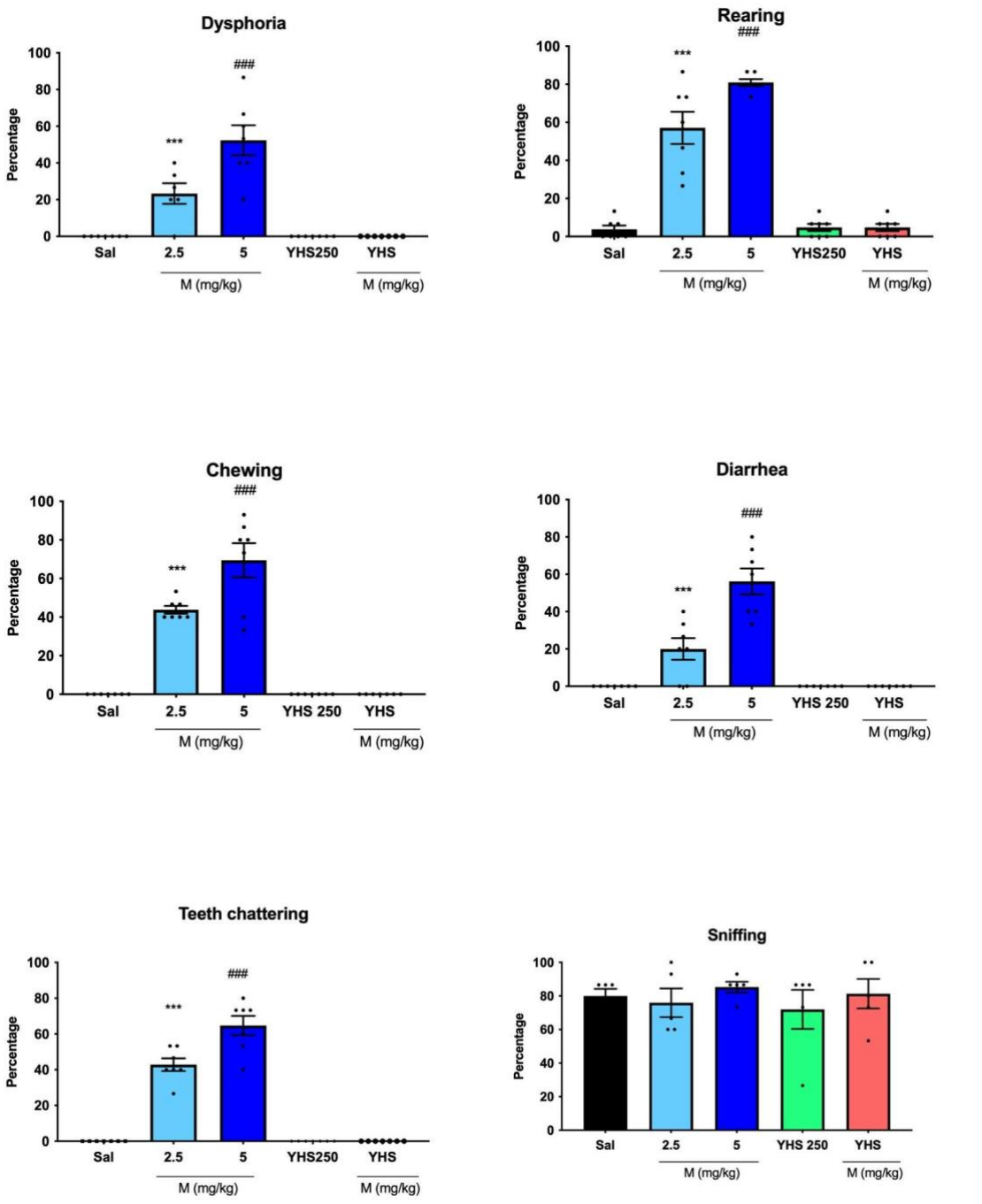

Figure 2.3 YHS inhibits morphine physical dependence after i.p. administration. Jumping, writhing, head shakes, genital licking, body grooming, face wiping, teeth chattering, dysphoria, rearing, chewing, diarrhea, and sniffing after naloxone injection (n = 8). One-way ANOVA

revealed significant percentage of jumping, writhing, head shakes, genital licking, body grooming, face wiping, teeth chattering, dysphoria, rearing, chewing, and diarrhea in both morphine groups, $F = 65.51$ $p < 0.0001$, followed by Tukey's multiple comparison test M2.5 *** $p < 0.0001$ compared with saline, M5, YHS 250, and M2.5YHS250; M5 ### $p < 0.0001$ compared with saline, M2.5, YHS 250, and M2.5 YHS250. YHS inhibits the rewarding properties of morphine.

Reward-related behavior was monitored in the CPP paradigm. A preference score was determined by observing the time that each animal spent in the drug-paired chamber vs. the saline-paired chamber during the pre- and post-training periods. As shown in Figure 2.4, M2.5 and M5 induced strong preference scores (100 and 250, respectively), indicative of addiction and the associated drug-seeking. When YHS 250 was added to M2.5 or M5 during the training, preference scores decreased strongly, showing that YHS is able to significantly limit the rewarding effects of morphine.

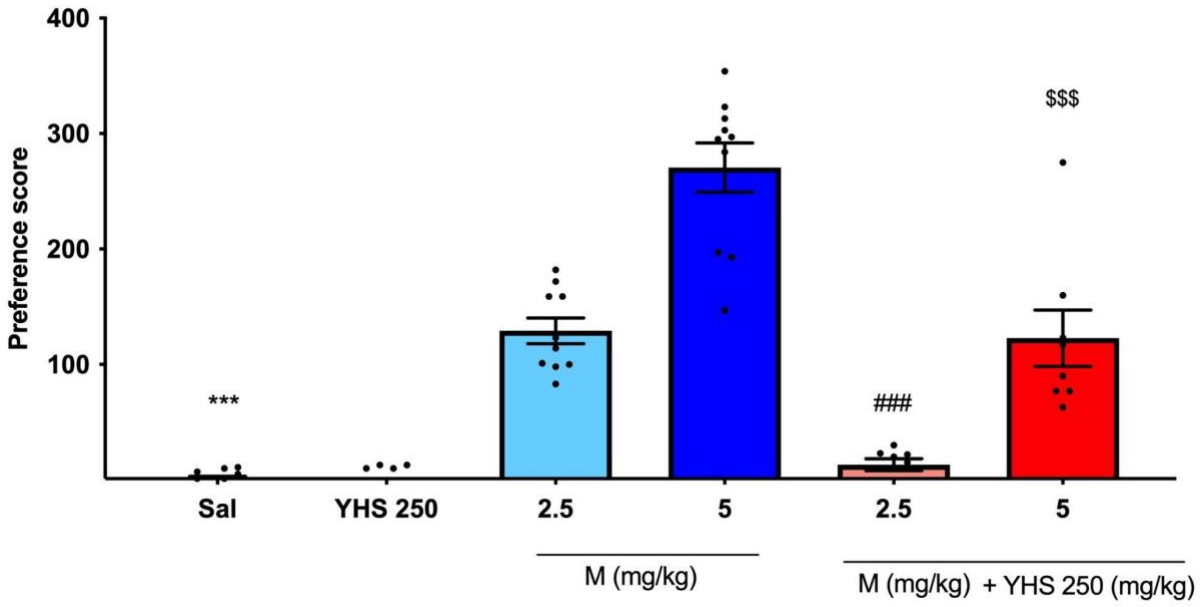

Figure 2.4 Morphine-induced CPP is inhibited by YHS after i.p. administration. Preference scores calculated based on animal's time spent in the drug-paired chamber vs. the non-drug-paired chamber during the pre- and post-preference periods (n = 8–11). The black dots correlate to the number of animals used in each experiment. One-way ANOVA revealed significant drug addiction in all morphine groups and a reduction in the combination groups $F = 62.50$ $p < 0.0001$, followed by Tukey's multiple comparison test, *** $p < 0.0001$ compared with M2.5, M5, and M5 YHS250, ### $p < 0.0001$ compared with M2.5, M5, and M5 YHS250, $$$ $p < 0.0001$ compared with M5 and M2.5 YHS 250. YHS reverses morphine tolerance and dependence.

The previous data suggest that co-administration of morphine and YHS could prevent development of tolerance and dependence in morphine-naive animals. We next investigated whether YHS might also be beneficial in already-dependent animals and could, thus, potentially be used to curb the opioid epidemic. For tolerance reversal, mice were treated for 3 days with

morphine (2.5 mg/kg twice daily), followed by four days of YHS (250 mg/kg) or YHS + morphine (250 mg/kg and 2.5 mg/kg, respectively) and then tested for analgesic tolerance (Figure 2.5). YHS alone or in combination with morphine reverses morphine tolerance and restores analgesia in previously tolerant animals.

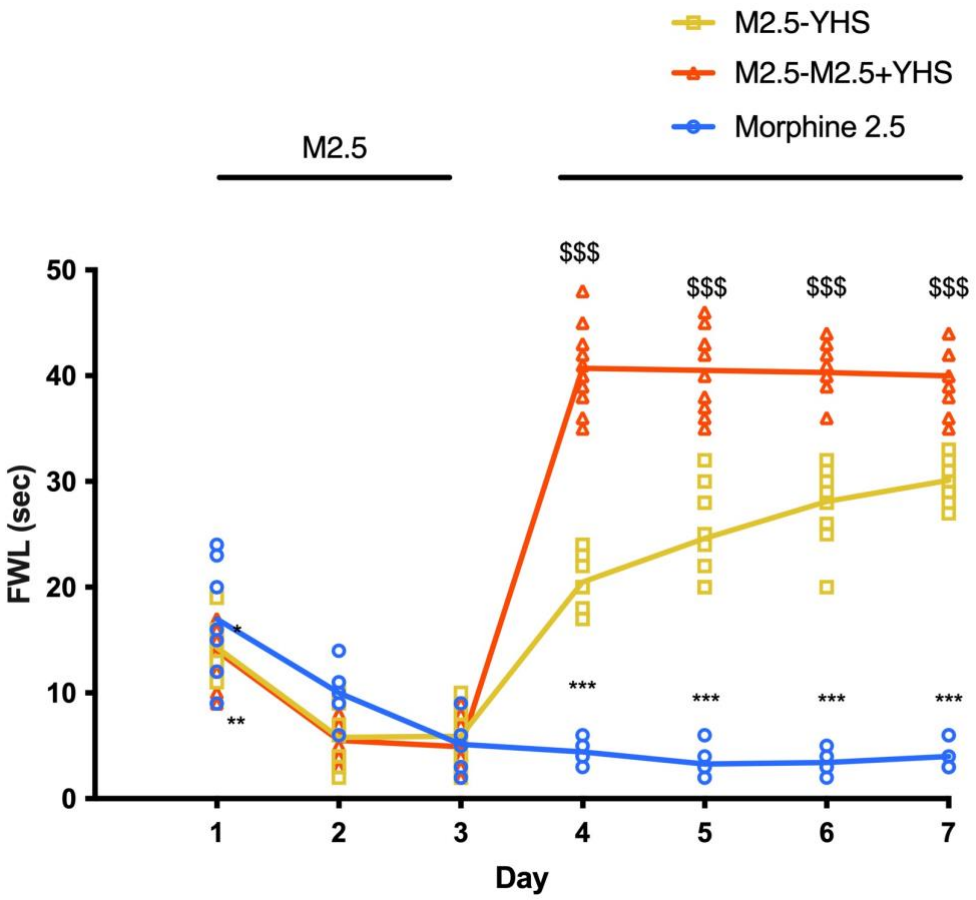

Figure 2.5 YHS reverses morphine tolerance. Analgesic response after 3 days (D) of Morphine, followed by 4 D of either YHS (250 mg/kg) or M2.5-M2.5+YHS (n = 10) (i.p. administration). Two-way ANOVA revealed significant drug effects F (6, 168) = 205.9 $p < 0.0001$, followed by Tukey's multiple comparison test, *** $p < 0.0001$ M2.5 compared with M2.5-YHS and M2.5-M2.5-YHS on D4-7, $$$ $p < 0.0001$ compared M2.5-YHS with M2.5-M2.5-YHS on D4-7.

The same animals were also tested for naloxone-precipitated withdrawal (Figure 2.8). As

expected, mice treated with morphine at 2.5 mg/kg for seven days exhibited significant signs of withdrawal behaviors (Figure 2.8). Switching treatment from morphine alone to morphine 2.5 mg/kg + YHS 250 mg/kg completely prevented—and may indeed have reversed—opioid dependence. Similarly, animals treated with morphine 2.5 mg/kg for 3 days and then switched to YHS also showed no signs of persisting morphine dependence, although we cannot rule out the possibility that these mice already underwent morphine withdrawal during the four days of YHS treatment. Importantly, adding YHS to an ongoing morphine treatment regimen appears to reverse pre-existing morphine dependence while maintaining high antinociceptive efficacy. For reversal of morphine rewarding properties, mice were either treated with saline or morphine (2.5 mg/kg) for 7 days. After this initial treatment, mice were kept on saline or saline treatment, or switched to YHS (250 mg/kg) or morphine (2.5 mg/kg) + YHS (250 mg/kg) for another 7 days. Conditioned place preference was tested to observe for any addiction-like properties. Mice that were treated initially with morphine and then switched to either YHS (250 mg/kg) or morphine (2.5 mg/kg) + YHS (250 mg/kg) reversed any addiction-like behavior in mice (Figure 2.6).

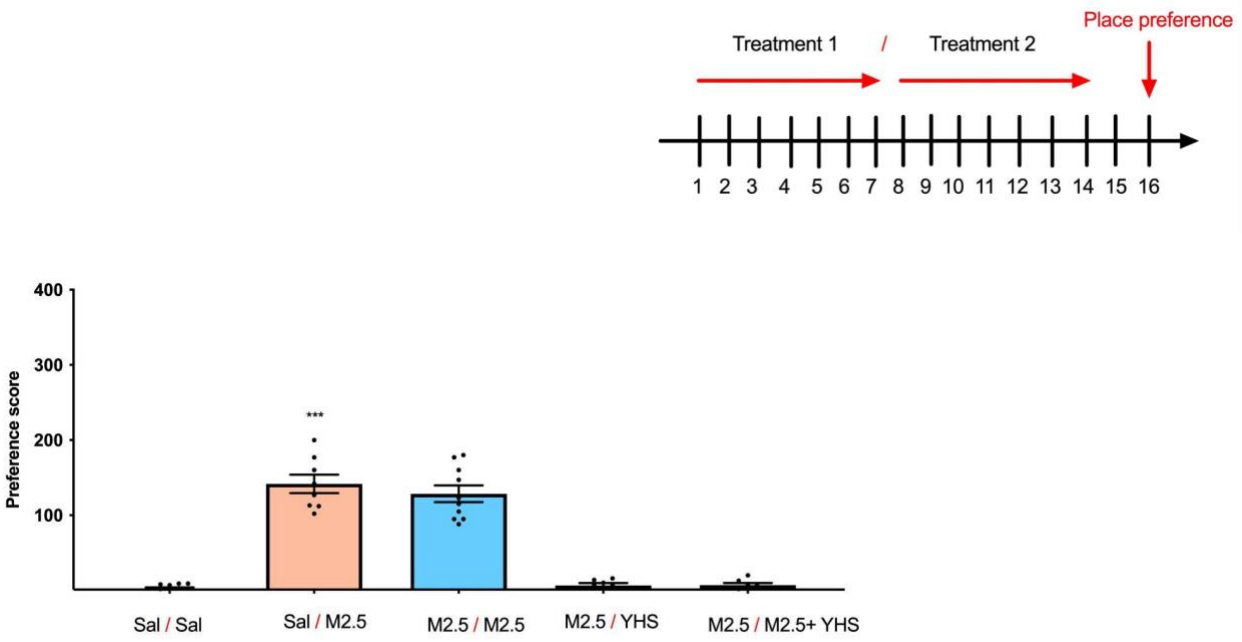

Figure 2.6 YHS reverses morphine-induced CPP. CPP responses for the following groups: 14 days of Sal injections (Sal–Sal), 7 days of Sal followed by 7 days of M2.5 injections (Sal-M2.5), 14 days of M2.5 injections (M2.5-M2.5), 7 days of M2.5 followed by 7 days of YHS (250 mg/kg) or M2.5-YHS injections (i.p. administration). (n = 7–11). The black dots correlate to the number of animals used in each experiment. One-way ANOVA revealed significant drug preference $F = 8.131$ $p < 0.0001$, followed by Tukey's multiple comparison test, *** $p < 0.0001$ compared with Sal and M2.5-YHS, $$$ $p < 0.0001$ compared with Sal-Sal, M2.5-YHS, and M2.5-M2.5+YHS.

Discussion

The opioid epidemic resulted in an increase in opioid prescriptions to treat neuropathic and other forms of chronic pain. Opioids are effective for treating severe acute pain, but display less effectiveness in treating chronic pain. Chronic pain requires repetitive administration of an antinociceptive agent. When opioids are administered repeatedly, they induce analgesic tolerance, which is a time-dependent loss of efficacy requiring increasing doses to reach the same antinociceptive state [73 ,96, 97]. Repeated administrations of opioids then lead to physical dependence, i.e., the need for maintained administration to prevent withdrawal symptoms. Dependence manifests itself in withdrawal when the use of opioids is abruptly discontinued [74, 98] and is accompanied by addictive behaviors to re-experience the rewarding effects of the opioids or at least avoid withdrawal [99, 100, 101].

The opioid epidemic stems from pain-sufferers becoming addicts because they have to simultaneously cope with pain, opioid tolerance, and dependence. To fight the epidemic, the CDC has recommended using NSAIDS alone or in combination with opioid drugs to reduce their use. However, NSAIDs often lack efficacy against neuropathic pain [75, 90]. A safer pain medication would be one that could limit or inhibit all three opioid-related phenomena: tolerance, dependence, and addiction [73, 92, 102]. In the present study, we present evidence that the extract of the plant *Corydalis yanhusuo* (YHS) may be able to maintain the analgesic benefits of opioids while curbing their adverse liabilities when administered as a co-medication.

We first show that adding YHS to morphine potentiates its analgesic activity in a dose- and time-dependent manner. While a single low dose of morphine (2.5 or 5 mg/kg) induces analgesia 30 min after its administration but begins to display tolerance 30 min later, YHS alone or morphine with YHS retain most of their antinociceptive activities for over a 2 h period. When co-

administered, YHS at all doses tested increases the antinociceptive effect of morphine, showing that it could serve as an adjuvant to opiates in managing pain. This would allow for lowering the doses of morphine at the same level of antinociceptive effectiveness, thus decreasing the risk of addiction.

An important clinical limitation of opioid treatment is the development of tolerance. Over repeated administrations, opioids lose their potencies [82, 99, 103]. We assessed the effect of adding YHS to morphine on tolerance. While morphine induces definitive tolerance over 7 days of repeated administration, the addition of YHS prevents morphine tolerance. This implies that the need to increase morphine doses to maintain antinociception would not occur in the presence of YHS, a factor that could significantly help to reduce addiction. Moreover, we show that co-administration of YHS with morphine can prevent the establishment of opioid dependence in drug-naive animals. More clinically relevant is the observation that a combination of YHS and morphine can reverse a preexisting morphine dependence and could thus help addicted patients to escape the vicious cycle of continued opioid exposure.

In trying to understand the mechanism underlying YHS mode of action, we have to recognize that YHS is a complex extract and that its activity may rely on several components. YHS contains over 100 chemical components [98]. Of these, some 81 are protoberberine, apomorphine, opiate-like, and other alkaloids [104, 105]. Several YHS components have been pharmacologically analyzed and found to display antagonism at dopamine receptors [92], agonism at opioid receptors [106], or inhibition of acetylcholinesterase activity [107]. These components act at their respective receptors at high nanomolar or micromolar concentrations. Of the YHS components, possibly the most studied is L-tetrahydropalmatine (L-THP) [108]. L-THP has been shown to exhibit sedative, anti-epileptic, antidepressant, and anxiolytic effects in addition to its analgesic activity [109]. With

regard to drugs of abuse, L-THP has been shown to attenuate cocaine-associated reward [109], self-administer cocaine, and promote recovery from cocaine-induced effects in rats [109,110]. L-THP was used to treat heroin withdrawal syndrome in patients [107]. L-THP was found to significantly reduce heroin craving and withdrawal symptoms and to improve the abstinence rate of heroin addicts. In these experiments L-THP was given at a dose of 60 mg twice daily. L-THP represents approximately 0.2% of the total dry mass of YHS [109], which is usually taken at about 5–10 g per day. L-THP should therefore not account for the full efficacy of YHS. Dehydrocorybulbine (DHCB), another YHS component and chemically related to L-THP, may also partially contribute to YHS effects in models of drug addiction or analgesia [109]. However, it has been shown that a combination of L-THP and DHCB does not account for the entire YHS analgesic effect [111]. It is therefore probable that several of the YHS components may participate in its efficacy and that YHS polypharmacological profiles are required for its full efficacy against morphine tolerance and dependence. Alternatively, undiscovered YHS component(s) may be responsible for these beneficial effects. Further studies will be needed to fully understand YHS mode of action.

Materials and Methods

Animals

CD-10 male mice obtained from Charles River aged 8 weeks were used for all behavior experiments. Mice were group housed and maintained on a 12 h light/dark cycle with food and water available ad libitum. All behaviors and treatments are approved by the Institutional Animal Care and Use Committee of the University of California, Irvine (AUP #20-015). Animals were frequently weighed and observed after injections to ensure proper health and weight gain. Any animals that seemed to be in distress or abnormal were excluded from the study.

Drugs

Morphine

Morphine injectable C II obtained from Patterson Veterinary (10 mg/mL concentration) (07-892-4699) was used according to the assigned groups and behavioral experiment. Three doses were used: 10 mg/kg, 5 mg/kg, and 2.5 mg/kg. Morphine was injected twice daily (morning and afternoon) for seven days intraperitoneally (i.p.) in a volume of 5 uL/g. The dosage for each animal was determined based on the animal's body weight. Morning and afternoon injections were spaced out for about 10 h. The varied doses of morphine used was dissolved in sterile saline. The vehicle used for all experiments was sterile saline.

Naloxone

Naloxone hydrochloride dihydrate obtained from Sigma Aldrich (N7758) at a dose of 6 mg/kg was given to precipitate withdrawal-like symptoms in mice at the end of the hot plate assay. The

dosage for each animal was determined based on the animal's body weight in a volume of 5 uL/g. Naloxone was injected via intraperitoneal administration.

YHS

The *Corydalis yanhusuo* extract (YHS) obtained from Dongyang County (Zhejiang, China) and authenticated by Institute of Medication, Xiyuan Hospital of China Academy of Traditional Chinese Medicine, as previously described [94]. A dose of 250 mg/kg dose [94] in a volume of 5 uL/g was used for most assays. To demonstrate a dose response of YHS, both the 125-mg/kg and the 500-mg/kg doses were used. The YHS powder was dissolved in saline solution and injected via intraperitoneal administration.

Animal Groups and Treatments

Mice were divided into various groups: control (saline only), YHS (125, 250, 500 mg/kg), morphine (10, 5, 2.5 mg/kg), and the combination of YHS and morphine at varying YHS concentrations (125, 250, 500 mg/kg). Drugs or vehicle were injected twice daily for seven days in the hot plate assay, and twice daily for 6 days in the conditioned place preference assay (CPP). The same mice are used for the pain, tolerance, and withdrawal assay. Behavioral testing was performed according to each model explained below.

Behavioral Assays

Pain Model

To establish the antinociceptive effects of YHS and morphine in combination on acute pain, foot withdrawal latency (FWL) in the hot plate assay was measured 30, 60, and 120 min after

injections, as well as before to establish a baseline on day 1 at 52 degrees Celsius. A hotplate assay was performed, as described in the literature [95, 96]. The cutoff time for the hotplate assay was 50 s.

Tolerance Assay

Mice were injected twice daily and the hot plate assay was tested on day 7 for tolerance-like behavior. FWL on the hotplate was measured at 30, 60, and 120 min after injections. Day 1 and Day 7 responses were compared to observe any tolerance to the drugs.

Withdrawal Assay

The withdrawal assay was tested on day 8 for withdrawal-like behaviors. Mice were observed for withdrawal symptoms, such as teeth chattering, genital licking, face wiping, head shakes, etc. [7]. The total time for this assay was about 50 min. All sessions were videotaped and analyzed later by individuals blinded to the experiment. Mice were habituated to a 40-x 40 locomotor test chamber for 5 min. After 5 min, the mice were injected according to their previous treatment (YHS, Morphine, Saline, or YHS+M2.5). Mice were observed for 30 min after injection and then were injected with naloxone followed by observation for 15 min.

Conditioned Place Preference (CPP)

The CPP assay consisted of multiple stages: a habituation period, conditioning sessions, and a test day as previously described [95]. The CPP assay consisted of a three chamber box. The middle chamber is considered the neutral side, where the mouse is placed and is allowed to explore the other two sides of the chamber. One side of the chamber is decorated with stripes and the other

side with circles. Mice were then habituated to all three compartments of the chamber for 3 days for 10 min. Animals that display a preference during the habituation period are omitted from the study. After the habituation period was conducted, mice were conditioned to both sides of the chamber (morning and afternoon) for 7 days and were injected with their corresponding drug (i.e., morphine group animals are injected with saline on the circles side in the morning and then morphine on the stripes at night). After the conditioning sessions, mice were given a day in between with no injections to induce drug craving, as previously described [89]. The next day, mice were tested for their preference in a total duration of 10 min. Preference score was calculated by using the equation: $((A2 - A1)/A1) * 100$, where A2 represents the percent time spent on the most preferred side during the final preference test and A1 represents the percent time spent on this same side during the initial habituation period.

To test CPP in mice dependent on morphine, animals were first treated with morphine and then switched to a treatment of YHS or the combination of M2.5 and YHS. This experiment was conducted the same way as described above, except it includes 7 days of morphine conditioning, and then an additional 7 days of the alternative treatment (either YHS or M2.5 + YHS). Once again, the mice were given a day with no injections before testing their CPP the next day. The groups that started with morphine were never taken off it to avoid any withdrawal symptoms that may arise and interfere with analyzing addiction-like behavior. All CPP testing sessions were videotaped and analyzed by individuals blinded by the experiment. A preference score for each mouse was calculated based on the equation described above.

Statistical Analysis

GraphPad Prism (GraphPad Software, Inc., San Diego, CA, USA) was used for statistical analysis, and all data are presented as mean ± standard error mean (SEM). One-way ANOVA followed by Tukey post-test was used to analyze morphine antinociception, dependence, morphine-induced CPP, reversal of CPP, and reversal of dependence. Two-way ANOVA followed by multiple comparisons tests was used to analyze inhibition of morphine tolerance and reversal of morphine tolerance. p value < 0.05 was deemed statistically significant.

Conclusions

In summary, although therapeutic plants were studied for many years for various ailments, the combination of opioids and herbal medicine for the management of pain and addiction has not been effectively explored. We show that the extract of the plant *Corydalis yanhusuo* (YHS) is able to reduce required doses of morphine in pain management and can successfully block development of morphine tolerance and dependence. Moreover, YHS is able to reverse a previously established opioid dependence. YHS therefore displays advantageous properties in our aim to curb the opioid epidemic. The fact that it is safe and readily available implies that it could have an immediate effect on this epidemic and that clinical trials are warranted.

Supplementary Materials

The following are available online at **https://www.mdpi.com/article/10.3390/ph14101034/s1**, Figure 2.7: FWL at 30 min after morphine 2.5 mg/kg (M2.5), YHS (250 mg/kg), and morphine +YHS (M2.5+YHS) over a period of 7 days (n = 7–11, i.p. administration) to display tolerance. Two way ANOVA revealed significant drug tolerance of morphine (M2.5) over 7 days (D) $F(6, 168) = 7.023$ $p < 0.0001$, followed by Tukey's multiple comparison test. Two way ANOVA revealed significant analgesic effects between M2.5, YHS 250, and M2.5+YHS $F(6, 168) = 7.023$ $p < 0.0001$, followed by Tukey's multiple comparison test M2.5*** $p < 0.0001$ compared to YHS on D1–7, YHS ### $p < 0.0001$ compared to M2.5 + YHS on D1–7, M2.5 $$$ $p < 0.001$ compared to M2.5 + YHS on D1–7., Figure 2.8: Jumping, writhing, head shakes, genital licking, body grooming, face wiping, teeth chattering, dysphoria, rearing, chewing, diarrhea, sniffing after naloxone i.p. administration (n = 7). One way ANOVA revealed significant percentage of jumping, writhing, head shakes, genital licking, body grooming, face wiping, teeth chattering, dysphoria, rearing, chewing, and diarrhea in animals treated with morphine only, $F(3, 24) = 81.05$ $p < 0.0001$, followed by Tukey's multiple comparison test, *** $p < 0.0001$, M2.5*** $p < 0.0001$ compared with M2.5-YHS and M2.5-M2.5 + YHS.

Materials and Methods

The mice used in the tolerance reversal assay were also used to assess withdrawal behaviors shown in Figure 2.7. The withdrawal assay was carried out as previously described in the manuscript.

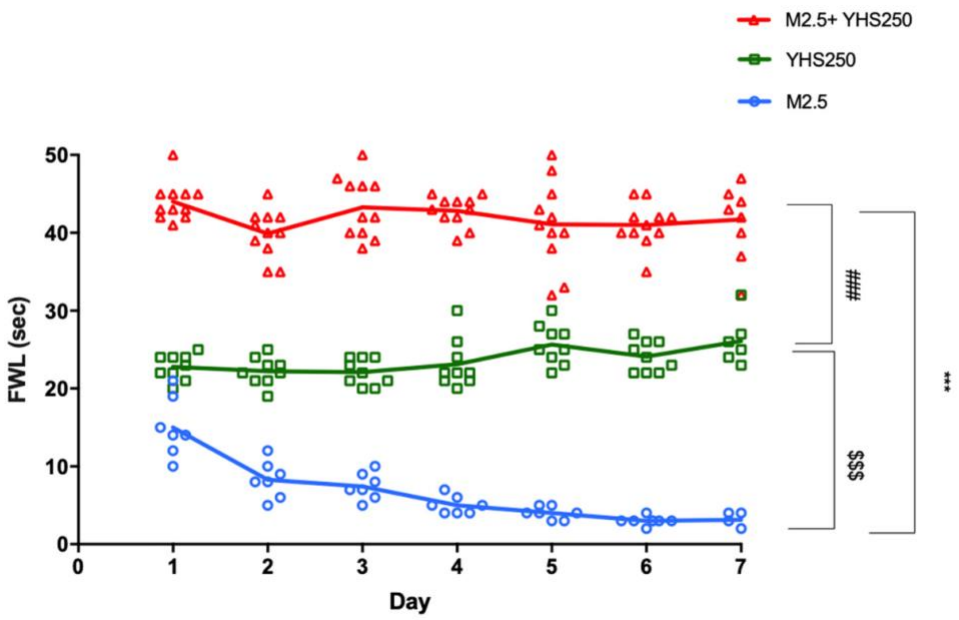

Figure 2.7: FWL at 30 min after morphine 2.5 mg/kg (M2.5), YHS (250 mg/kg), and morphine +YHS (M2.5 + YHS) over a period of 7 days (n = 7–11, i.p. administration) to display tolerance. Two way ANOVA revealed significant drug tolerance of morphine (M2.5) over 7 days (D) $F(6,168) = 7.023$ $p < 0.0001$, followed by Tukey's multiple comparison test. Two way ANOVA revealed significant analgesic effects between M2.5, YHS 250, and M2.5+YHS $F(6,168) = 7.023$ $p < 0.0001$, followed by Tukey's multiple comparison test M2.5*** $p < 0.0001$ compared to YHS on D1–7, YHS ### $p < 0.0001$ compared to M2.5 + YHS on D1–7, M2.5 $$$ $p < 0.001$ compared to M2.5 + YHS on D1–7.

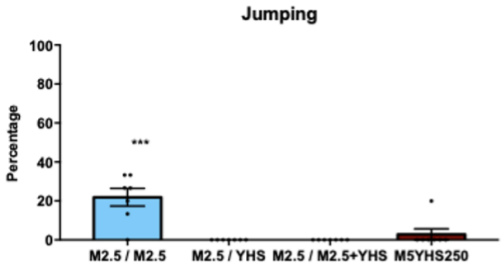
Jumping
Percentage
100
80
60
40
20
0
***
M2.5 / M2.5
M2.5 / YHS
M2.5 / M2.5+YHS
M5YHS250

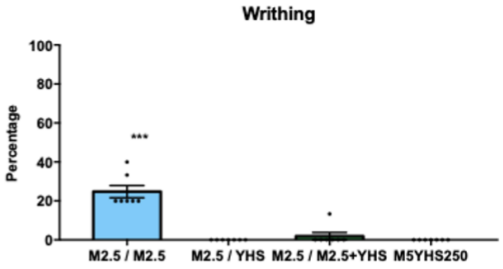
Writhing
Percentage
100
80
60
40
20
0
***
M2.5 / M2.5
M2.5 / YHS
M2.5 / M2.5+YHS
M5YHS250

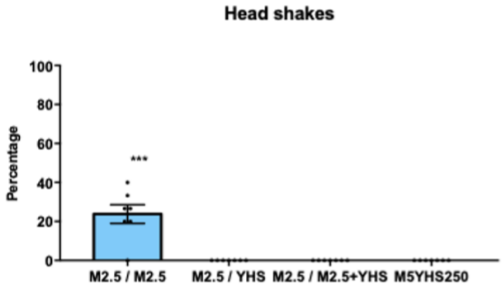
Head shakes
Percentage
100
80
60
40
20
0
***
M2.5 / M2.5
M2.5 / YHS
M2.5 / M2.5+YHS
M5YHS250

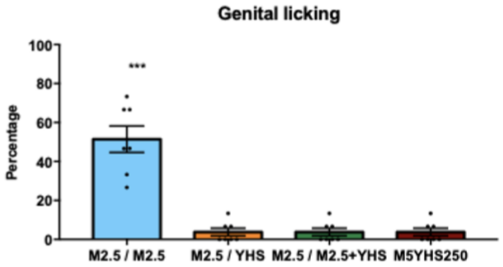
Genital licking
Percentage
100
80
60
40
20
0
***
M2.5 / M2.5
M2.5 / YHS
M2.5 / M2.5+YHS
M5YHS250

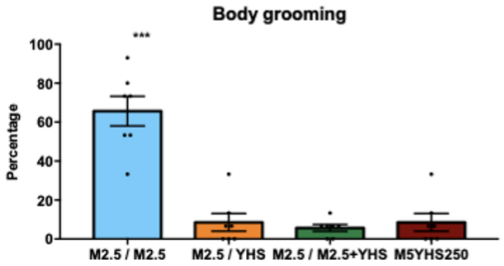
Body grooming
Percentage
100
80
60
40
20
0
***
M2.5 / M2.5
M2.5 / YHS
M2.5 / M2.5+YHS
M5YHS250

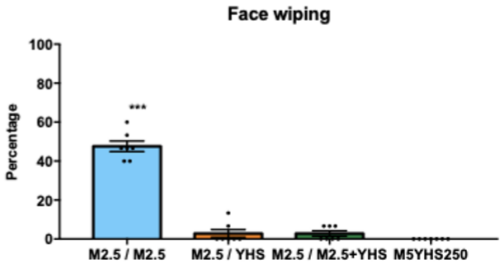
Face wiping
Percentage
100
80
60
40
20
0
***
M2.5 / M2.5
M2.5 / YHS
M2.5 / M2.5+YHS
M5YHS250

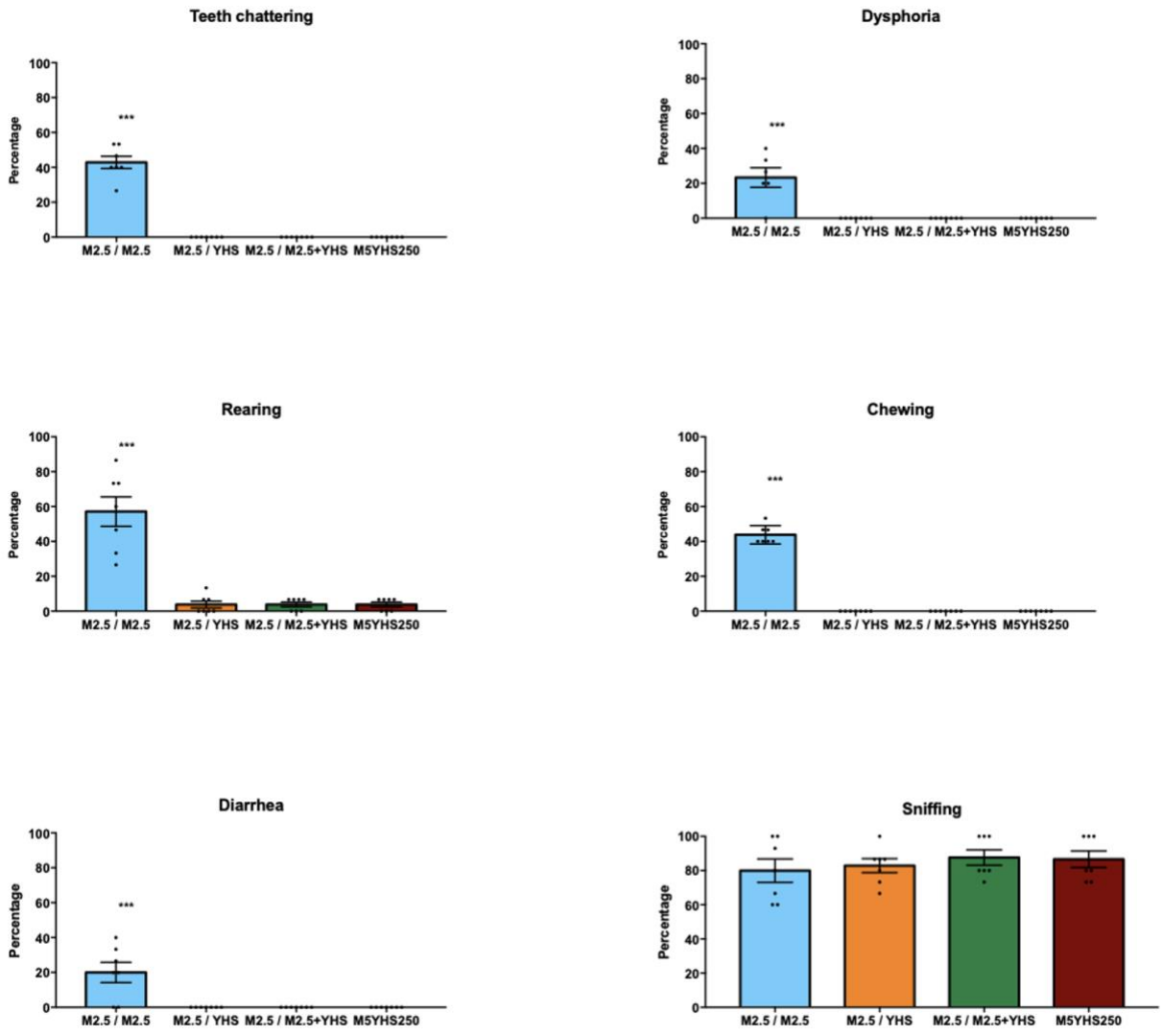

Figure 2.8: Jumping, writhing, head shakes, genital licking, body grooming, face wiping, teeth chattering, dysphoria, rearing, chewing, diarrhea, sniffing after naloxone i.p. administration (n = 7). One way ANOVA revealed significant percentage of jumping, writhing, head shakes, genital licking, body grooming, face wiping, teeth chattering, dysphoria, rearing, chewing, and diarrhea in animals treated with morphine only, $F(3, 24) = 81.05$ $p < 0.0001$, followed by Tukey's multiple comparison test, *** $p < 0.0001$, M2.5 *** $p < 0.0001$ compared with M2.5-YHS and M2.5-M2.5 + YHS.

Informed Consent Statement

Not applicable.

Data Availability Statement

All data is contained within the article and **supplementary files**.

Acknowledgments

We thank Amal Alachkar for discussions and Arman Zograbyan, Travis Dabbous, Zicheng Wang and Ayesha Noor for all the help during the course of this project.

Conflicts of Interest

The authors declare no conflict of interest.

Chapter 3: Morphine and an extract of Corydalis Yanhusuo Effects on Mu Receptor levels in the Mouse Brain

Abstract

Morphine, a potent mu opioid receptor (MOR) agonist, is known for its robust analgesic properties but is associated with the development of tolerance. We have previously shown that an extract of the therapeutic plant, Corydalis Yanhusuo (YHS), can reduce morphine tolerance. We hypothesize that YHS regulates MOR levels to prevent the development of tolerance and thus sought out to assess this using immunocytochemical and protein analyses. This study explores the potential impact of YHS upregulation of MOR expression within distinct brain regions, including the lateral septal nucleus, primary and secondary motor cortex, anterior cingulate cortex, caudal lateral septal nucleus, thalamus, and amygdala. The knowledge derived from our study holds the promise of illuminating the complex mechanisms involved in tolerance development, with a particular emphasis on how these mechanisms can be improved through the use of YHS.

Introduction

Morphine is historically known for its unparalleled analgesic properties [112-114]. To date, morphine is regarded as the gold standard treatment for pain management [74]. Morphine primarily exerts its analgesic (pain-relieving) properties through its interaction via the μ-opioid receptors (MOR) and the central nervous system [115]. μ-opioid receptors are found in various regions of the central nervous system, particularly in the thalamus, amygdala, periaqueductal gray matter, spinal cord, the cerebral cortex, and many other regions [116, 117]. The widespread presence of mu opioid receptors is a key reason why opioid treatments can have numerous effects beyond pain relief, and why they also carry the potential for side effects and misuse.

When morphine activates MOR, it initiates a cascade of biochemical events that ultimately alleviate pain [118]. Repeated administration of morphine for pain management is a common medical practice, especially in cases of chronic or severe pain. However, this repeated morphine administration results in the phenomenon of tolerance, defined as a loss of efficacy over time. Furthermore, pain afflicted individuals require higher doses of morphine to maintain their initial analgesic response.

Several brain regions have been implicated in opioid tolerance, more specifically the reward and pleasure pathways, which encompass the nucleus accumbens and ventral tegmental area [77]. The hypothalamus, which governs responses to pain and stress, may also experience adaptations under prolonged opioid exposure, affecting pain perception and stress responses [119]. Additionally, the limbic system, encompassing the amygdala and hippocampus, has been linked to the emotional and memory aspects of opioid tolerance [120]. Opioid-induced changes within the limbic system can influence emotional responses to opioids and affect the formation of memories associated with drug use [121]. The prefrontal cortex, responsible for decision-making

and cognitive control, may also play a role, as adaptations in this region can influence an individual's capacity to manage opioid use and cravings [122]. In essence, opioid tolerance is a multifaceted phenomenon that emerges from intricate interactions among these brain regions and their associated neural networks. Prolonged opioid exposure induces changes in the functional dynamics of these regions, ultimately leading to the need for escalated opioid doses to achieve these desired effects: a hallmark of opioid tolerance.

Studies have shown that morphine tolerance is closely related to MOR expression in the brain [38]. It often manifests through downregulation of opioid receptors, especially in areas where these receptors are abundant, such as the spinal cord and specific brainstem nuclei [123]. This downregulation is accompanied by receptor desensitization, which collectively reduces the efficacy of opioids [124]. Thus, morphine tolerance can lead to a decrease in both the number and sensitivity of MOR receptors [125].

Corydalis yanhusuo (YHS), is a medicinal herb employed in traditional medicine for its analgesic and anti-inflammatory properties [126]. Previous research has demonstrated that YHS exhibits promising analgesic properties in animal assays. Our lab has shown that YHS is analgesic on its own, as well as in combination with morphine treatment in mice. We have also shown that YHS treatment can inhibit morphine developed tolerance and dependence in mice [126]. In this study, our objective is to elucidate the potential role of YHS in upregulating MOR expression throughout the brain, specifically in the lateral septal nucleus, primary and secondary motor cortex, anterior cingulate cortex (CTX), caudal lateral septal nucleus (LSN), thalamus (THA), and amygdala (AMG). Additionally, we aim to assess the impact of morphine (M), YHS, and the combination of both (MYHS) in altering MOR protein levels in the brain following 1- and 7-day treatment regimens. Furthermore, we endeavor to compare brain regions implicated in the

development of tolerance during morphine or morphine and YHS treatment in mice. Our hypothesis posits that the capacity of YHS to mitigate morphine tolerance may be attributed to an augmentation of MOR expression in various cerebral regions. Overall, our findings are poised to provide valuable insights into the mechanisms underlying tolerance development and its amelioration by YHS region specifically.

Methods & Materials

Animals

Experiments were conducted using male CD-10 mice, aged 8 weeks, sourced from Charles River. These mice were housed in groups, and maintained on a 12-hour light/dark cycle, with free access to food and water. All experimental procedures and treatments were conducted in accordance with the approval granted by the Institutional Animal Care and Use Committee at the University of California, Irvine (IACUC# 23-059). Regular weight measurements and post-injection observations were performed to ensure their well-being and healthy weight gain. Any animals displaying signs of distress or abnormalities were excluded from the study.

Injections

Morphine injectable (C II) (10 mg/mL), was obtained from Patterson Veterinary (Product ID: 07-892-4699). Mice received intraperitoneal (i.p.) injections of morphine at a dosage of 2.5 mg/kg. YHS, obtained from Dongyang County in Zhejiang, China, and authenticated by the Institute of Medication at Xiyuan Hospital of China Academy of Traditional Chinese Medicine (as previously described), was administered at a dose of 100 mg/kg in a volume of 5 μL/g via intraperitoneal administration [126]. Mice were categorized into various groups and injected with either saline (S), YHS (100 mg/kg), morphine (at 2.5 mg/kg), or both morphine and YHS. The injection volume was 5 μL/g, and individual dosages were determined based on each animal's body weight. Drugs were administered twice daily in the morning and afternoon approximately 10 hours apart, for a duration of 7 days. Drugs were dissolved in sterile saline, which served as the vehicle for all experimental procedures. Brains were either harvested or perfused after 30 minutes following the first injection on day 1 or 30 minutes following the first injection on the 7th day.

Harvesting

Mice were euthanized in accordance with approved ethical guidelines after 30 minutes following the first injection or 30 minutes following the first injection on the 7th day. Following carbon dioxide overdose, the mouse's skull was carefully opened to expose the brain, and the brain was gently extracted from the skull. Subsequently, the isolated brains were promptly frozen by immersion in pre-chilled isopentane (below freezing point of the tissue). Frozen brain tissue was then transferred and stored in -80°C for further analysis.

ELISA

Harvested brains were extracted for membrane proteins. Microtiter plates with 96 wells were coated with the capture antibody (monoclonal anti-target antigen, catalog No. NB1001620 purchased from Fisher Scientific, 1:1000 dilution). The plates were then incubated at 4°C overnight to allow antibody binding to the plate surface. Following incubation, the plates were washed three times with phosphate-buffered saline (PBS) containing 0.05% Tween-20 (PBST) to remove unbound antibodies. After washing, 200 µL of blocking buffer (5% bovine serum albumin in PBS) was added to each well. The plates were incubated at room temperature for 2 hours to prevent non-specific binding. Subsequently, the plates were washed with PBST to remove excess blocking buffer. Brain samples, which contained the target antigen, were added to the wells at a volume of 100 µL per well. The plates were incubated at 37°C for 1 hour to facilitate antigen binding to the capture antibody. After the sample incubation, the plates were washed four times with PBST to remove unbound samples and other contaminants. The detection antibody (monoclonal anti-target antigen conjugated with horseradish peroxidase, catalog No. 7TM0319N

purchased from 7TM antibodies, 1:1000 dilution) was added to each well at a concentration of 0.5 μg/mL in a volume of 100 μL. The plates were incubated at 37°C for 1 hour to allow the detection antibody to form a "sandwich" with the captured antigen. To initiate the enzyme reaction, 100 μL of a substrate solution (3,3',5,5'-tetramethylbenzidine) was added to each well. The reaction was allowed to proceed for 15 minutes in the dark at room temperature. The absorbance of each well was measured at 450 nm using a microplate reader (BioTek Synergy H1). The absorbance values were recorded as a measure of the color change, indicating the presence of the target antigen.

Immunohistochemistry

Immunohistochemistry procedures for the examination of MOR-positive neurons were executed following previously established protocols. Mice were subjected to perfusion under isoflurane anesthesia, utilizing a 4% paraformaldehyde (PFA) solution. Subsequently, brains were extracted, post-fixed in 4% PFA for an overnight period at 4 °C, and ultimately preserved in a 30% sucrose solution. Coronal brain sections, measuring 30 μm in thickness, were obtained, and three to four sections were selected from each region of interest. Sections were subjected to blocking buffer consisting of 4% normal goat serum dissolved in PBS with 0.3% Triton X-100 for 1 hour. Subsequently, sections were incubated in a blocking buffer containing the primary antibody specific for MOR (catalog: 7TM0319N purchased from 7TM antibodies). After rinsing with PBS, the sections were incubated with a secondary antibody (goat anti rabbit, 1:500 dilution, red) for a period of 1 hour, followed by staining with 4′,6-diamidino-2-phenylindole (DAPI). Finally, sections were mounted on slides for analysis.

Image acquisition

Imaging was executed utilizing the Leica Sp8 TCS confocal microscope available at the UCI Optical Biology Core Facility and Keyence. Mor-positive neurons were quantified within the bilateral regions of interest in each section. The mean counts were calculated based on analysis of three non-consecutive sections per brain, with a total of 4-8 brains included in the study. Cell counts were determined using ImageJ software and were further verified through manual confirmation. Brain regions were identified using the Mouse Brain Atlas (2nd edition) from G. Paxinos and K.B.J. Franklin.

Statistical analysis

Statistical analyses of behavioral data were carried out using GraphPad Prism (GraphPad Software, Inc.). One-way and two-way ANOVA followed by Tukey post-test was used to analyze the data mentioned.

Results

Two cohorts of mice were injected with saline, morphine, YHS, and morphine + YHS for 1 and 7 days. Mice were euthanized 30 minutes following the first injection (Day 1) or the last injection on Day 7. Brains were collected and analyzed by enzyme-linked immunosorbent assay (ELISA) and immunohistochemistry analysis using a specific MOR antibody. This monoclonal antibody has been shown to be specific to the mu-opioid receptor (MOR) receptor. The levels of MOR expression were determined on Day 1 (left) or Day 7 (right) upon treatment with saline, morphine, YHS, and MYHS (Figure 3.1). On Day 1, although there was a weak but significant increase in MOR expression upon YHS treatment when compared to saline, the different treatments did not show significant changes. On Day 7, while the morphine treatment did not show a difference with saline treatment, the YHS or M+YHS treatments display significant increases in MOR expression.

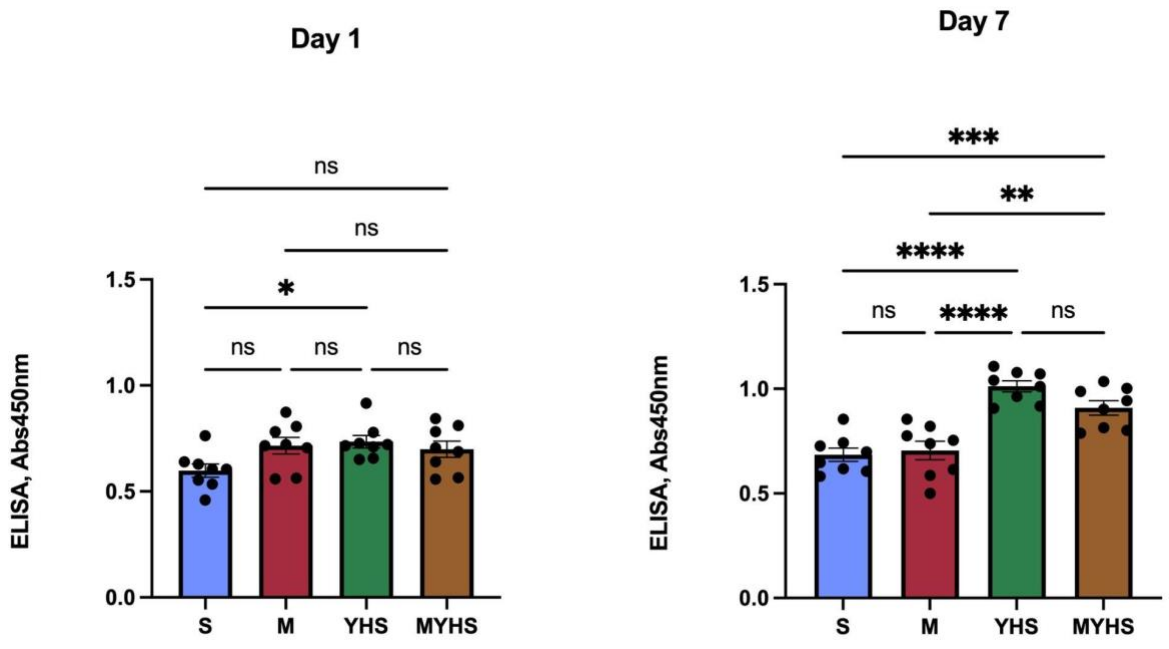

Figure 3.1 Intensity of MOR expression measured in ELISA assay at 450 nm on full brains treated with 1 day (left) or 7 days (right) of saline (S), morphine (M), YHS, or the combination of morphine and YHS (MYHS). One-way ANOVA followed by Tukey's multiple comparison test revealed an increase in MOR expression after 1 day, $F=3.039$, $*p<0.05$ compared with S and YHS. One-way ANOVA followed by Tukey's multiple comparison test revealed an increase in MOR expression after 7 days, $F= 20.79$, $****p<0.0001$ compared with YHS, M, and S, $***p<0.001$ compared with MYHS and S, $**p<0.01$ compared with MYHS and M.

To assess which specific levels of the brain contributed to the changes in MOR expression, immunocytochemical analyses were performed on Day 1 and Day 7 groups following saline, morphine, YHS, and morphine+YHS treatment on the second cohort of mice. The mice subjected to the protocol described in Figure 1 were perfused, and their brains were harvested, sectioned and subsequently immunostained using a specific MOR antibody (refer to the Materials and Methods section for details on the specific antibody used). Because it would be impossible to cover the entire brain, five different sections (1-5), representative of most of the brain, were chosen and further subdivided into specific regions of interest (highlighted in white in Figure 3.2A). MOR-positive neuron quantification was conducted in bilateral regions of interest for each section and sub regions, and the resulting average MOR counts are presented in a heatmap. Figure 3.2B illustrates the methodology employed to acquire the positive MOR+/DAPI counts under consideration. Specifically, five distinct subregions (DBN-2, CTX-2, THA-4, AVA-5, and HIP-5) were selected following a 1-day treatment with saline. The variability among these subregions is visually depicted via confocal imaging post-immunostaining, complemented by the accompanying

mean counts. These mean counts are subsequently transformed into a heat map, where the color gradation corresponds to the quantity of MOR in each sub region.

A.

Section 1

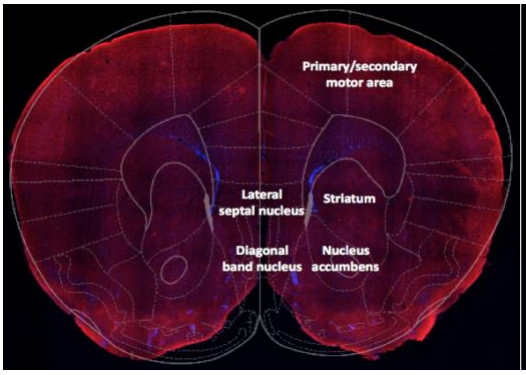

Section 2

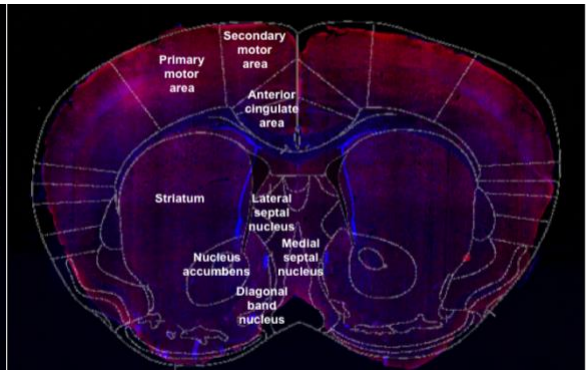

Section 3

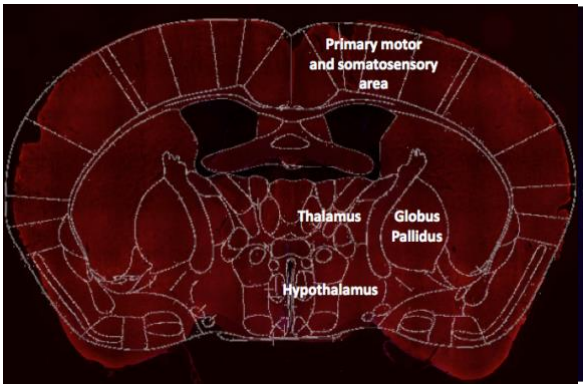

Section 4

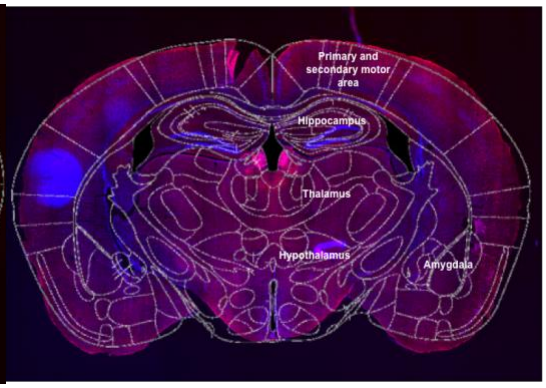

Section 5

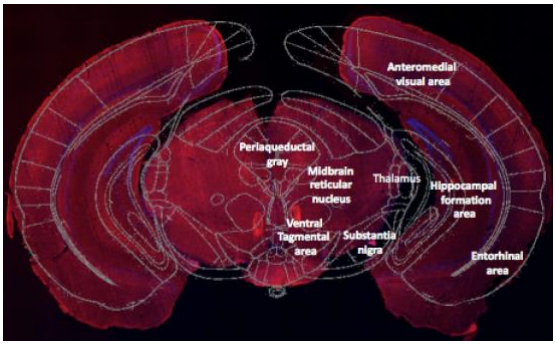

B.

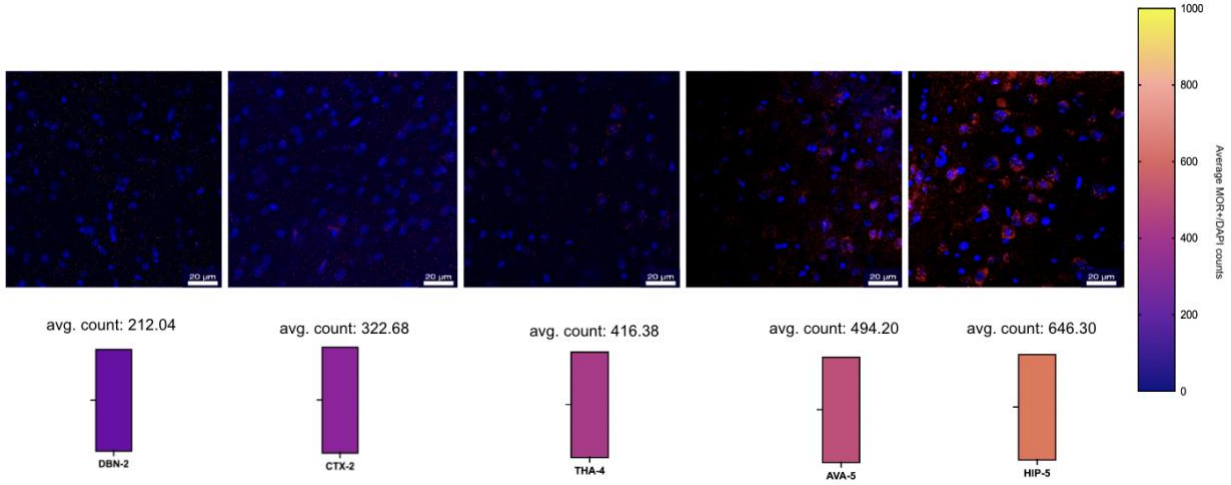

Figure 3.2 Immunostaining with a MOR specific receptor antibody in 5 sections of the mouse brain. **A**. 5 sections of the mouse brain were analyzed for positive MOR cells/DAPI expression after 1 or 7 days of saline, morphine, YHS, or MYHS injections. Sub regions are labeled in white. Section 1 sub regions analyzed include primary/ secondary motor area (CTX), striatum (STR), lateral septal nucleus (LSN), diagonal band nucleus (DBN), and the nucleus accumbens (NAc). Section 2 sub regions analyzed include primary/ secondary motor area (CTX), striatum (STR), lateral septal nucleus (LSN), diagonal band nucleus (DBN), medial septal nucleus (MSN) and the nucleus accumbens (NAc). Section 3 sub regions analyzed include primary motor and somatosensory area (CTX), globus pallidus (GP), hypothalamus (HYT), and thalamus (THA). Section 4 sub regions analyzed include hippocampus (HIP), primary/ secondary motor area (CTX), amygdala (AMG), thalamus (THA) and hypothalamus (HYT). Section 5 sub regions analyzed include anterior medial visual area (AVA), entorhinal area (ETA), midbrain reticular nucleus (MRN), ventral tegmental area (VTA), substantia nigra reticular and compact part (SN), thalamus (THA), hippocampal formation (HIP), and periaqueductal gray area (PG). **B.** Representative

images of MOR+ cells (red) and DAPI (blue) at 40x objective following 1 (left) and 7 day treatment (right) of S, M, YHS, and MYHS in mice in the primary and secondary motor and anterior cingulate area (CTX-section 2). Scale bar 20 um.

Heat maps depicting the expression of MOR following 1 day of exposure to S, M, YHS, and MYHS are provided in Figure 3.3. Notable alterations in MOR expression were not discerned across the various treatment groups and subregions. Nevertheless, it can be deduced that a predominant portion of MOR expression is situated within the CTX-4, AVA-5, and HIP-5 areas.

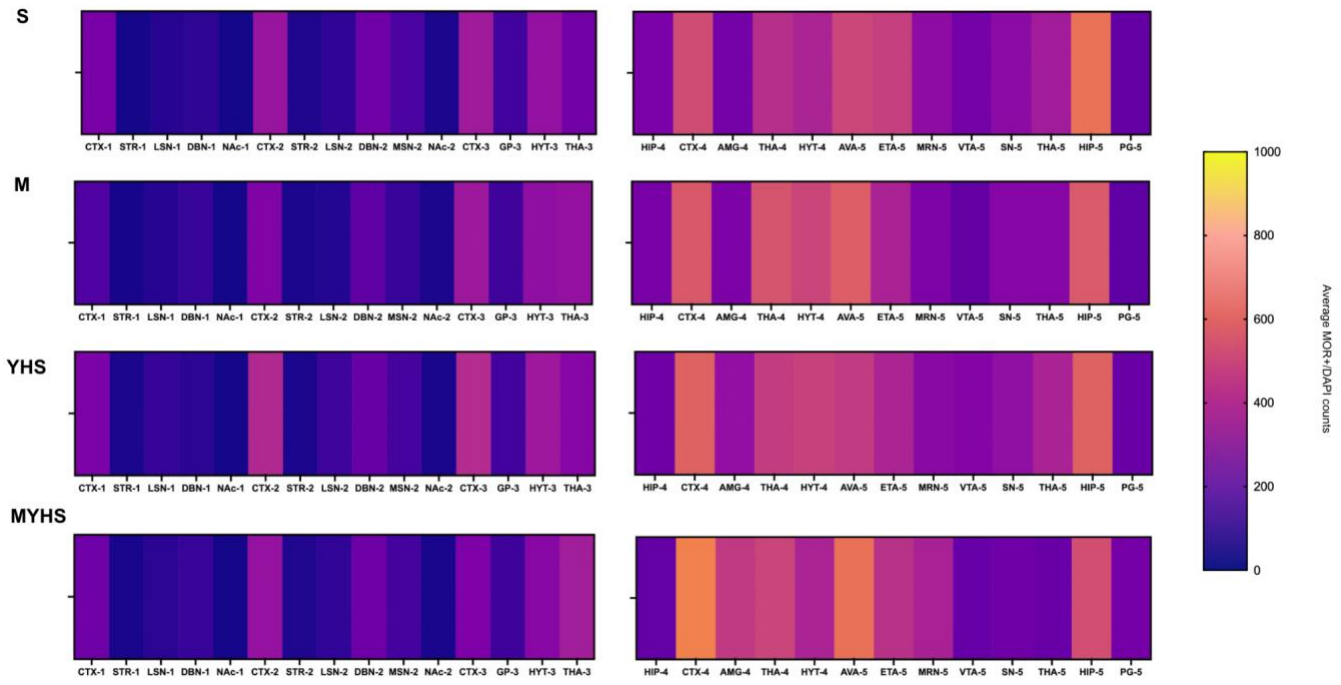

Figure 3.3 Heat maps of MOR expression in all sections after 1 day treatment of saline, morphine, YHS and MYHS. Heat map displaying MOR expression after 1 day of S, M, YHS, and MYHS treatment. X axis displays all sub regions at section 1-5. Scale bar ranges from 0-1000, which corresponds to counts of positive MOR cells/DAPI after immunostaining.

Heat maps depicting the expression of MOR following 7 days of exposure to S, M, YHS, and MYHS are provided in Figure 4. After 7 day treatment with S, M YHS, and MYHS we found that specific sub regions, CTX-2, AMG-4, and THA-4 were of particular interest. MOR expression was changed in all these regions following 7 days of morphine, YHS, and MYHS (Figure 3.4). All other subregions stayed relatively the same or had a small change in MOR expression. Small changes and confocal images between treatment groups and regions are further highlighted in the Supplementary section.

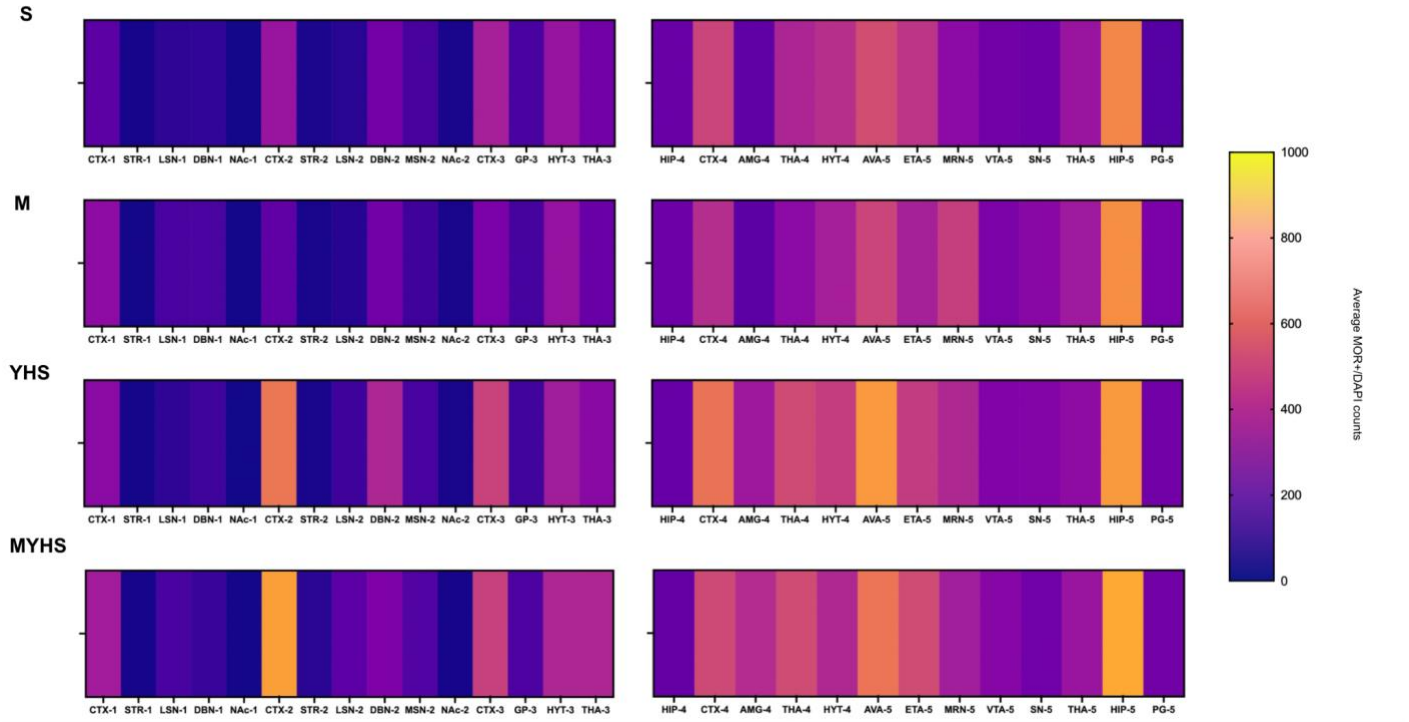

Figure 3.4 A. Heat maps of MOR expression in all sections after 7 day treatment of saline, morphine, YHS and MYHS. X axis displays all sub regions at section 1-5. Scale bar ranges from 0-1000, which corresponds to counts of positive MOR cells/DAPI after immunostaining.

Discussion

Repeated exposure to opioids results in diminished responsiveness to the drugs' analgesic and euphoric properties and leads to the development of tolerance, dependence, and ultimately, addiction. The brain regions responsible for the development of tolerance are still under study. We have previously shown that mice subjected to a 7-day regimen of morphine when co-injected with YHS do not display morphine tolerance [16]. In the course of this study, we employed two distinct methodologies to elucidate the expression of MOR in the mouse brain following treatments with saline (S), morphine (M), YHS, and MYHS for durations of 1 and 7 days. Initially, we conducted ELISA assays on whole-brain samples to comprehensively evaluate alterations in overall MOR expression. Subsequently, our second methodology involved a region-specific analysis, aiming to discern MOR changes within specific brain regions following the same treatments. Mouse brains were sectioned, and immunohistochemistry analysis was undertaken. Our initial findings reveal that the administration of a 7-day regimen of morphine does not elicit significant changes in MOR expression in whole brains. However, intriguingly, when YHS is administered alone or in combination with morphine, notable alterations in MOR expression are observed. In our pursuit to unravel the underlying mechanisms contributing to the role of YHS in morphine tolerance, we posited that the heightened MOR expression might be region-specific. To explore this hypothesis, we employed immunocytochemical analyses, focusing on different brain regions to pinpoint the selectivity of MOR expression induced by the combined YHS and morphine treatment.

We quantified MOR-positive neuronal cells using immunostaining across five strategically chosen brain sections, covering a comprehensive spectrum of the brain, excluding the cerebellum. The construction of a MOR expression heat map was facilitated and validated by correlating positive cell numbers with color intensity. At the 30-minute mark following a single injection on

Day 1, minimal variations were observed in the heat maps among brain sections treated with saline (S), morphine (M), YHS, or the combination MYHS. However, distinctive outcomes emerged following the 7-day regimens. Notably, a 7-day morphine treatment failed to yield significant differences compared to saline treatment in the heat maps. In contrast, the administration of YHS, either alone or in combination with morphine, resulted in noteworthy increases in MOR expression over the 7-day period. The most pronounced enhancements were observed in multiple cortex sections (CTX1-4 AVA), the thalamus (THA3-4), the amygdala (AMG4), as well as smaller regions, such as the lateral septal nucleus (LSN). Remarkably, the cortex exhibited the most prominent increases after YHS and MYHS treatment. Importantly, our immunohistochemistry experiments consistently indicated that the presence of YHS for 7 days consistently led to increases, with no instances of significant decrease, in MOR expression.

The lateral septal nucleus (LSN) is of particular significance due to its potential role in the neurobiological processes linked to the development of opioid tolerance and dependence [127]. Our immunohistochemistry results demonstrate that there is an upregulation of MOR expression subsequent to exposure to YHS and in combination with morphine. Given the well-established connection between MOR expression in the LSN and the central nervous system's response to opioid compounds, an augmentation in MOR expression within this region may hold significant implications for the phenomenon of morphine tolerance. The capacity of YHS to induce heightened MOR expression within the more caudal level of the LSN may potentially result in heightened analgesic effects, with the potential to mitigate the development of tolerance, a pattern previously shown in our previous behavioral studies [126]. It's important to note that the relationship between MOR expression in the LSN and tolerance is complex and not fully understood. The development of tolerance involves various factors, including the type of opioid,

the dose, the duration of use, and genetic predispositions [127]. Additionally, MOR expression is regulated by various other factors, which makes this phenomenon more complex.

Similar to the LSN region, our investigation revealed that the administration of YHS and MYHS over a period of 7 days led to a notable enhancement in MOR expression specifically within the primary and secondary motor cortex, as well as the anterior cingulate area (CTX), when compared to a 7-day regimen of morphine treatment. There is a well-established association between the somatosensory cortices and the formation of associative memories induced by morphine, and similarly, the anterior cingulate region has been linked to the processing of pain signals [128-130]. Notably, we observed a reduction in MOR expression after 7 days of morphine treatment alone, while the coadministration of YHS and MYHS effectively led to an upregulation of MOR expression at this same juncture. Because the primary and secondary motor cortex and anterior cingulate area play a broader role in the neural network in pain, they may also be influenced indirectly by opioid exposure in the development of tolerance. In certain cases, the potential of YHS to enhance MOR expression could potentially mitigate the development of tolerance. This hypothesis is rooted in the idea that an augmentation of receptors within the primary and secondary motor cortex as well as the anterior cingulate cortex would create a surplus of binding sites for opioids. Consequently, this surplus could translate to a heightened responsiveness to opioids, potentially reducing the need for escalating doses, as observed in our study involving mice subjected to repeated YHS and morphine treatments.

Lastly, we found that YHS and MYHS treatment for 7 days also enhanced MOR expression in the amygdala and thalamus region when compared to 7 days of morphine treatment. The thalamus and amygdala hold pivotal roles in the context of morphine tolerance, with each playing a unique part in this phenomenon [131]. The thalamus is more directly

associated with the sensory and pain-related aspects of tolerance [132], while the amygdala plays a role in the emotional and memory-related components of opioid tolerance and dependence [128]. Studies have suggested that prolonged morphine use can induce alterations in how the thalamus perceives and interprets pain, potentially resulting in a diminished responsiveness to such signals over time [133, 134]. This decreased thalamic sensitivity contributes to the declining efficacy of morphine in alleviating pain as reported in previous studies [135, 136], and aligns with our reported data after 7 days of chronic morphine treatment. Conversely, the amygdala assumes a crucial role with the emotional facets of pain perception and the establishment of emotional associations linked to pain and drug usage [137]. In the context of morphine tolerance, the amygdala can contribute to the emotional dimensions of opioid withdrawal [138]. Moreover, the capacity of YHS to enhance MOR expression within both the amygdala and thalamus, juxtaposed with the decrease in MOR expression resulting from prolonged morphine use, implies the pivotal role these regions play in the tolerance development process. We hypothesize that YHS may expand the reservoir of accessible receptors within regionally specific sites, like the thalamus and amygdala; this expansion could potentially serve as a mechanism to mitigate the development of morphine tolerance.

Conclusions

In summary, morphine tolerance involves complex neural changes leading to reduced responsiveness to opioids, culminating in tolerance, dependence, and addiction. Although the specific brain regions driving these alterations remain unidentified, chronic opioid exposure necessitates higher doses for pleasurable effects, perpetuating drug use. Our study explores these changes, revealing increased MOR expression in certain regions with chronic morphine, and further enhancement with YHS treatment. This suggests YHS could mitigate tolerance by creating more binding sites for morphine. These findings provide valuable insights into the mechanisms of tolerance and offer potential avenues for managing opioid dependence, showcasing the promise of YHS in this regard. Additional investigations are imperative to provide conclusive evidence supporting the ability of YHS to enhance MOR expression in specific brain regions. Furthermore, these studies will be essential for establishing a direct correlation between the observed MOR expression increases and the underlying mechanisms contributing to tolerance development.

Supplementary Materials:

Suppl. 3.5

Section 1: Day 1

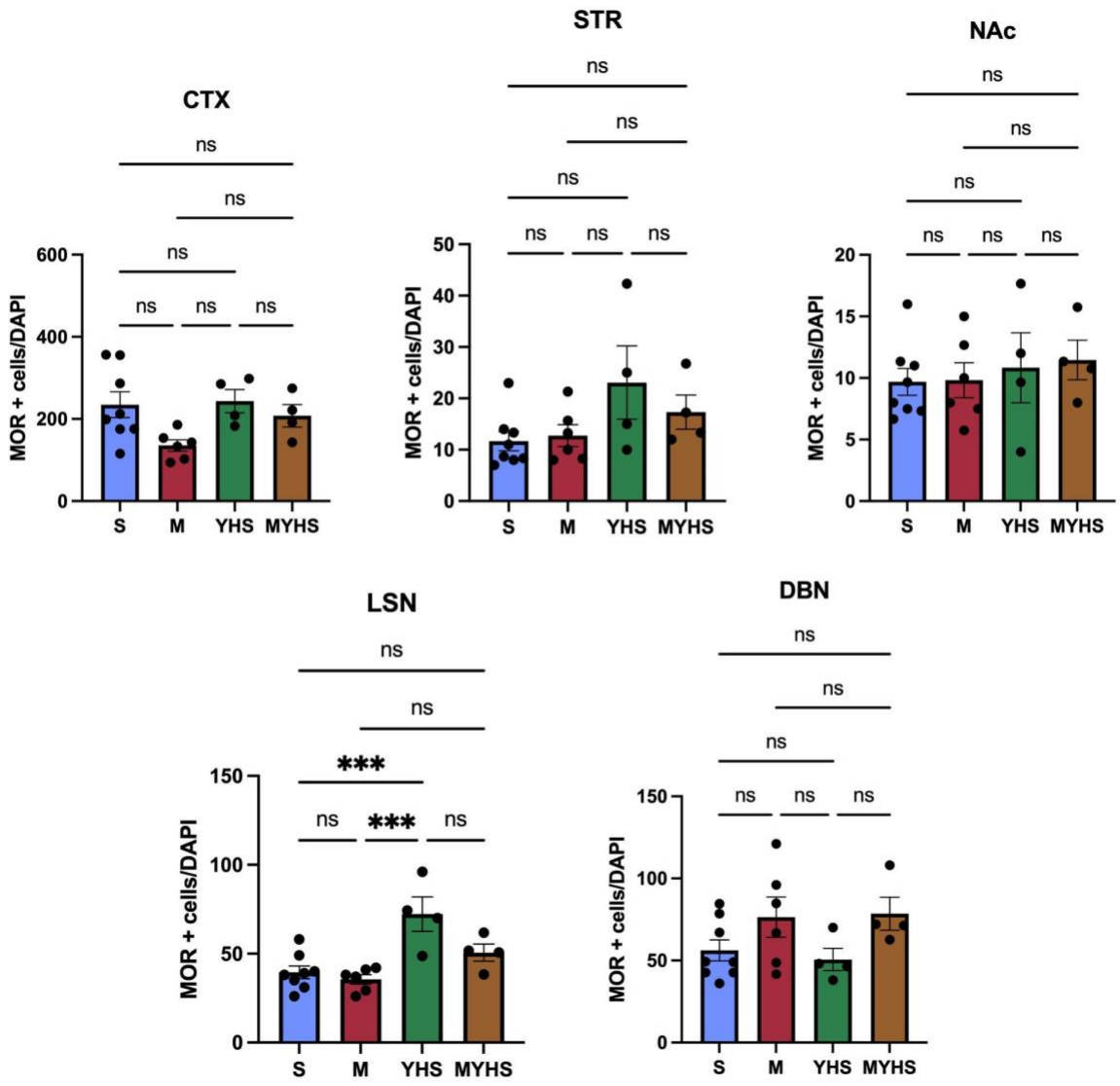

Section 1: Day 7

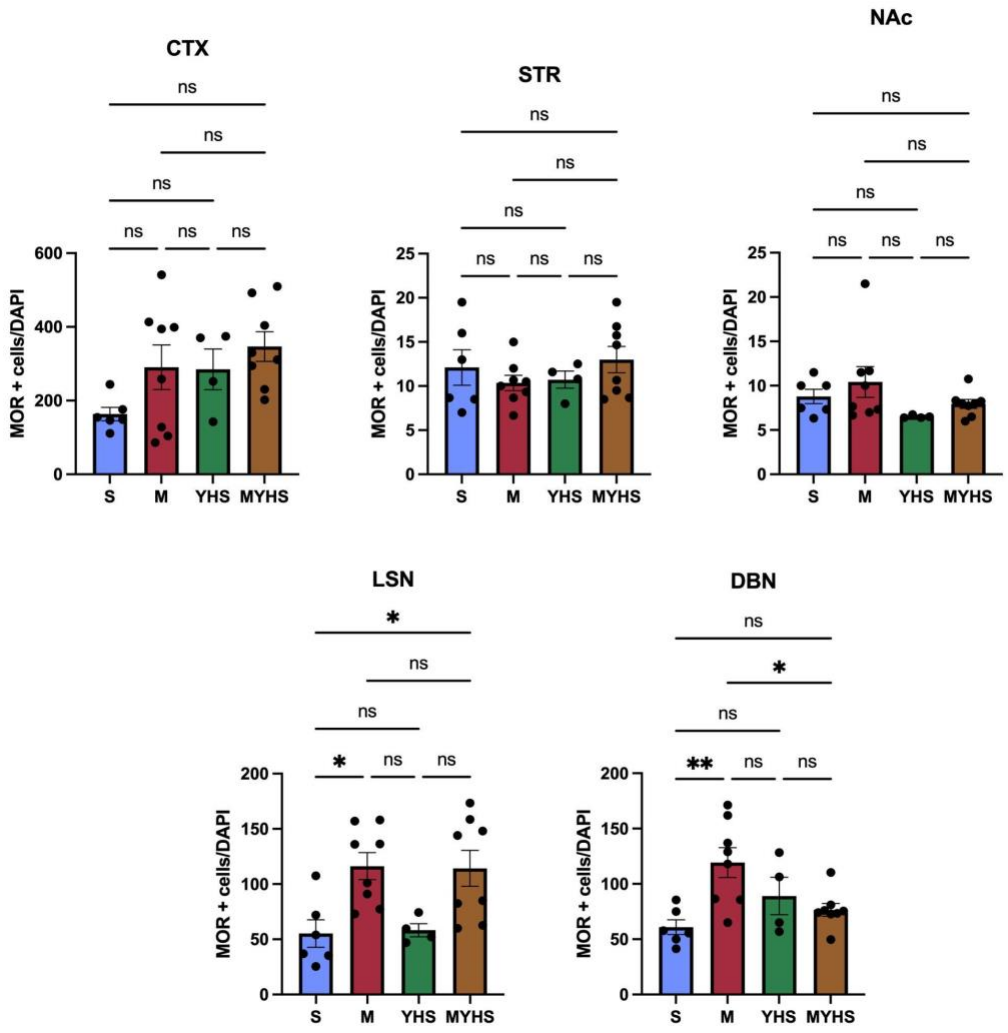

Suppl. 3.5 Day 1: Quantification of MOR+ cells/DAPI in the LSN after 1 day of S, M, YHS, and MYHS injection. One-way ANOVA followed by Tukey's multiple comparison test revealed significant drug effects in the LSN, F= 9.885, ***p<0.001 compared with YHS, M, S, n= 4-8. Quantification of MOR+ cells/DAPI in the CTS, STR, NAc, and DBN after 1 day of S, M, YHS, or MYHS injection. One-way ANOVA followed by Tukey's multiple comparison test revealed no significant drug effects on MOR expression. Day 7: Quantification of MOR+ cells/DAPI in the LSN and DBN region after 7 days of S, M, YHS, or MYHS injection. One-way ANOVA followed

by Tukey's multiple comparison test revealed significant drug effects in the LSN, F= 5.494, *p<0.05 compared with S, M, and MYHS, n= 4-8. One-way ANOVA followed by Tukey's multiple comparison test revealed significant drug effects in the DBN, F= 5.815, **p<0.01 compared with S and M, *p<0.05 compared with M and MYHS. Quantification of MOR+ cells/DAPI in the CTX, STR, and NAc after 7 days of S, M, YHS, and MYHS injection. One-way ANOVA followed by Tukey's multiple comparison test revealed no significant drug effects on MOR expression.

Suppl. 3.6
Section 2: Day 1

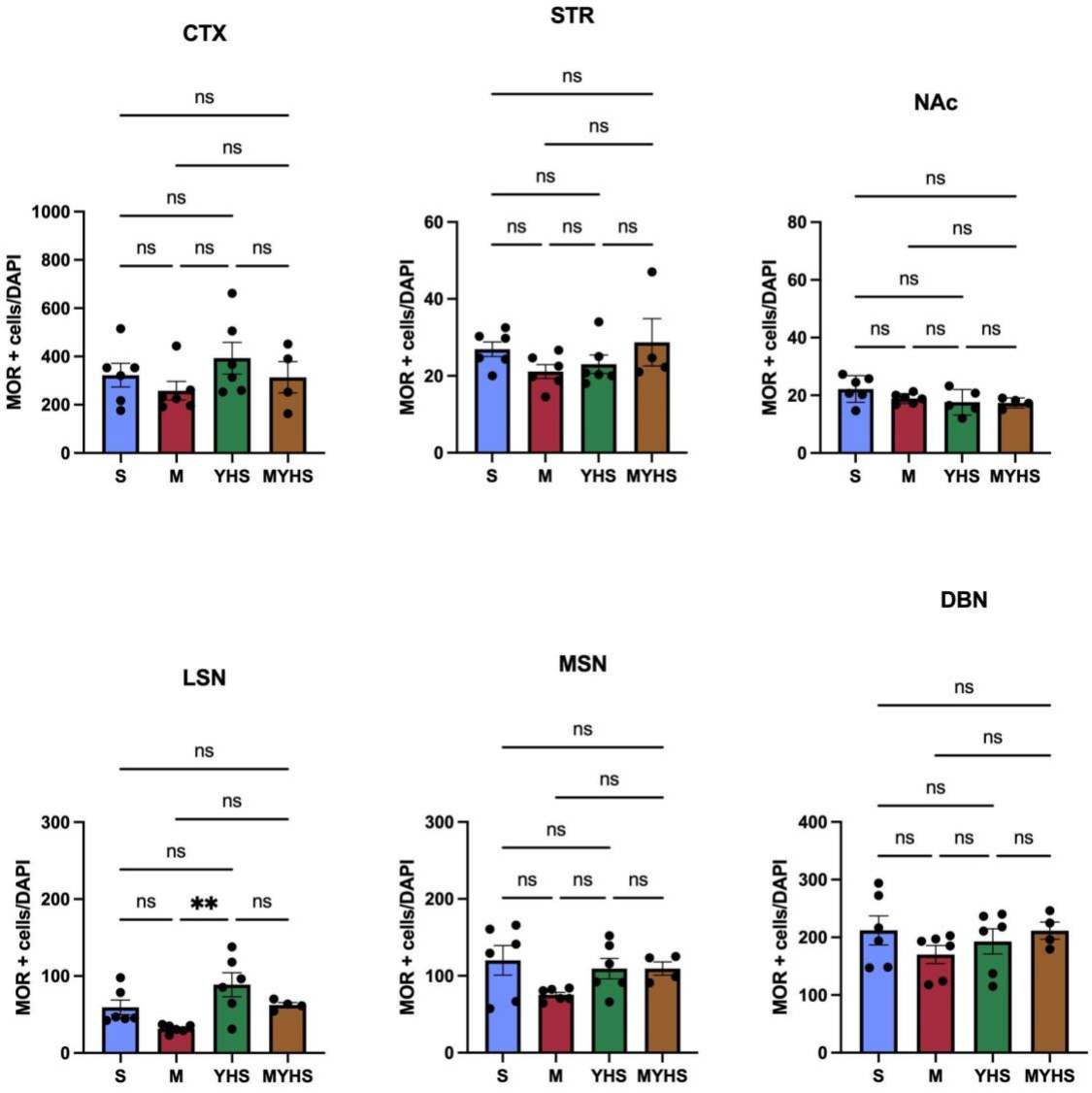

Section 2: Day 7

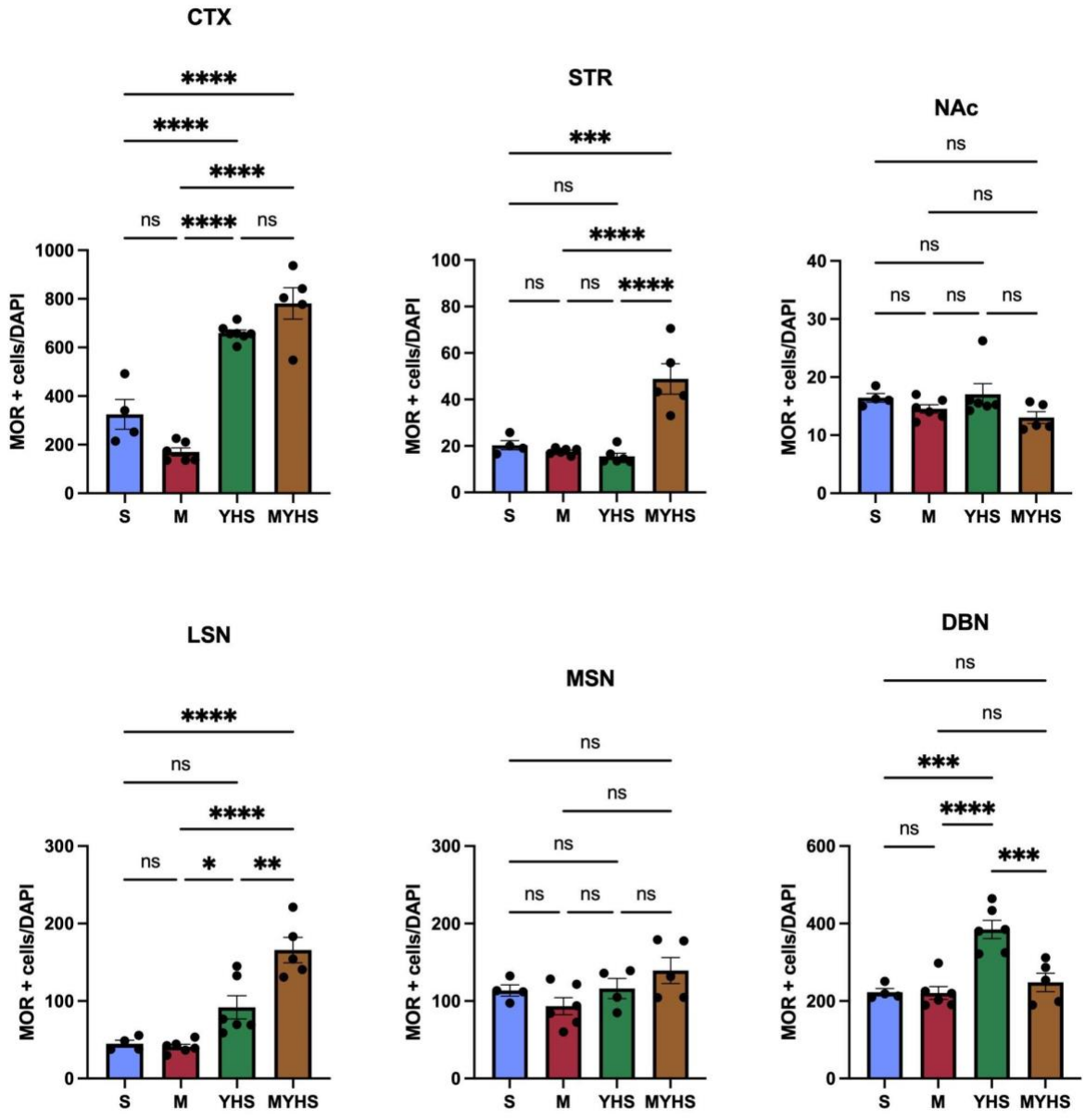

Suppl. 3.6 Day 1: Quantification of MOR+ cells/DAPI in the LSN after 1 day of S, M, YHS, and MYHS injection. One-way ANOVA followed by Tukey's multiple comparison test revealed significant drug effects in the lateral septal nucleus (rostral), F= 22.79, p**< 0.01 compared with M and YHS, n=4-6. Quantification of MOR+ cells/DAPI in the CTX, STR, NAc, MSN and DBN

after 1 day of S, M, YHS, or MYHS injection. One-way ANOVA followed by Tukey's multiple comparison test revealed no significant drug effects on MOR expression. Day 7: Quantification (right) of MOR+ cells/DAPI in the CTX. One-way ANOVA followed by Tukey's multiple comparison test revealed significant drug effects in the CTX, F= 56.30, ****p<0.0001 compared with S, M, YHS, and MYHS. Quantification of MOR+ cells/DAPI in the STR. One-way ANOVA followed by Tukey's multiple comparison test revealed significant drug effects in the F= 22.45, ****p<0.0001 compared with morphine, YHS, and M+YHS,***p<0.001 compared with S and MYHS. Quantification of MOR+ cells/DAPI in the LSN in mice following day 7 injection of S, M, YHS, and MYHS. One-way ANOVA followed by Tukey's multiple comparison test revealed significant drug effects in the LSN F= 22.79, ****p<0.0001 compared with S, M, and MYHS, **p<0.01 compared with YHS and M+YHS, *p<0.05 compared with M and YHS. Quantification of MOR+ cells/DAPI in the DBN in mice following day 7 injection of S, M, YHS, and MYHS. One-way ANOVA followed by Tukey's multiple comparison test revealed significant drug effects in the DBN, F= 15.99, ****p<0.001 compared with morphine and YHS, ***p<0.001 compared with S, YHS, and MYHS, n=4-6. Quantification of MOR+ cells/DAPI in the NAc and MSN after 7 days of S, M, YHS, or MYHS injection. One-way ANOVA followed by Tukey's multiple comparison test revealed no significant drug effects on MOR expression.

Suppl. 3.7
Section 3: Day 1

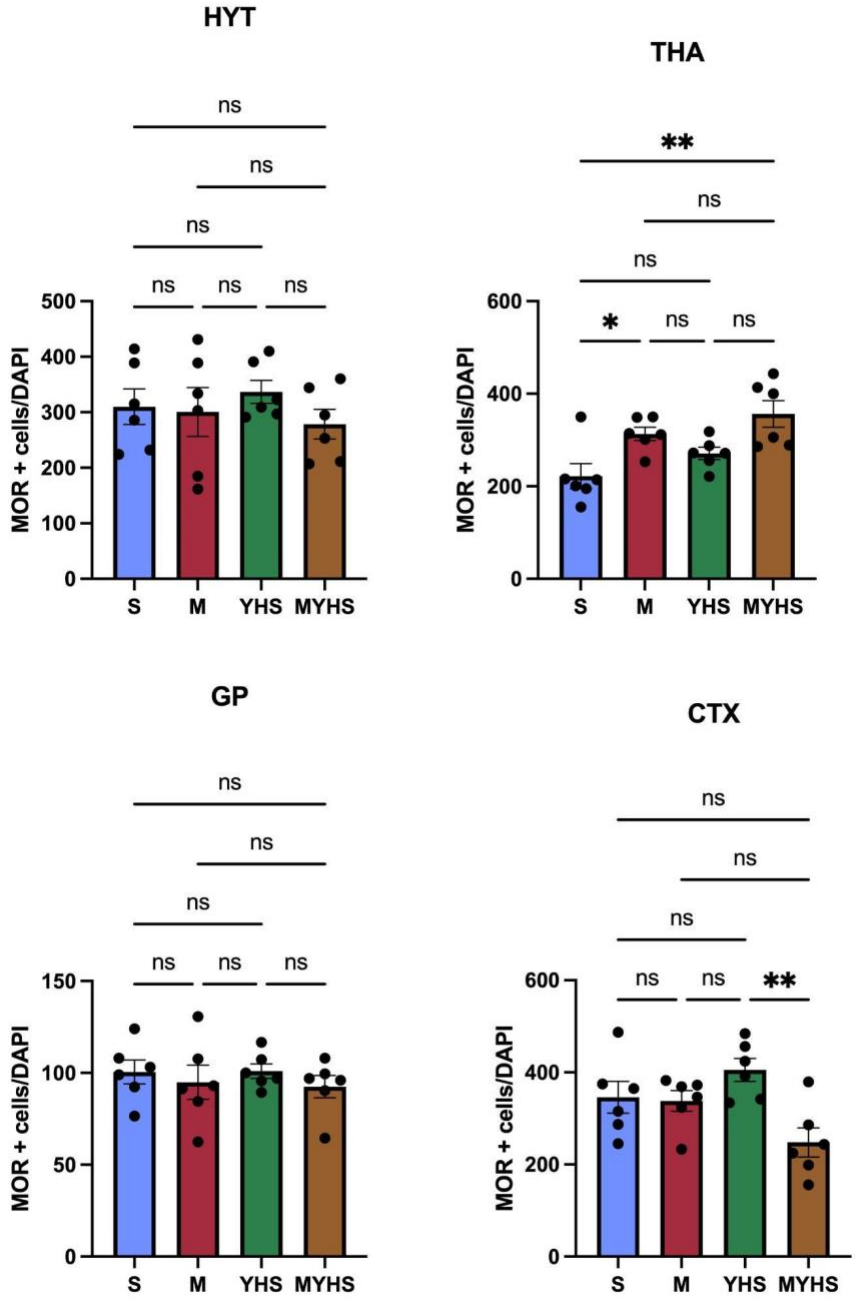

Section 3: Day 7

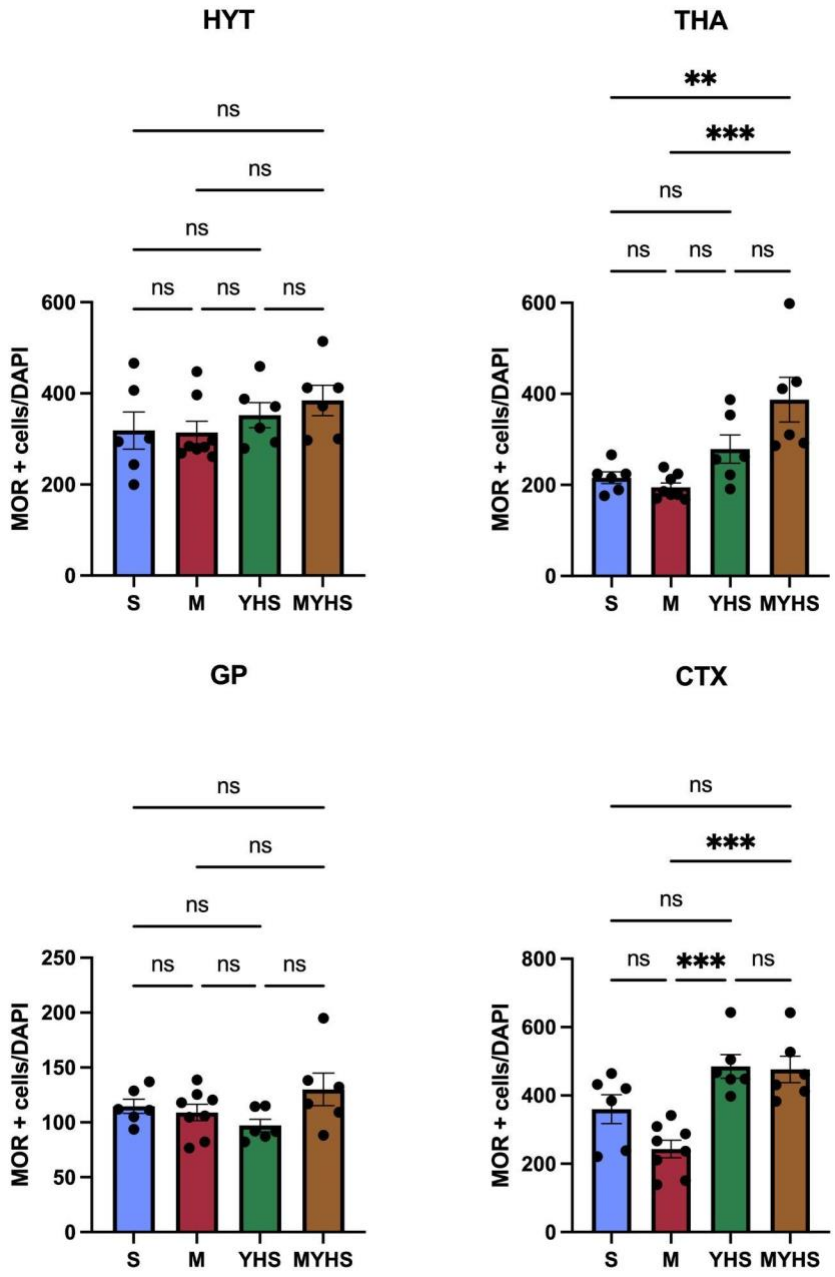

Suppl. 3.7 Day 1: Quantification of MOR+ cells/DAPI in the THA after 1 day of S, M, YHS, and MYHS injection One-way ANOVA followed by Tukey's multiple comparison test revealed significant drug effects in the THA, F= 6.761, p**< 0.01 compared with S and MYHS, *p<0.05

compared with S and M, n=6. Quantification of MOR+ cells/DAPI in the CTX after 1 day of S, M, YHS, and MYHS injection One-way ANOVA followed by Tukey's multiple comparison test revealed significant drug effects in the CTX, p**< 0.01 compared YHS and MYHS. Quantification of MOR+ cells/DAPI in the HYT and GP after 1 day of S, M, YHS, and MYHS injection. One-way ANOVA followed by Tukey's multiple comparison test revealed no significant drug effects on MOR expression. Day 7: Quantification of MOR+ cells/DAPI in the THA after 7 days of S, M, YHS, and MYHS injection. One-way ANOVA followed by Tukey's multiple comparison test revealed significant drug effects in the THA, F= 9.580,***p<0.001 compared with M and MYHS, p**< 0.01 compared with S and MYHS, n=6. Quantification of MOR+ cells/DAPI in the CTX after 7 days of S, M, YHS, and MYHS injection. One-way ANOVA followed by Tukey's multiple comparison test revealed significant drug effects in the CTX, F=11.65, ***p<0.001 compared with M, YHS, and mYHS. Quantification of MOR+ cells/DAPI in the HYT and GP after 7 days of S, M, YHS, and MYHS injection. One-way ANOVA followed by Tukey's multiple comparison test revealed no significant drug effects on MOR expression.

Suppl. 3.8
Section 4: Day 1

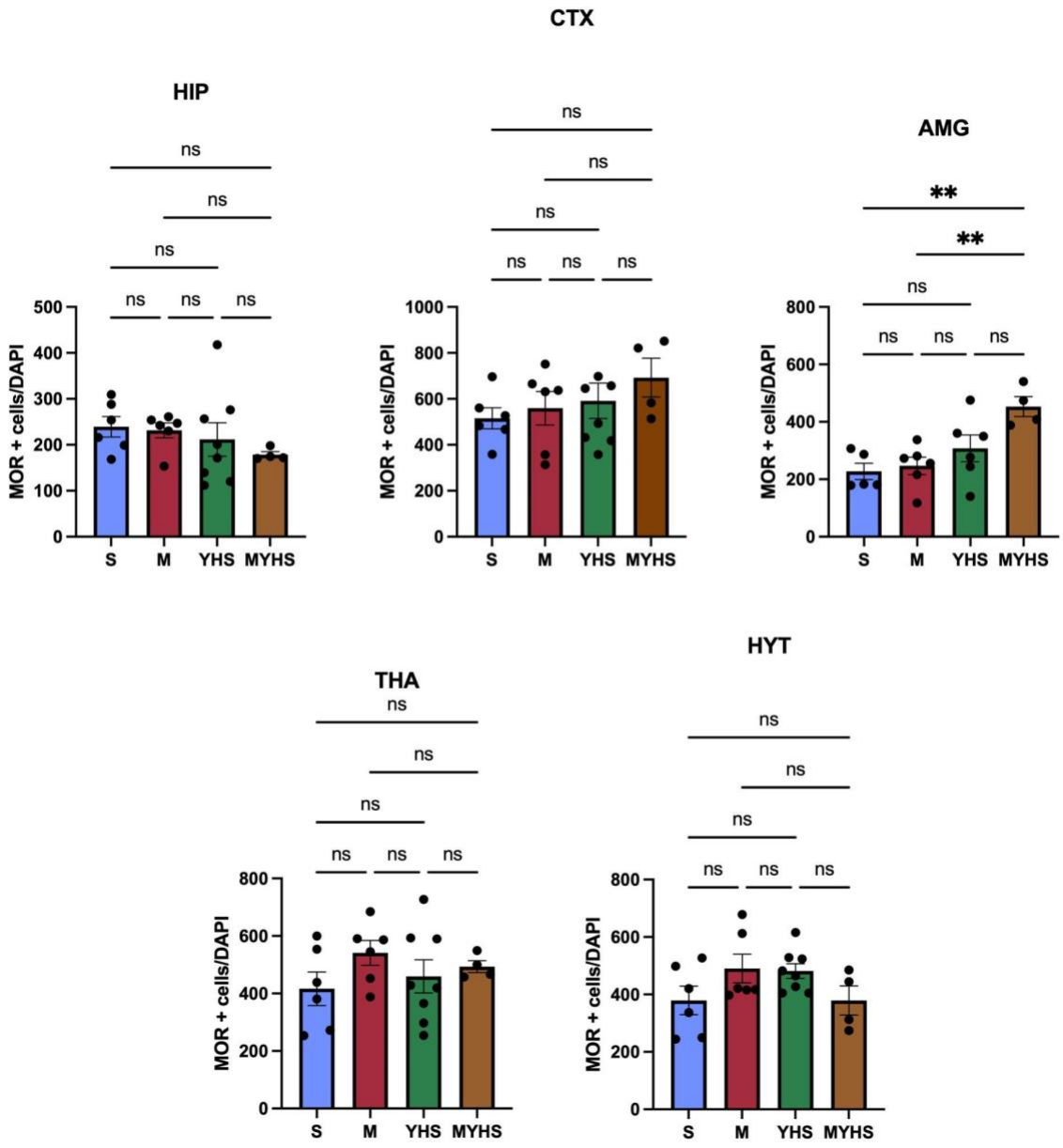

Section 4: Day 7

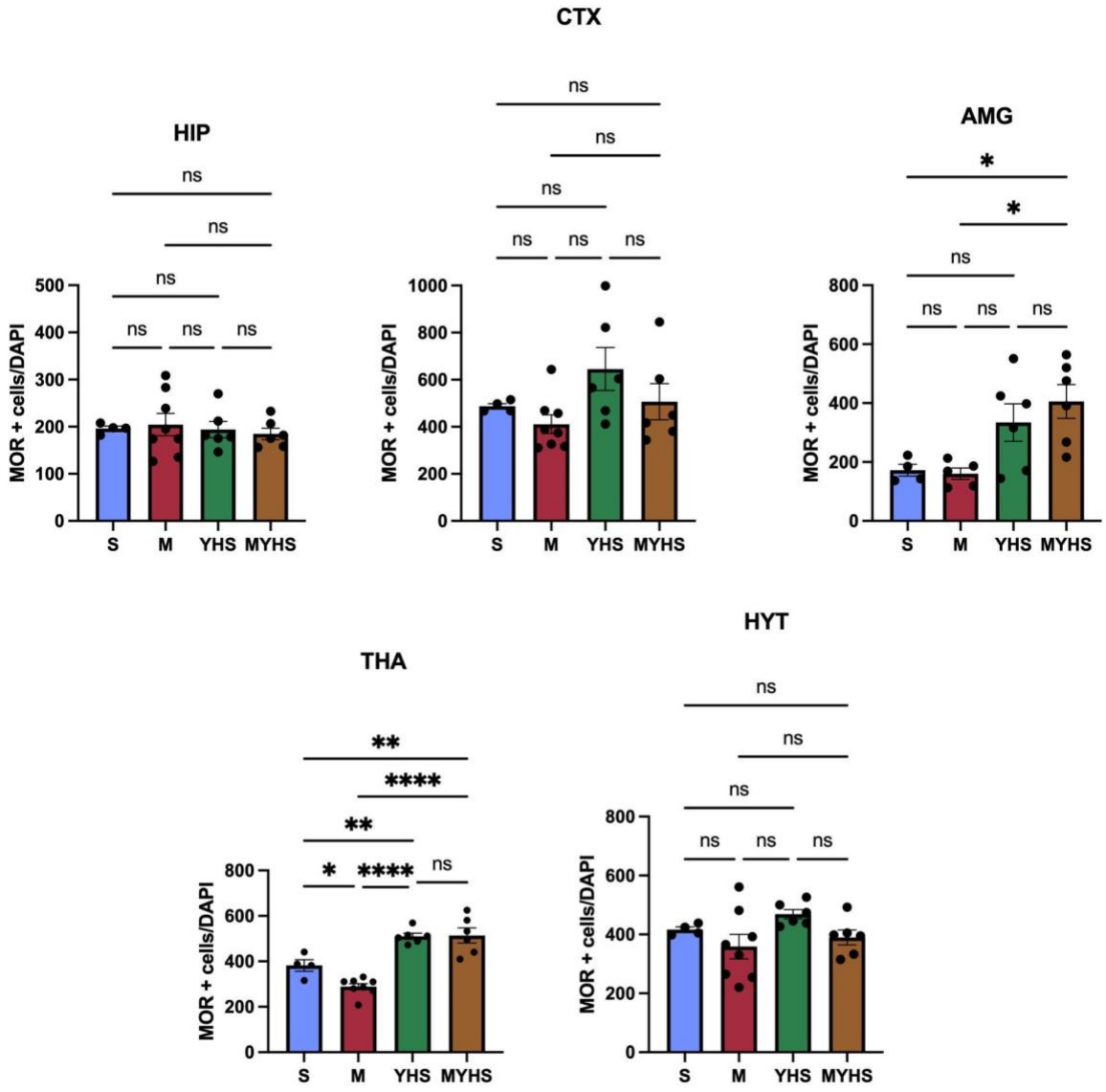

Suppl. 3.8. Day 1: Quantification of MOR+ cells/DAPI in the AMG after 1 day of S, M, YHS, and MYHS injection. One-way ANOVA followed by Tukey's multiple comparison test revealed significant drug effects in the AMG, F=6.262 ** $p<0.01$ compared with S, M, and MYHS. Quantification of MOR+ cells/DAPI in the CTX, HIP, THA, and HYT after 1 day of S, M, YHS, and MYHS injection. One-way ANOVA followed by Tukey's multiple comparison test revealed no significant drug effects on MOR expression, n=4-8. Day 7: Quantification of MOR+ cells/DAPI

in the AMG after 7 days of S, M, YHS, and MYHS injection. One-way ANOVA followed by Tukey's multiple comparison test revealed significant drug effects in the AMG, $F=5.612$, $*p<0.05$ compared with S, M, YHS, and MYHS, n= 4-6. Quantification of MOR+ cells/DAPI in the THA after 7 days of S, M, YHS, and MYHS injection. One-way ANOVA followed by Tukey's multiple comparison test revealed significant drug effects in the THA, $F= 28.45$, $****p<0.0001$ compared with M, YHS, and MYHS, $p**<0.01$ compared with S, YHS, and MYHS, $*p<0.05$ compared with S and M. Quantification of MOR+ cells/DAPI in the CTX, HYT, and HIP after 7 days of S, M, YHS, and MYHS injection. One-way ANOVA followed by Tukey's multiple comparison test revealed no significant drug effects on MOR expression, n= 4-6.

Suppl. 3.9
Section 5: Day 1

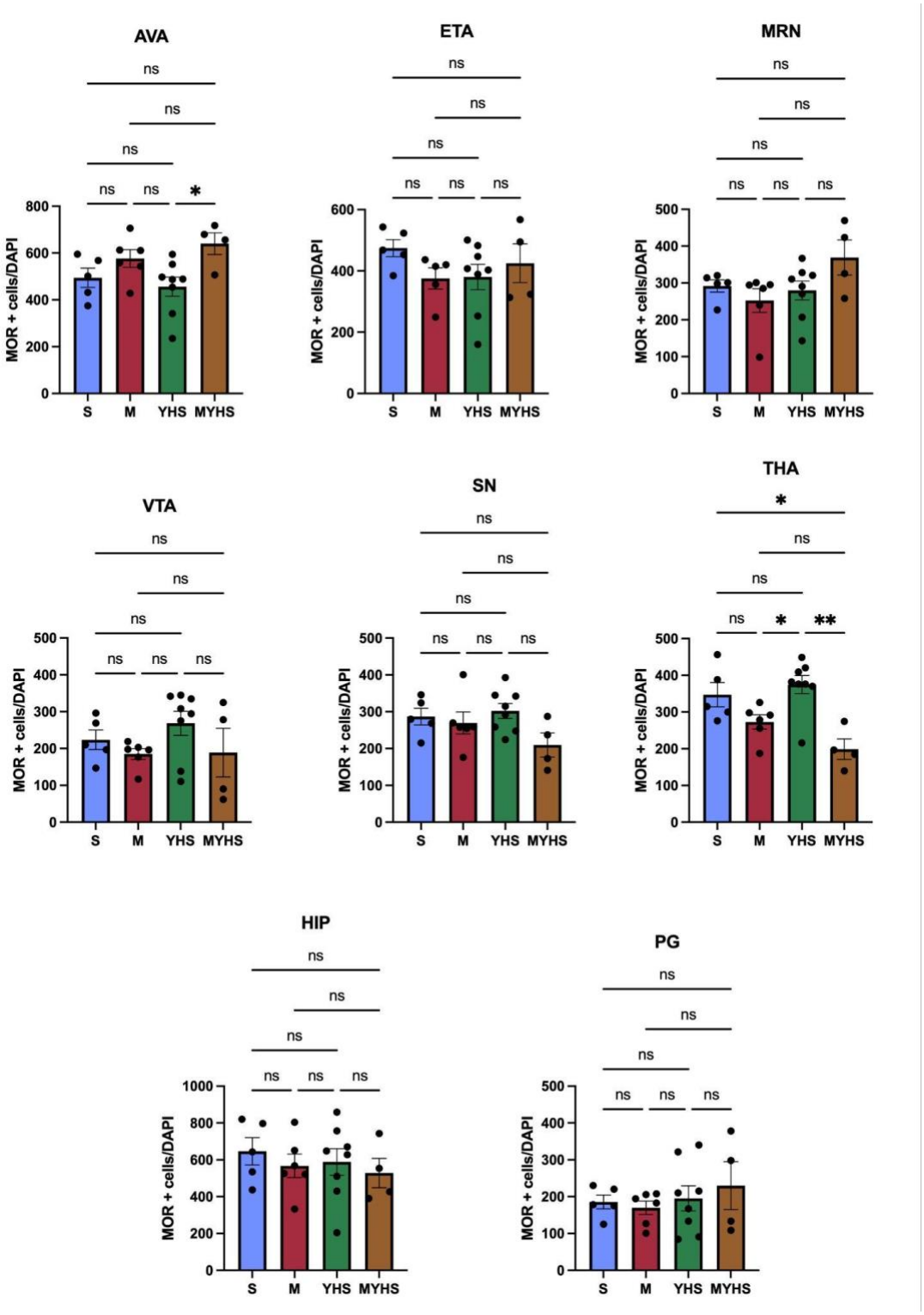

Section 5: Day 7

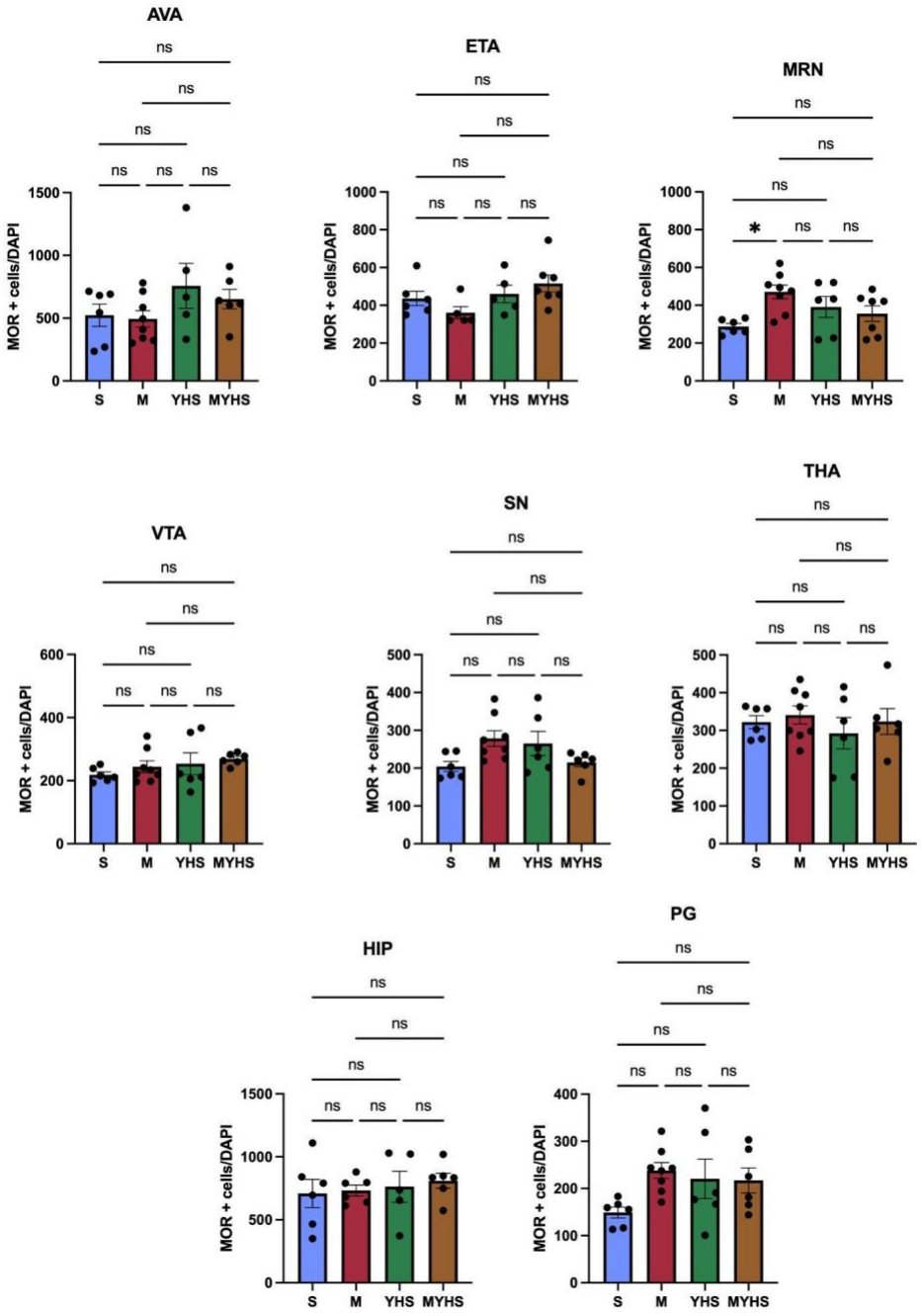

Suppl. 3.9 Day 1: Quantification of MOR+ cells/DAPI in the AVA after 1 day of S, M, YHS, and MYHS injection. One-way ANOVA followed by Tukey's multiple comparison test revealed

significant drug effects in the AVA, F= 3.597, *p<0.05 compared with YHS and MYHS, n= 4-8. Quantification of MOR+ cells/DAPI in the THA after 1 day of S, M, YHS, and MYHS injection. One-way ANOVA followed by Tukey's multiple comparison test revealed significant drug effects in the THA, F= 8.096, p**<0.01 compared with YHS and MYHS, *p<0.05 compared with S, M, YHS and MYHS, n= 4-8. Quantification of MOR+ cells/DAPI in the ETA, VTA, SN, MRN, HIP, and PG after 1 day of S, M, YHS, and MYHS injection. One-way ANOVA followed by Tukey's multiple comparison test revealed no significant drug effects on MOR expression, n= 4-8. Day 7: Quantification of MOR+ cells/DAPI in the MRN after 7 days of S, M, YHS, and MYHS injection. One-way ANOVA followed by Tukey's multiple comparison test revealed significant drug effects in the MRN, F= 3.774, *p<0.05 compared with S and M, n= 4-8. Quantification of MOR+ cells/DAPI in the ETA, VTA, SN, THA, HIP, and PG after 7 days of S, M, YHS, and MYHS injection. One-way ANOVA followed by Tukey's multiple comparison test revealed no significant drug effects on MOR expression.

Suppl. 3.10

A.

CTX-2

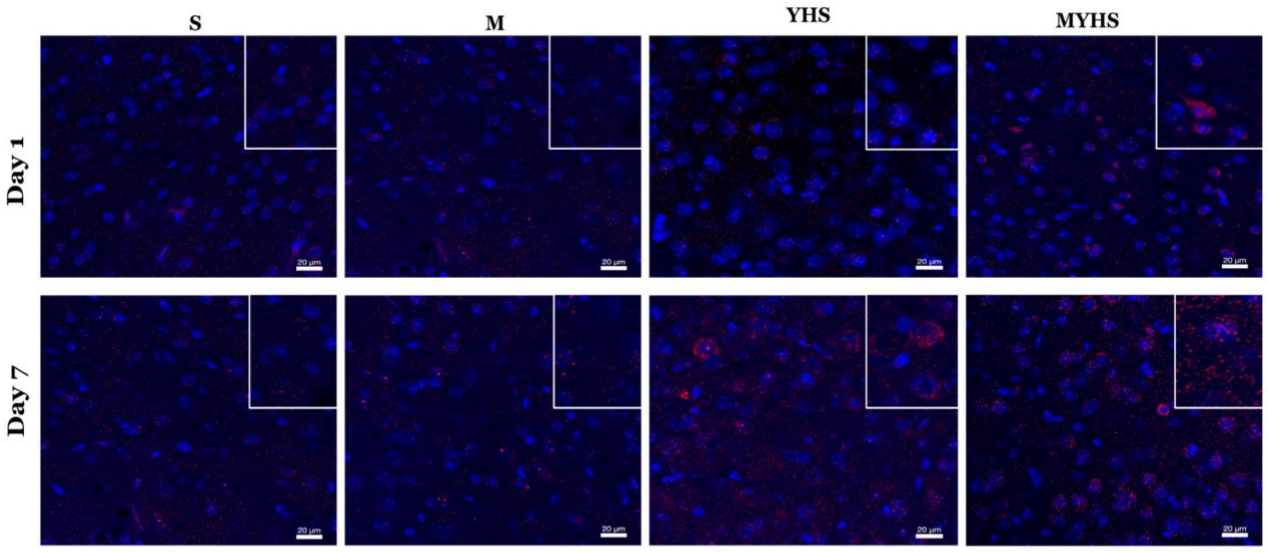

B.

AMG-4

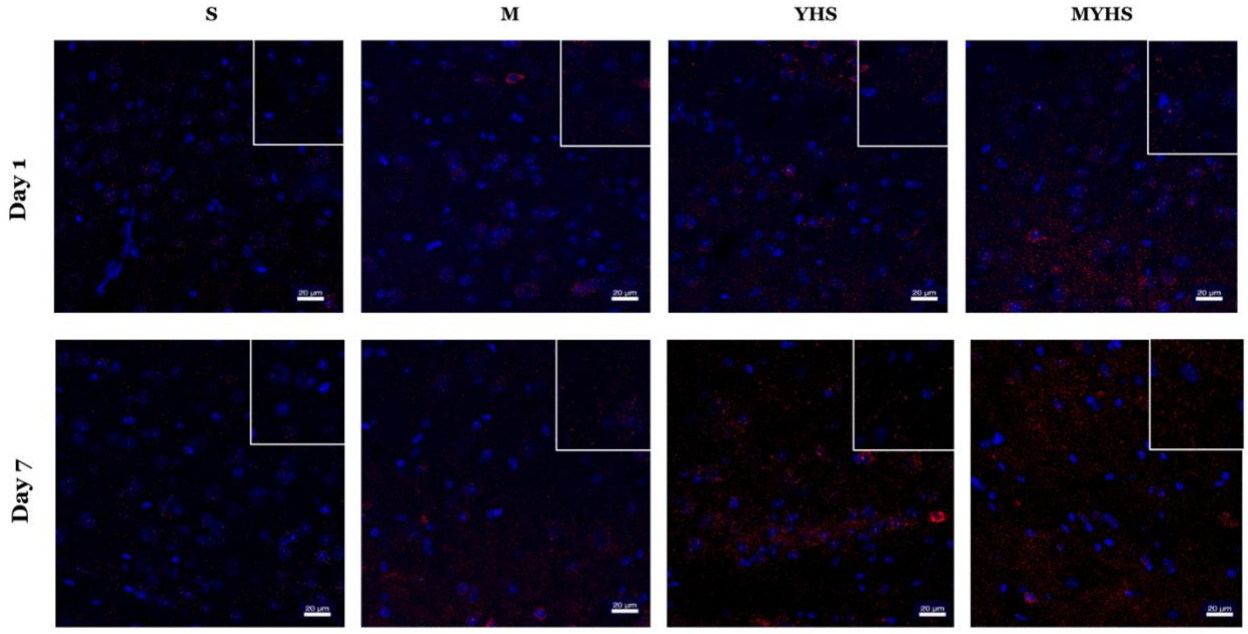

C.

THA-4

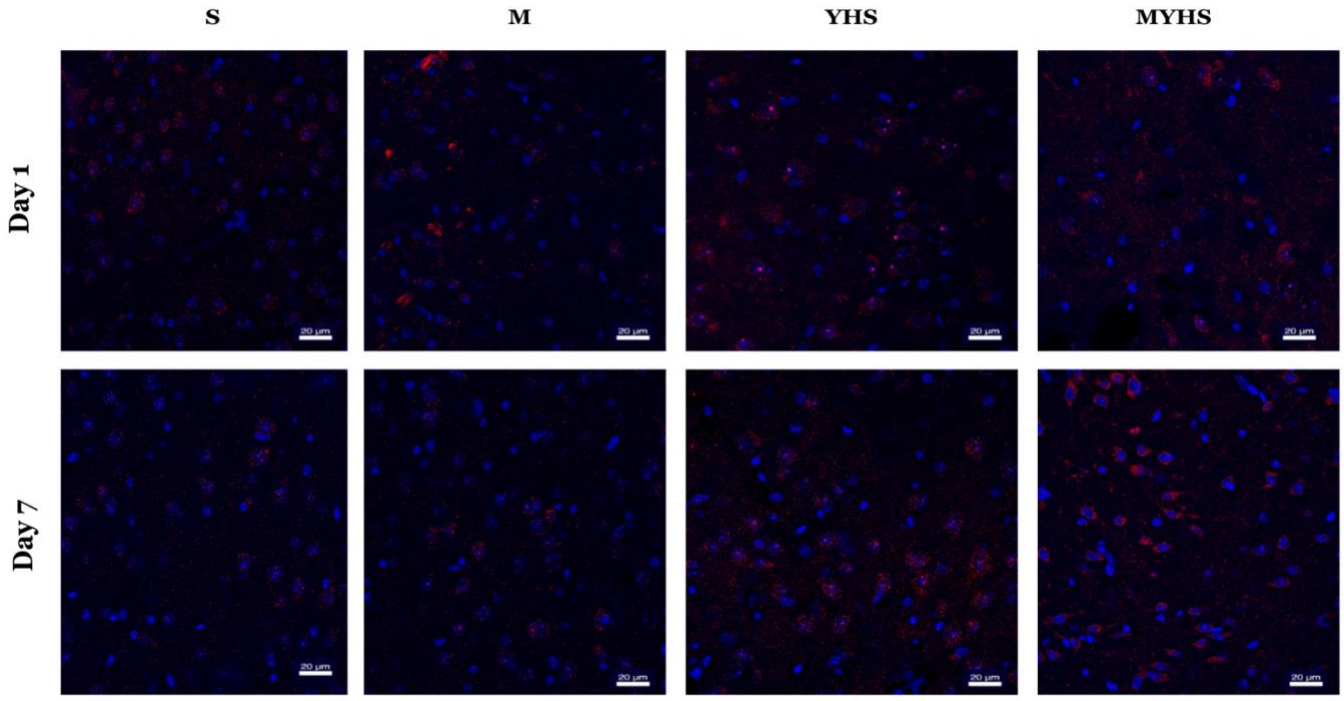

D.

LSN-2

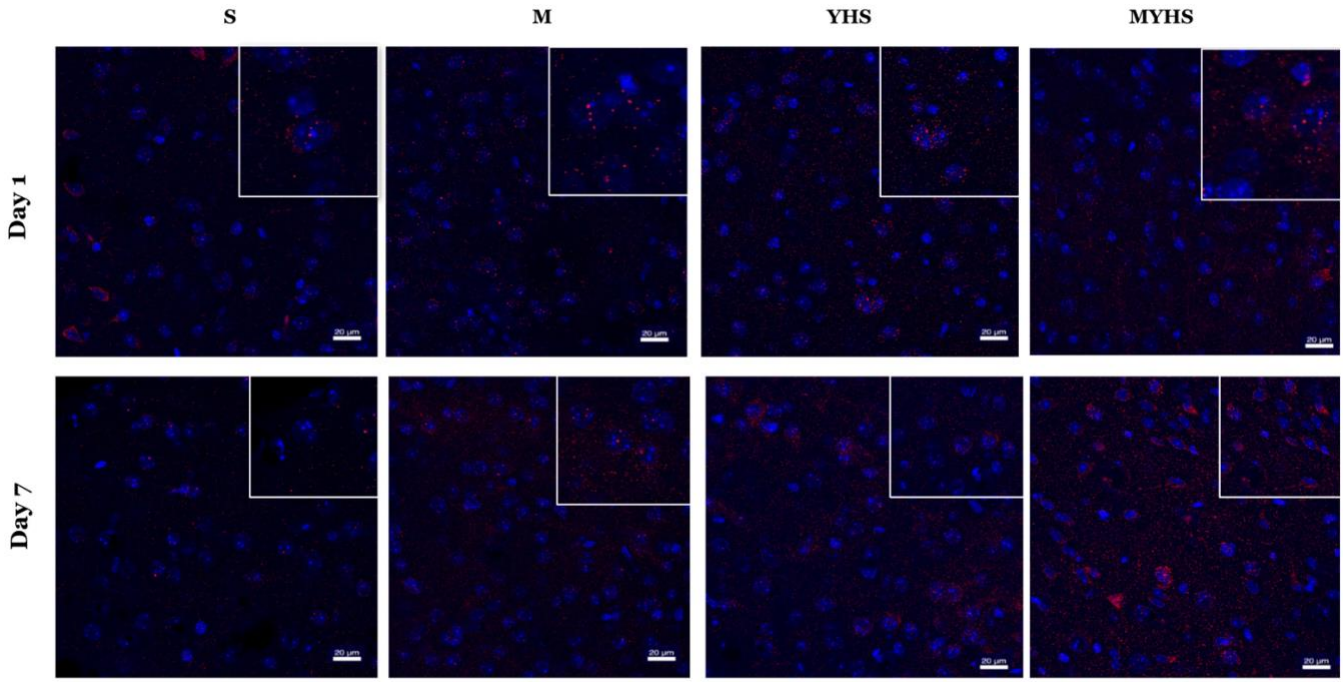

E.

STR-2

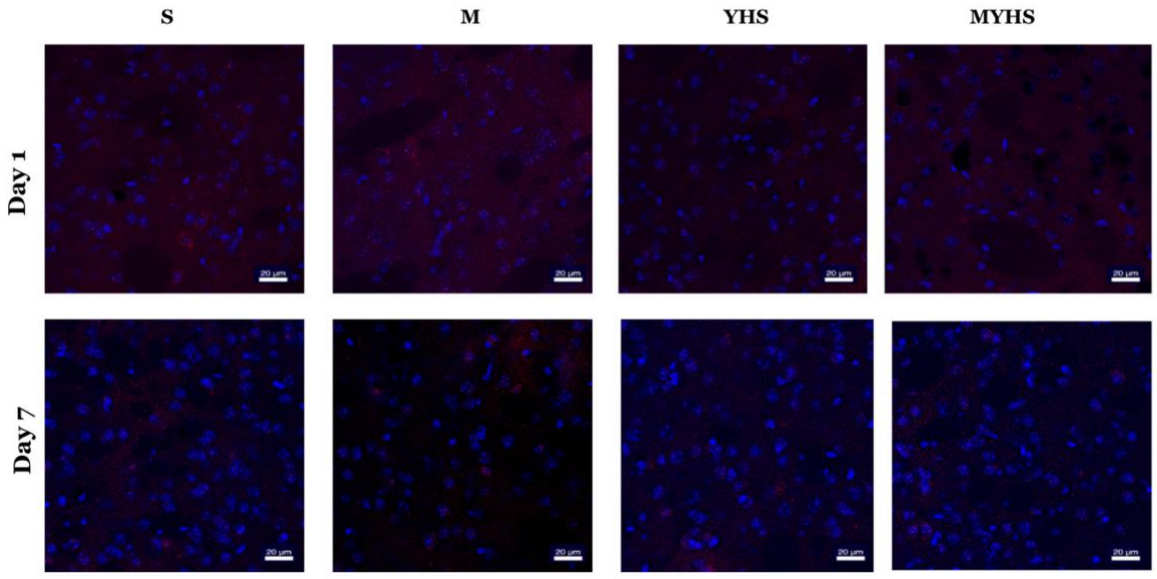

Suppl. 3.10

A. Representative images MOR+ cells (red) and DAPI (blue) at 40x objective following day 1 (top) and 7 days (bottom) injection of S, M, YHS, and MYHS in mice at CTX level 2. Scale bar=20 um. **B.** Representative images MOR+ cells (red) and DAPI (blue) at 40x objective following day 1 (top) and 7 days (bottom) injection of S, M, YHS, and MYHS in mice at AMG level 4. Scale bar=20 um. **C.** Representative images MOR+ cells (red) and DAPI (blue) at 40x objective following day 1 (top) and 7 days (bottom) injection of S, M, YHS, and MYHS in mice at THA level 4. Scale bar=20 um. **D.** Representative images MOR+ cells (red) and DAPI (blue) at 40x objective following day 1 (top) and 7 days (bottom) injection of S, M, YHS, and MYHS in mice at LSN level 2. Scale bar=20 um. **E.** Representative images MOR+ cells (red) and DAPI (blue) at 40x objective following day 1 (top) and 7 days (bottom) injection of S, M, YHS, and MYHS in mice at STR level 2. Scale bar=20 um.

Chapter 4: The active components in *Corydalis yanhusuo*

Abstract

The Corydalis yanhusuo extract (YHS), celebrated in traditional Chinese medicine for its analgesic properties, encompasses a diverse composition of over 160 compounds, including alkaloids, organic acids, volatile oils, amino acids, alcohols, and sugars. Noteworthy among these constituents are 81 protoberberine, apomorphine, opiate-like, and other alkaloids recognized as pivotal bioactive agents in YHS. Previous work in our laboratory demonstrated YHS's efficacy in mitigating morphine tolerance in mice, underscoring its potential in pain management. Additionally, we have identified and characterized dehydrocorybulbine (DHCB) through high-performance liquid chromatography (HPLC), highlighting its antinociceptive and dopamine receptor antagonistic activities. This current study utilizes HPLC to fractionate YHS, aiming to identify the specific components responsible for mitigating morphine tolerance. Fraction A emerges as a promising candidate, sustaining morphine's analgesic effects over an extended period. This comprehensive investigation enhances our understanding of YHS's therapeutic potential, paving the way for targeted interventions in pain management.

Introduction

Exploring the intricate mechanisms underlying the analgesic effects of Corydalis yanhusuo extract (YHS), particularly its capacity to alleviate morphine tolerance in mice, stands as a pivotal area of investigation, substantiated by our prior experimental findings [126]. Morphine, a cornerstone in pain management, often leads to the development of tolerance, necessitating higher doses for sustained efficacy [139]. This phenomenon poses challenges in clinical settings, as increased dosage may contribute to undesirable side effects and potential opioid dependence [140]. The imperative to address morphine tolerance and the growing need for alternative medicines in pain management underscore the significance of our inquiry into the multifaceted properties of YHS [140]. Acknowledging the complexity of YHS as an extract underscores the likelihood that its therapeutic efficacy may hinge on the synergistic interactions among a myriad of components.

To date, YHS has yielded over 160 isolated compounds, encompassing alkaloids, organic acids, volatile oils, amino acids, alcohols, and sugars [63]. Of these, alkaloids emerge as the most pivotal biological active constituents within YHS [63]. The spectrum of alkaloids extracted and identified from YHS surpasses 80, including tertiary amines, quaternary alkaloids, and various non-alkaloid compounds [63]. Despite this wealth of chemical diversity, a comprehensive review examining the phytochemical and pharmacological aspects of YHS, specifically in the context of its analgesic properties, is notably absent from the existing literature. Some components of YHS have been identified as protoberberine, apomorphine, opiate-like, and various alkaloids [62, 63, 141]. These constituents, subjected to pharmacological scrutiny, have exhibited notable interactions, including antagonism at dopamine receptors, agonism at opioid receptors, and inhibition of acetylcholinesterase activity, all occurring at concentrations in the high nanomolar or micromolar range [142].

Berberine stands as a well-established active constituent of YHS, recognized for its prominent analgesic contributions in various pathological pain conditions [143]. Belonging to the protoberberine alkaloid group, it has been demonstrated to exhibit robust analgesic efficacy [144]. A study delving into its impact on visceral pain revealed that the antinociceptive activity of berberine was effectively nullified through the administration of the opioid receptor antagonist naloxone or selective antagonists targeting mu and delta morphine receptors (MOR and DOR) [144]. These findings strongly indicate that the analgesic effects of berberine in visceral pain are likely attributed to its binding activities at MOR and DOR [143].

Palmatine, an isoquinoline alkaloid belonging to the protoberberine class and closely structurally related to berberine [145], exhibits a diverse range of beneficial activities, with a notable emphasis on its role in analgesia and anti-inflammation [146]. Investigations have revealed that palmatine effectively diminishes the levels of proinflammatory cytokines IL-6 and TNF-α in lipopolysaccharide (LPS)-induced murine macrophage-like cells and BALB/c mice [146]. Magnoflorine, also known as thalictrine and escholine, stands as an isoquinoline alkaloid featuring an aporphine configuration [147]. As a quaternary ammonium alkaloid, it typically exhibits solubility in water, methanol, and ethanol, while remaining insoluble in low-polar organic solvents such as petroleum ether and chloroform [147]. Notably, magnoflorine draws attention due to its structural resemblance to morphine and its potential association with analgesic properties [147]. A study has underscored its significance by demonstrating anti-inflammatory effects, particularly at higher doses [148]. This investigation further revealed its capacity to inhibit nitric oxide (NO) inflammation production and safeguard murine macrophage cells (RAW 264.7) from lipopolysaccharide-induced apoptosis [148].

Foremost among the elucidated YHS components is L-tetrahydropalmatine (L-THP),

constituting approximately 0.2% of the total dry mass of YHS [149]. L-THP boasts a multifaceted pharmacological profile, encompassing sedative, anti-epileptic, antidepressant, anxiolytic, and analgesic effects [150]. Its impact extends to the modulation of drug abuse-related behaviors, including attenuation of cocaine-associated reward, self-administration of cocaine, and recovery from cocaine-induced effects in rats [151, 152]. Furthermore, L-THP has proven effective in treating heroin withdrawal syndrome, significantly reducing cravings and withdrawal symptoms while enhancing abstinence rates in heroin addicts [153, 154]. While L-THP represents a significant component of YHS, questions persist about its ability to solely account for the observed effects, given its minute representation in typical YHS consumption (5–10 g per day) [64].

Another YHS constituent, dehydrocorybulbine (DHCB), has emerged as a potential contributor to YHS effects in models of drug addiction and analgesia [62,]. Following the synthesis of DHCB through reverse-phase high-performance liquid chromatography (HPLC), our lab has previously shown that it displays moderate antagonist activities towards dopamine receptors [62]. Utilizing selective pharmacological compounds and dopamine receptor knockout (KO) mice, we also showed that DHCB's antinociceptive effect is predominantly attributed to its interaction with D2 receptors, particularly evident at lower doses [62]. Furthermore, this study demonstrates the efficacy of DHCB in addressing inflammatory pain and injury-induced neuropathic pain, accompanied by the noteworthy observation that it does not induce antinociceptive tolerance [62].

It is noteworthy that a combination of L-THP and DHCB does not fully replicate the comprehensive analgesic effects of YHS, implying the involvement of additional, yet-to-be-discovered components [126]. This underscores the complexity of YHS's polypharmacological profiles and the imperative need for a detailed exploration of its chemical composition.

Through reverse-phase HPLC fractionation, our objective is to dissect YHS into its

constituent parts, elucidating their individual contributions, and potentially uncovering novel compounds responsible for the observed beneficial effects against morphine tolerance and dependence. In our initial findings, certain fractions, specifically B and C, displayed inherent tolerance effects, contrasting with the sustained analgesic effects observed in Fraction A. These unexpected results highlight the intricate interplay of YHS fractions and their diverse pharmacological profiles, reinforcing the need for a meticulous investigation into the active components contributing to the modulation of morphine tolerance. Notably, Fraction A has emerged as a promising candidate, demonstrating the ability to sustain morphine's analgesic effects over an extended period. This promising outcome positions Fraction A as a potential key player in reversing tolerance, prompting further fractionation and rigorous testing to isolate the active component(s) responsible for this. Further elucidation of YHS's intricate pharmacological profile could pave the way for novel and more effective pain management strategies.

Materials and Methods

Fractionation and Identification of Corydalis yanhusuo Extract Components Using Reverse Phase HPLC Technique

YHS was fractionated into various samples for assessment in mice tolerance assays, as previously detailed [126]. Reverse phase high-performance liquid chromatography (HPLC) was employed as a technique for the separation and identification of components in a mixture [62]. In the initial step of column chromatography, the mobile phase (the liquid containing the mixture) was passed through a stationary phase (a solid) packed in a column [62]. The components then traversed the solid phase at different rates, depending on the compound, allowing for their separation over time. Methanol/water was utilized as the mobile phase in reversed-phase chromatography [62]. Due to methanol's polar-protic nature, it increased the retention of hydrophobic compounds in the reversed phase [62].

The choice of the column in HPLC was crucial, as the physical and chemical characteristics of the specific column determined the degree of separation. In reverse-phase HPLC, where the mobile phase is hydrophilic and the stationary phase is hydrophobic, molecules were eluted by decreasing polarity through the use of an organic solvent. For the separation of YHS, a C18 column was employed [62]. All tested fractions were appropriately diluted based on the total mass collected during the HPLC process. Subsequently, individual fractions were subjected to testing in mice to observe their analgesic response. Following this initial assessment, morphine was administered alongside each individual fraction to monitor tolerance over a 7-day period. Fractions that successfully blocked morphine tolerance underwent further fractionation until single compounds (or compound combinations) were identified.

Animal Handling

Male CD-10 mice, aged 8 weeks and sourced from Charles River, were utilized in all behavioral experiments. The mice were group-housed and maintained under a 12-hour light/dark cycle, with access to food and water ad libitum. All procedures and treatments were ethically approved by the Institutional Animal Care and Use Committee of the University of California, Irvine (AUP #20-015). To ensure their well-being, animals were regularly weighed and observed post-injections. Any mice exhibiting signs of distress or abnormalities were excluded from the study.

Drug Administration
Morphine

Morphine injectable C II, obtained from Patterson Veterinary (concentration: 10 mg/mL, catalog number: 07-892-4699), was administered according to assigned groups and specific behavioral experiments. Morphine dosed at 2.5 mg/kg was intraperitoneally (i.p.) injected twice daily (morning and afternoon) for seven consecutive days, with a dosage of 5 μL/g based on the individual animal's body weight. The morning and afternoon injections were spaced approximately 10 hours apart.

Corydalis yanhusuo extract (YHS) and fractions

YHS was sourced from Dongyang County (Zhejiang, China) and validated by the Institute of Medication, Xiyuan Hospital of China Academy of Traditional Chinese Medicine, as detailed previously [126]. The introduction of YHS into the HPLC column resulted in the collection of various fractions (designated as A-E) using a fraction collector. In our prior mice experiments, YHS at a dose of 100 mg/kg was administered, and the dosages of the collected fractions were

calculated proportionally based on the percentage contribution of each fraction to the total weight of all fractions; the cumulative weight of the collected fractions amounted to approximately 77 mg. All fractions were diluted in a vehicle solution of cremophor EL: ethanol: saline (2:1:17).

Animal Grouping and Treatments

Mice were categorized into distinct groups: vehicle, Fraction A-E, morphine 2.5 mg/kg (M2.5), and the combination of Fractions A-E with M2.5. Drugs or vehicle were administered twice daily for seven days in the hot plate assay. Behavioral testing was conducted in accordance with the models explained below.

Behavioral Assessments

Tolerance Assay

Mice received injections twice daily, and the hot plate assay was conducted on day 7 to assess tolerance-like behavior. FWL on the hotplate was measured at 30, 60, and 120 minutes after injections. Responses on Day 1 and Day 7 were compared to observe any tolerance to the administered drugs.

Statistical analysis

GraphPad Prism (GraphPad Software, Inc., San Diego, CA, USA) was used for statistical analysis, and all data are presented as mean ± standard error mean (SEM). One-way ANOVA followed by Tukey's post-test was used to analyze the data in this paper.

Results

Fractionation of YHS was achieved through reverse phase chromatography. Figure 1 illustrates the methodology for reversed phase high-performance liquid chromatography (HPLC). Briefly, YHS is injected into the stationary phase (labeled HPLC column).The liquid phase is propelled through the column by a binary gradient, meticulously regulated by two pumps, operating under high pressure. As the constituents within YHS traverse the solid phase, they exhibit distinct rates of movement, facilitated by the unique characteristics of each compound. This differential migration enables the temporal separation of the components. Upon exiting the column, the individual components encounter an ultraviolet detector, which quantifies their presence. The detector output is subsequently transmitted to a computer system, where it is processed to generate a chromatogram, providing a visual representation of the separated components in YHS.

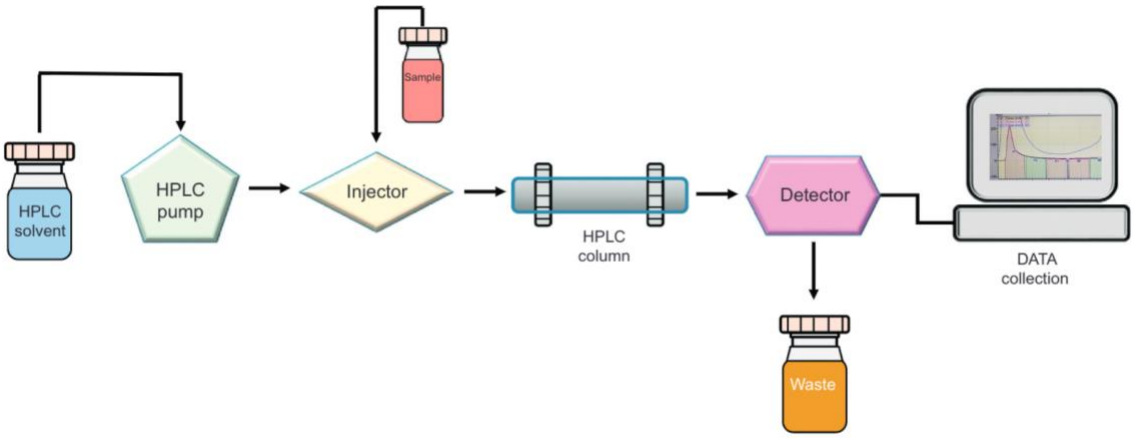

Figure 4.1 Methodology of reverse phase high performance liquid chromatography of. YHS undergoing separation within the stationary phase of the HPLC column, driven by a binary gradient

under high pressure. As individual components traverse the solid phase at varying rates, the ultraviolet detector captures their presence, producing a chromatogram for detailed analysis.

The fractionation process of YHS resulted in the generation of 5 discernible fractions designated as A, B, C, D and E. The chromatogram of YHS presented in Figure 4.2 displays absorbance and retention time over a 5-minute period. Retention time, defined as the interval between sample injection and the detection of substances, is a crucial parameter for characterizing the separated components. The chromatogram highlights different wavelengths, color-coded for clarity, with specific attention directed towards the absorbance at 254 nm represented by the black line (Figure 2). This wavelength was selected due to its relevance to our research focus on alkaloids and aromatic rings. Conversely, other wavelengths, such as 210 nm, exhibit broad absorbance characteristics, including methanol, while the 280 nm wavelength is more sensitive to conjugated compounds. Conjugated compounds are characterized by alternating single and multiple bonds, exemplified by compounds possessing two aromatic rings. Five distinct pools, designated as Fractions A, B, C, D, and F, were successfully isolated through this chromatographic process (Figure 4.2). These fractions have been earmarked for further in vivo testing.

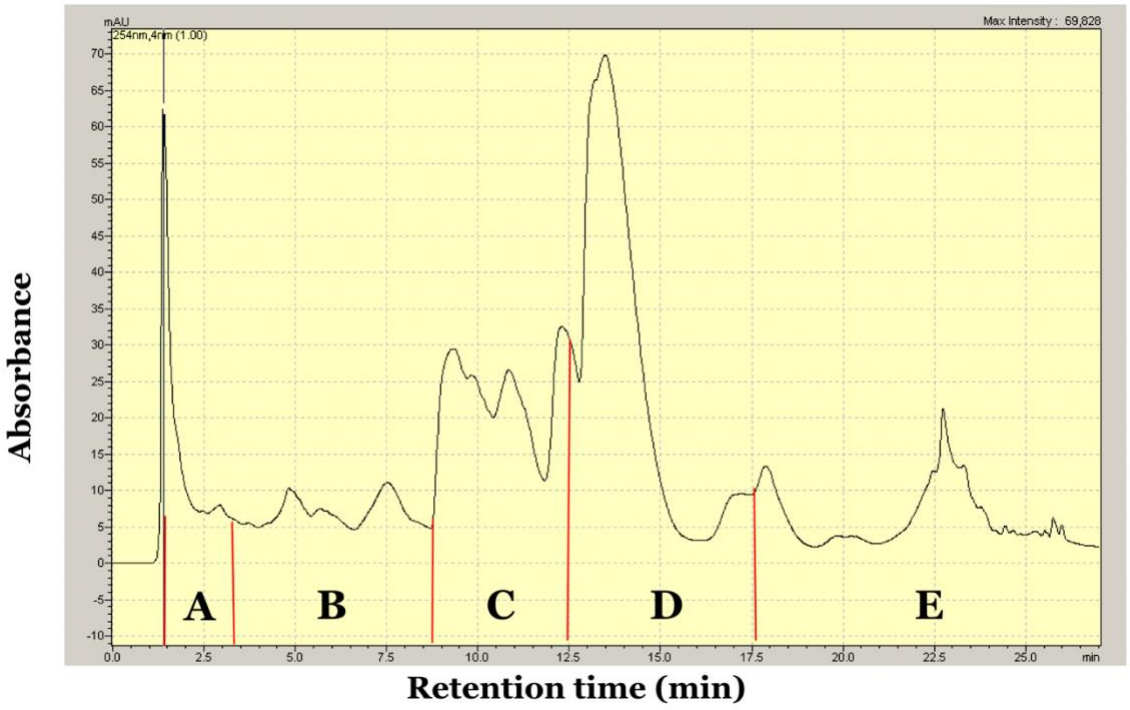

Figure 4.2 Chromatogram of YHS. The graph depicts absorbance and retention time (min) dynamics over a 25-minute period. Notably, the absorbance at 254 nm (represented by the black line) is of particular significance, aligning with our focus on alkaloids and aromatic rings. Five distinct fractions (A, B, C, D, and E) were successfully isolated for further in vivo testing, showcasing the effectiveness of the chromatographic process.

Two sets of mouse cohorts underwent evaluation through the hot plate assay. The first cohort received injections of Fractions A, B, C, D, and E individually and underwent tests for analgesia and tolerance over a 7-day period. Figure 4.3 illustrates the analgesic effects of Fractions A, B, C, D, and E administered alone for 7 days (D), with the vehicle serving as the control. FWL was determined 30 minutes after injections. Fractions B, C, and D demonstrated some analgesic effects, while other fractions either exhibited minimal effects or none at all in comparison to the vehicle.

Fractions B and C when administered independently displayed some tolerance effects throughout the days. However, all other fractions did not manifest any significant tolerance effects.

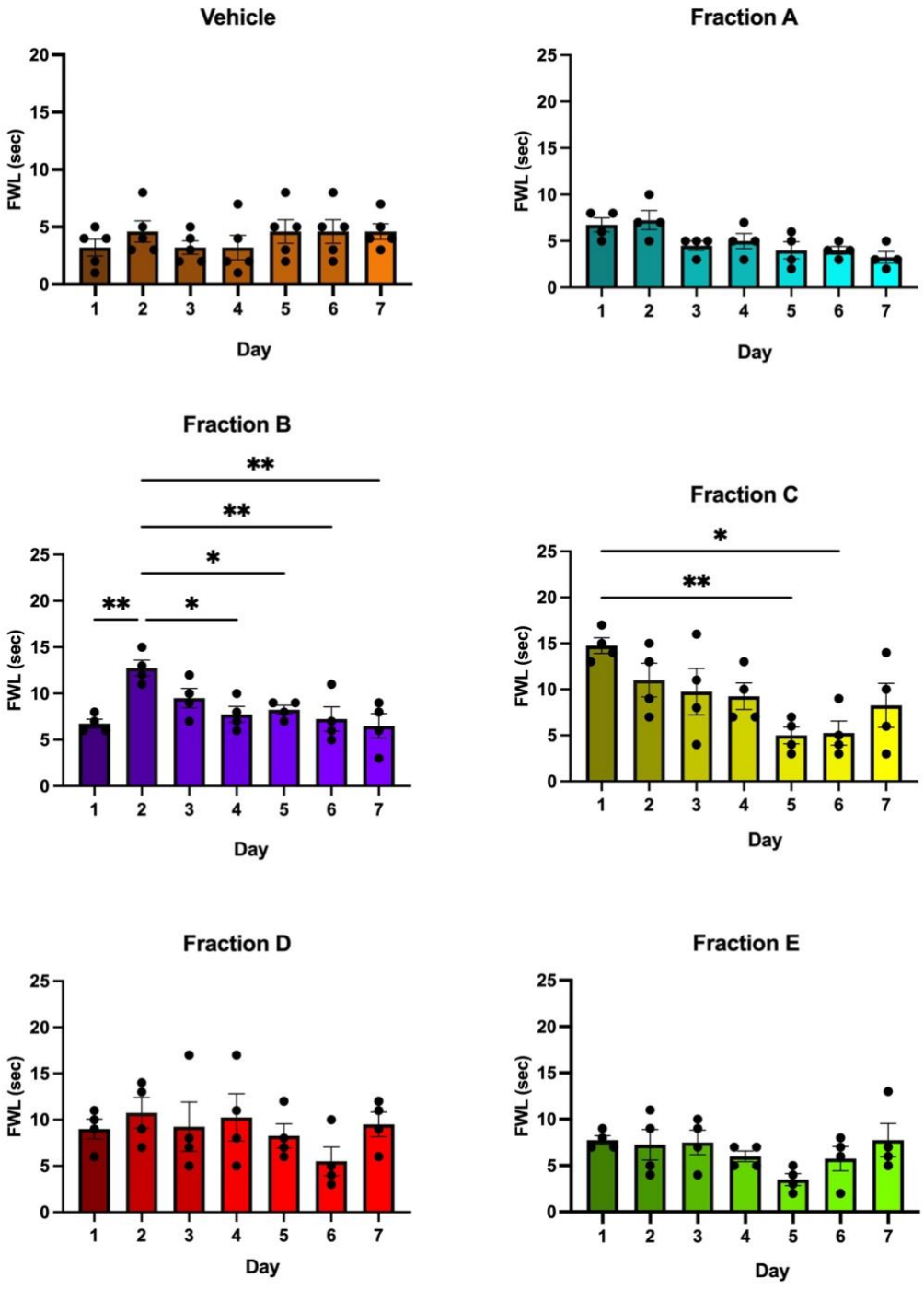

Figure 4.3. Analgesic and tolerance profiles of fractions A, B, C, D and E in mice. FWL at 30 min after treatment with Fraction A, B, C, D, and E (i.p. administration) over a period of 7 days (D) (n = 4-5) to display analgesia and tolerance. One-way ANOVA followed by Tukey's test revealed significant drug tolerance over 7 days after Fraction B administration F= 5.084, $^{**}p < 0.01$ compared with D1, D2, D6, D7, $^{*}p < 0.05$ compared with D2, D3, and D5. One-way ANOVA followed by Tukey's test revealed significant drug tolerance over 7 days after Fraction C administration F= 3.829, $^{**}p < 0.01$compared with D1 and D5, $^{*}p < 0.05$ compared with D1 and D6. All other fractions displayed no significant drug effects.

The second cohort of mice underwent a comprehensive evaluation, receiving combined administrations of Fractions A, B, C, D, and E with morphine, as well as morphine alone, spanning a duration of 7 days. This experimental design aimed to scrutinize the potential reversal of tolerance. Figure 4.4 presents a detailed depiction of the responses exhibited by each fraction when administered with morphine for the reversal of tolerance. Notably, Fractions C, D, and E demonstrated pronounced tolerance effects throughout the 7-day period, while Fractions A and B did not exhibit comparable effects.

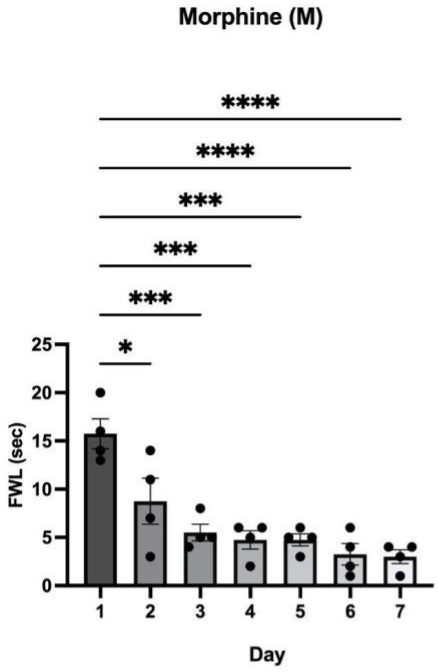
Morphine (M)
****
****
***
***
***
*
FWL (sec)
25
20
15
10
5
0
1
2
3
4
5
6
7
Day

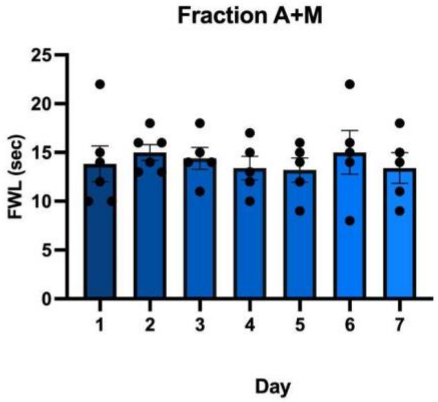
Fraction A+M
FWL (sec)
25
20
15
10
5
0
1
2
3
4
5
6
7
Day

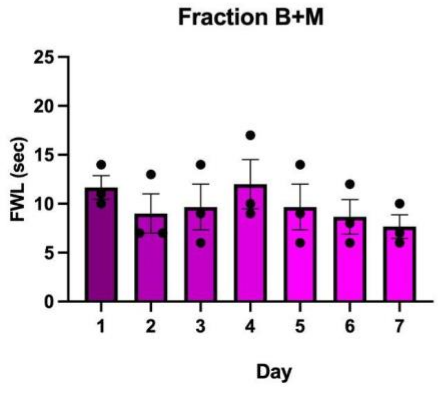
Fraction B+M
FWL (sec)
25
20
15
10
5
0
1
2
3
4
5
6
7
Day

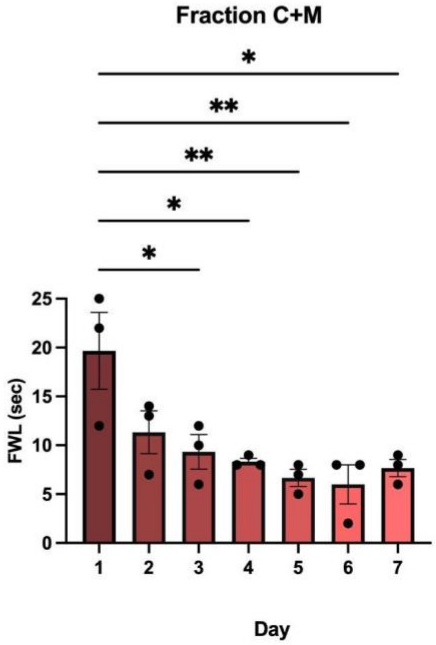
Fraction C+M
*
**
**
*
*
FWL (sec)
25
20
15
10
5
0
1
2
3
4
5
6
7
Day

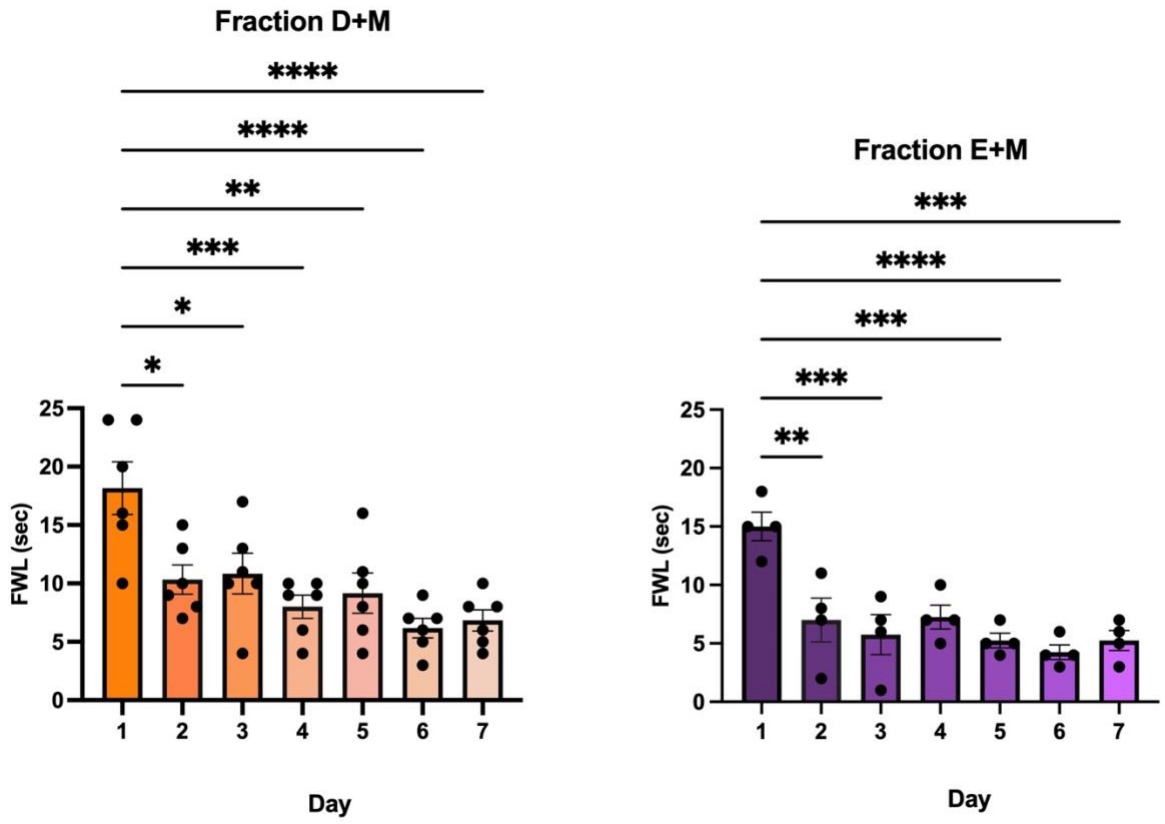

Figure 4.4 Analgesic and tolerance profiles of fractions A, B, C, D and E in combination with morphine in mice. FWL at 30 min after treatment with Fraction A, B, C, D, and E with morphine (i.p. administration) over a period of 7 days (D) (n = 4-6) to display reversal of tolerance. One-way ANOVA followed by Tukey's test revealed significant drug tolerance over 7 days after morphine administration, F=11.82, ****p<0.0001 compared with D1, D6, and D7, ***p<0.001 compared with D1, D3, D4, and D5, *p<0.05 compared with D1 and D2. One-way ANOVA followed by Tukey's test revealed significant drug tolerance over 7 days after Fraction C+M administration, F=8.252, ***p<0.001 compared with D1, D4, D5, and D6, ** p<0.01 compared with D1, D3, and D7. One-way ANOVA followed by Tukey's test revealed significant drug tolerance over 7 days after Fraction D+ M administration, F=7.444, ****p<0.0001 compared D1, D6, and D7, ***p<0.001 compared with D1 and D4, ** p<0.01 compared with D1 and D5,

*p<0.05 compared with D1, D2, and D3. One-way ANOVA followed by Tukey's test revealed significant drug tolerance over 7 days after Fraction E+ M administration, F= 8.821, ****p<0.0001 compared with D1 and D6, ***p<0.001 compared with D1, D3, D5, and D7, ** p<0.01 compared with D1 and D2. Fractions A+M and B+M displayed no significant drug effects.

Discussion

In our investigation, we sought to delineate the specific components of the YHS extract responsible for reversing morphine tolerance. Initially, we fractionated YHS into distinct fractions and subjected them to in vivo testing in mice using a hot plate assay over a 7-day period as previously described [126]. Given our prior evidence indicating that the combination of YHS and morphine effectively blocked morphine tolerance, we aimed to identify which fractions could individually reverse this tolerance [126].

Surprisingly, our results revealed that some fractions, namely Fraction B and C, exhibited tolerance effects on their own. This observation prompted us to hypothesize that the component responsible for blocking morphine tolerance might reside in a fraction distinct from those exhibiting inherent tolerance. Notably, Fraction A, D, and E did not induce tolerance when administered alone. Furthermore, our assessment of analgesic responses demonstrated that certain fractions, such as A and F, did not elicit significant analgesic effects, while B, C, and D exhibited heightened responses compared to our control. This discrepancy in analgesic efficacy prompted us to investigate the interactive effects of each fraction when combined with morphine.

Combining morphine with all fractions and testing them in mice over 7 days, alongside administering morphine alone, revealed intriguing findings. Fractions C, D, and E, when combined with morphine, failed to reverse morphine tolerance. Conversely, Fraction B, while not exhibiting inherent tolerance effects, did not enhance the analgesic response of morphine. Instead, the combined effects resembled those of Fraction B alone over the 7-day period, indicating a potential blockage of morphine's effects rather than a reversal of tolerance. The most promising results emerged with Fraction A+M, where the combination was able to sustain the analgesic effect of morphine over the 7-day period. Although Fraction A alone did not exhibit substantial analgesic

responses, its ability to preserve the effects of morphine makes it a compelling candidate for further exploration.

Moving forward, Fraction A warrants additional fractionation and tolerance testing to isolate the active component(s) responsible for blocking morphine tolerance. Advanced techniques such as liquid chromatography mass spectrometry (LC/MS) can be employed to identify and quantify known and unknown compounds within this fraction. This meticulous analysis may contribute to unraveling the molecular basis of morphine tolerance reversal and guide future studies in refining therapeutic strategies for managing opioid tolerance.

Conclusions

In summary, our study marks a significant advancement in unraveling the intricate relationship between YHS fractions and morphine tolerance. Notably, Fraction A has emerged as a compelling focal point, showcasing its potential to sustain morphine's analgesic effects over an extended duration. Subsequent investigations will delve deeper into Fraction A, subjecting it to further fractionation and rigorous tolerance testing. These endeavors aim to pinpoint the specific active component(s) responsible for mitigating morphine tolerance. Our findings provide valuable insights, laying the foundation for future inquiries dedicated to refining therapeutic approaches in addressing opioid tolerance and optimizing the efficacy of pain management strategies.

Chapter 5: A selective agonist, JNJ-63533054, serves as a potential analgesic in mice

Abstract

GPR 139 discreetly manifests in the brain, with its apex expression discernible in the medial habenula. Its intricate involvement in interconnected circuits associated with mood, motivation, and anxiety is well-established. Furthermore, GPR 139's endogenous ligands, identified as catecholamine/serotonin precursors, underscore its pivotal role in modulating neurons engaged in vital physiological and psychological processes. The GPR 139 agonist, JNJ-63533054, has undergone scrutiny for its potential therapeutic applications in neurobehavioral circuits. Recent studies illuminate the nuanced functions of GPR 139, indicating its participation in adaptive or habituative processes in response to chronic states or stimuli. Additionally, JNJ-63533054 has exhibited the ability to inhibit morphine-induced analgesia in various pain models and morphine self-administration, highlighting its potential as a versatile pharmacological agent. However, exploration of JNJ-63533054 as an analgesic itself is currently lacking, notwithstanding its established links to the opioid receptor. In prior studies, our lab has demonstrated that YHS extract exerts its effects, at least in part, via the dopamine 2 receptor. Moreover, when YHS extract is combined with morphine, it effectively mitigates morphine tolerance. In this investigation, we aim to determine whether the mechanism by which YHS blocks morphine tolerance involves the GPR 139 receptor. This study builds upon the existing knowledge of this selective agonist, revealing that JNJ-63533054 serves as an analgesic in mice, as demonstrated in the hot plate assay. This discovery not only enhances our comprehension of the pharmacological effects of GPR 139 activation but also proposes an alternative avenue for targeting pain medications. The comprehensive insights presented here contribute significantly to the expanding knowledge base on GPR 139, offering a foundation for further exploration into its therapeutic applications in pain management.

Introduction

Opioids, renowned for their potent pain management through μ-opioid receptor (MOR) activation, carry a substantial risk of abuse and addiction [53]. Within the domain of orphan G protein-coupled receptors (GPCRs), approximately 100 receptors, characterized by ambiguous matches to neuromodulators, obscure signaling mechanisms, and poorly understood physiological roles, offer a promising avenue to unravel novel neuromodulatory systems and illuminate neuropsychiatric conditions [155]. Despite the challenges posed by orphan receptors, successful "de-orphanization" stories underscore their potential as innovative drug targets, including the intriguing GPR139 [155].

GPR139, exhibiting features akin to canonical peptide receptors within class A GPCRs, weakly activates in response to aromatic amino acids and peptides derived from α-MSH [156]. Studies link GPR139 to MOR, revealing its anti-opioid activity in C. elegans through forward genetics, making it a potential target for enhancing opioid safety [67]. Selective expression of GPR139 in brain circuits associated with motivated behaviors, movement control, nociception, and cognition has been unveiled [156].

Pharmacological and genetic investigations implicate GPR139 in the rewarding and analgesic effects of substances like alcohol and opioids, revealing its coordination with the μ-opioid system and its influence on dopamine D2 receptors (D2R) [66]. The intricate interplay between D2R and GPR139 represents a fascinating axis within neural signaling, suggesting a regulatory influence of D2R on GPR139-mediated processes [66]. This dynamic interaction may contribute to modulating circuits associated with motivated behaviors, movement control, nociception, and cognition [66]. Exploring the relationships between these receptors may provide

valuable insights into their coordinated impact on neural regulation and potential therapeutic applications.

One study focused on unraveling the functional interplay between GPR139 and DRD2 in vitro, utilizing a calcium mobilization assay in cells co-transfected with both receptors from multiple species. Interestingly, the dopamine DRD2 agonist failed to elicit a calcium response in cells expressing DRD2 alone, consistent with the Gi signaling transduction pathway [66]. However, in cells co-transfected with both DRD2 and GPR139, the DRD2 agonist successfully induced a calcium response, supporting an in vitro interaction between GPR139 and DRD2 [66]. These findings suggest their potential functional interaction in native tissue settings.

GPR139's pivotal role in modulating interconnected circuits associated with mood, motivation, and anxiety is well-documented, emphasizing its significance [157]. The selective agonist, JNJ-63533054, acting upon GPR139, has potential therapeutic applications in neurobehavioral circuits, influencing adaptive or habituation processes and demonstrating involvement in the modulation of sleep states [158]. The versatile pharmacological profile of JNJ-63533054, inhibiting morphine-induced analgesia and self-administration, suggests its multifaceted therapeutic potential [67].

To address the critical gap in understanding JNJ-63533054's standalone analgesic properties, our study aims to unveil its role using GPR139 transgenic KO models in mice, particularly in the hot plate assay. Our lab's prior research on YHS has shown its activity at the D2 receptor and its ability to block morphine tolerance [126]. To delve deeper into how YHS achieves this effect, we hypothesize that the GPR139 receptor may be involved, given in vitro studies indicating its co-localization and functionality with the D2 receptor. Beyond unveiling this novel pharmacological facet, our findings propose an alternative avenue for pain medication targeting,

enriching our comprehension of the pharmacological effects of GPR139 activation. These insights might contribute significantly to the expanding knowledge base on GPR139 and establish a solid foundation for further exploration into its therapeutic applications in pain management.

Materials and Methods

Animals

Two distinct mouse strains were employed in behavior experiments. Male CD-10 mice, aged 8 weeks, were procured from Charles River, while the GPR 139 knockout mouse strain (GPR139tm1.1(KOMP)Vleg), bred on a pure C57BL/6N background, originated from the embryonic stem cell clone 10338B-A5, generated by Regeneron Pharmaceuticals Inc. and obtained from the KOMP repository at the University of California, Davis [67]. Littermates used in the study were produced through the mating of heterozygous parents [67]. The mice were group-housed and maintained under a 12-hour light/dark cycle, with ad libitum access to food and water. Ethical approval for all procedures and treatments was obtained from the Institutional Animal Care and Use Committee of the University of California, Irvine (AUP #20-015). Regular weight monitoring and post-injection observations were conducted to ensure the animals' well-being. Any mice displaying signs of distress or abnormalities were excluded from the study.

Behavior assays

Locomotor activity

Locomotor activity was assessed following established protocols [159]. Mice underwent a 30-minute habituation period in a locomotion test chamber (Med Associates, Inc.), with subsequent recording of locomotor activity for 1 hour [159]. The obtained data were analyzed using Activity Monitor 5 software (Med Associates, Inc.).

Hotplate assay

To establish the antinociceptive effects JNJ-63533054 on acute pain, foot withdrawal latency (FWL) in the hot plate assay was measured 30 min after injections, as well as before to establish a baseline on day 1 at 52 degrees Celsius [126]. A hotplate assay was performed, as described in the literature [95, 96, 126]. The cutoff time for the hotplate assay was 50s.

Tolerance assay

Mice were injected twice daily and the hot plate assay was tested on day 7 for tolerance-like behavior. FWL on the hotplate was measured at 30 min after injections. Day 1 and Day 7 responses were compared to observe any tolerance to the drugs as previously described [126].

Drug Administration

Morphine injectable (C II) (10 mg/mL), was obtained from Patterson Veterinary (Product ID: 07-892-4699) [126]. Mice received intraperitoneal (i.p.) injections of morphine at a dosage of 2.5 mg/kg. YHS, obtained from Dongyang County in Zhejiang, China, and authenticated by the Institute of Medication at Xiyuan Hospital of China Academy of Traditional Chinese Medicine (as previously described), was administered at a dose of 100 mg/kg in a volume of 5 μL/g via intraperitoneal administration [126]. JNJ-63533054 was dissolved in a vehicle solution containing cremophor EL: ethanol: saline (2:1:17) [126]. JNJ dosed at 1, 3, 5 and 10 mg/kg were administered. The injection volume was 5 μL/g, and individual dosages were determined based on each animal's body weight. Drugs were administered twice daily in the morning and afternoon approximately 10 hours apart, for a duration of 7 days for tolerance assay [126].

Statistical analysis

GraphPad Prism (GraphPad Software, Inc., San Diego, CA, USA) was used for statistical analysis, and all data are presented as mean ± standard error mean (SEM). Unpaired t test and one-way ANOVA followed by Tukey post-test and unpaired t tests was used to analyze data presented in this paper.

Results

To ascertain the optimal dosage for JNJ-63533054 in subsequent hotplate and tolerance assays, GPR139 wild-type (WT) mice underwent injections with varied doses (1, 3, and 10 mg/kg). The locomotor activity assay, depicted in Figure 1, showcases the diverse JNJ doses administered alongside the respective distances traveled by each group. Remarkably, no statistically significant differences were detected in locomotor activity across all administered doses.

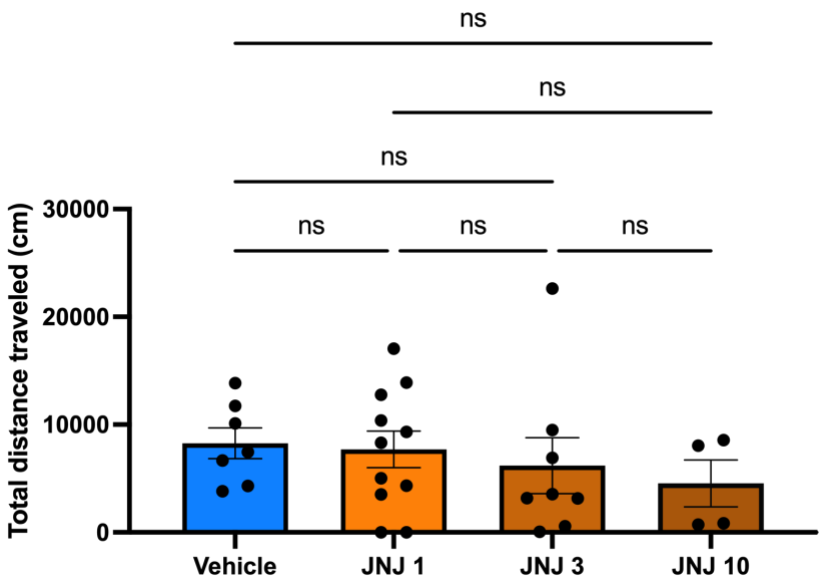

Figure 5.1. Lack of locomotor inhibition by JNJ 63533054 in WT mice. The graph depicts the distance traveled by mice during a 60-minute locomotion assay, illustrating the impact of varying doses of JNJ (1, 3, and 10 mg/kg). Statistical analysis, conducted through one-way ANOVA followed by Tukey's multiple comparison test, revealed no significant drug effects on locomotor activity ($F = 0.4774$) (n=4-11).

Having observed no significant inhibition of locomotor activity with various JNJ doses, we confirmed the drug's lack of influence on movement, crucial for the subsequent analgesia

assessment in the hotplate assay. Varying doses of JNJ (1, 3, 5, and 10 mg/kg) were systematically administered to determine the compound's potential analgesic properties. Initial investigations utilized the WT strain from the GPR139 mouse model to observe analgesic responses in the hotplate assay. Figure 5.2 illustrates the withdrawal latencies (FWL) at the 30-minute post-injection mark for vehicle, JNJ 1, JNJ 3, JNJ 5, and JNJ 10 (mg/kg). Notably, JNJ 3, JNJ 5, and JNJ 10 demonstrated analgesic effects compared to the vehicle group, establishing a dose-dependent trend.

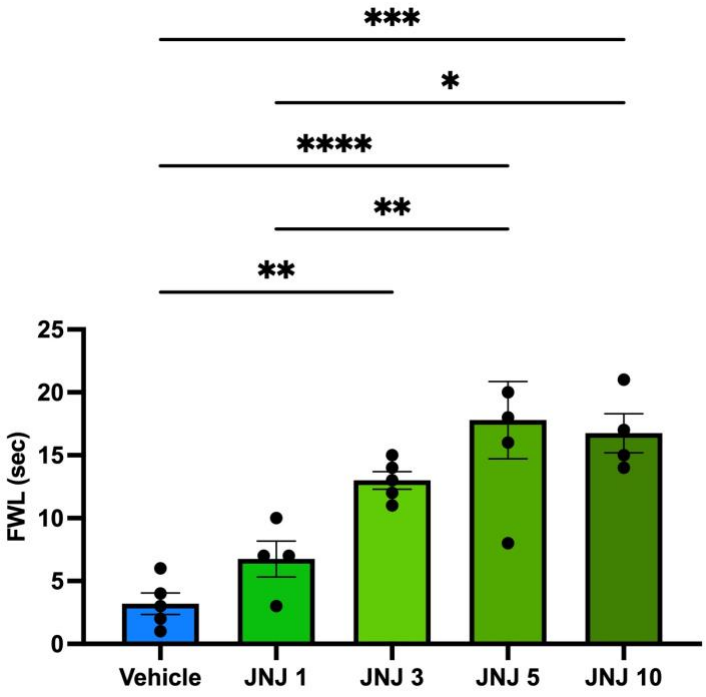

Figure 5.2 Evaluation of analgesic effects of JNJ 63533054 in the hotplate assay in WT mice. To ascertain the analgesic potential of JNJ 63533054, varying doses (1, 3, 5, and 10 mg/kg) were administered in the hotplate assay. The graph displays the withdrawal latencies (FWL) at the 30-minute mark after injections of vehicle, JNJ 1, JNJ 3, JNJ 5, and JNJ 10 (mg/kg). One-way ANOVA followed by Tukey's multiple comparison test revealed significant drug effects, F=

12.71, ****p<0.0001 compared with vehicle and JNJ 5, ***p<0.001 compared with vehicle and JNJ 10, **p<0.01 compared with vehicle, JNJ 1, JNJ 3, and JNJ 5, *p<0.05 compared with JNJ 1 and JNJ 10.

Following the analysis of dose-response data, we selected the JNJ dose of 3 mg/kg for subsequent investigations. In a comprehensive assessment of JNJ 63533054's analgesic potential, we employed this chosen dose in the hotplate assay, extending our observations to both GPR 139 WT and KO mice, as well as male and female subjects. Figure 5.3 presents the withdrawal latencies (FWL) of male and female WT and KO mice. Notably, JNJ 3 mg/kg demonstrated pronounced analgesic effects in both male and female WT mice, underscoring its efficacy. Conversely, this dose exhibited no analgesic effects in male and female KO mice as predicted, emphasizing the selectivity and critical role of GPR 139 in mediating JNJ 63533054's analgesic response. These findings highlight the nuanced interplay of gender and genotype in influencing the compound's efficacy in the hotplate assay.

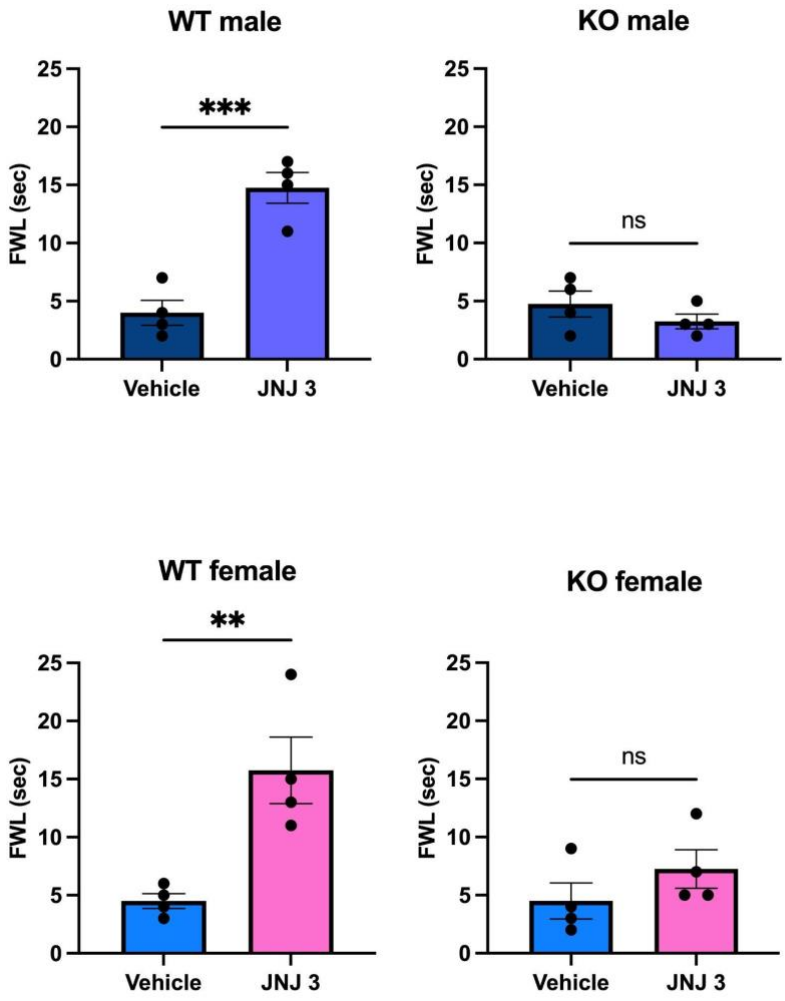

Figure 5.3 Sex and genotype influence on JNJ 63533054 analgesic efficacy in the hotplate assay. Top graphs display FWL results of WT male (left) and KO male (right). Unpaired t tests revealed significant differences in WT male after JNJ 3 treatment compared to vehicle (t= 6.317, p= 0.0007), ***p<0.001. Unpaired t tests revealed no significant differences in KO male mice after JNJ 3 and vehicle. Bottom graphs display FWL results of WT female (left) and KO female (right). Unpaired t tests revealed significant differences in WT female mice after JNJ 3 treatment compared to vehicle (t=3.826, p=0.087), **p<0.01. Unpaired t tests revealed no significant differences in KO female mice after JNJ 3 and vehicle

To investigate the potential interaction between YHS and the GPR 139 receptor, we administered a YHS dose of 100 mg/kg to male and female GPR 139 WT and KO mice. In Figure 5.4, the withdrawal latencies (FWL) following YHS and vehicle treatments are depicted for both male and female WT/KO mice. YHS exhibited analgesic effects in both GPR 139 WT and KO mice, suggesting that the observed analgesia is not mediated through the GPR 139 receptor. These findings challenge the hypothesis that the analgesic impact of YHS is linked to GPR 139, prompting further exploration into alternative mechanisms underlying the observed analgesic effects.

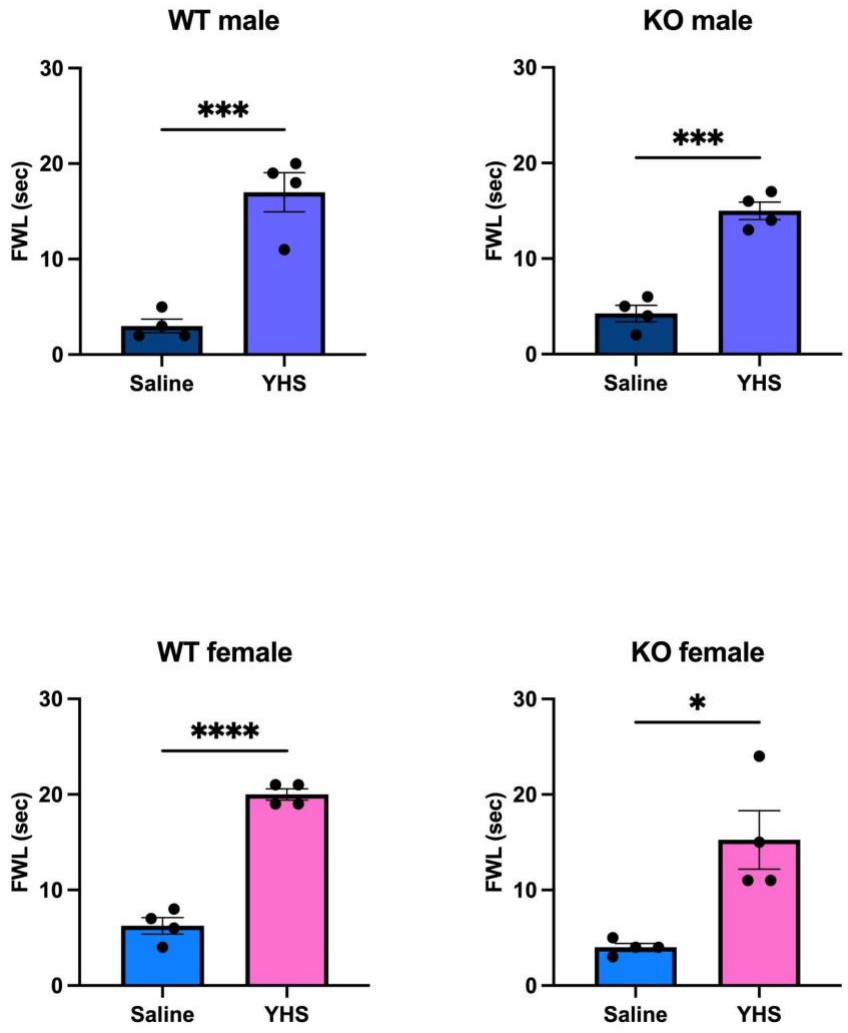

Figure 5.4 YHS analgesic effect is independent of GPR 139 receptor. Top graphs display FWL results of WT male (left) and KO male (right). Unpaired t tests revealed significant differences in WT and KO male after YHS treatment compared to vehicle, t=6.481, p=0.0006, and t=8.600, p=0.001 ***p<0.001. Bottom graphs display FWL results of WT female (left) and KO female (right). Unpaired t tests revealed significant differences in WT and KO female mice after YHS treatment compared to vehicle, t=13.34, p= 0.0001 and t=3.638, p=0.0109, ****p<0.0001 and *p<0.05.

To explore the potential involvement of the GPR 139 receptor in YHS's ability to counteract morphine tolerance, tolerance assays were conducted in both male and female GPR 139 WT and KO mice. Over a 7-day period, mice were treated with morphine (2.5 mg/kg) alone or in combination with YHS (100 mg/kg). Figure 5.5A illustrates the impact of morphine alone and morphine + YHS on WT male and female mice. As anticipated, morphine alone induces tolerance effects, while the co-administration of morphine and YHS prevents the development of tolerance.

The effects of morphine alone and morphine + YHS on KO male and female mice over the 7-day period are depicted in Figure 5.5B. While morphine alone induces tolerance in KO male and female mice, the combination of morphine and YHS prevents the development of tolerance. However, it's noteworthy that the overall analgesic responses in KO females and males with morphine + YHS are considerably lower compared to their WT counterparts. This suggests that while YHS retains its ability to block morphine tolerance in KO mice, the analgesic efficacy is diminished in the absence of the GPR 139 receptor, indicating a potential modulatory role of GPR 139 in this context.

A

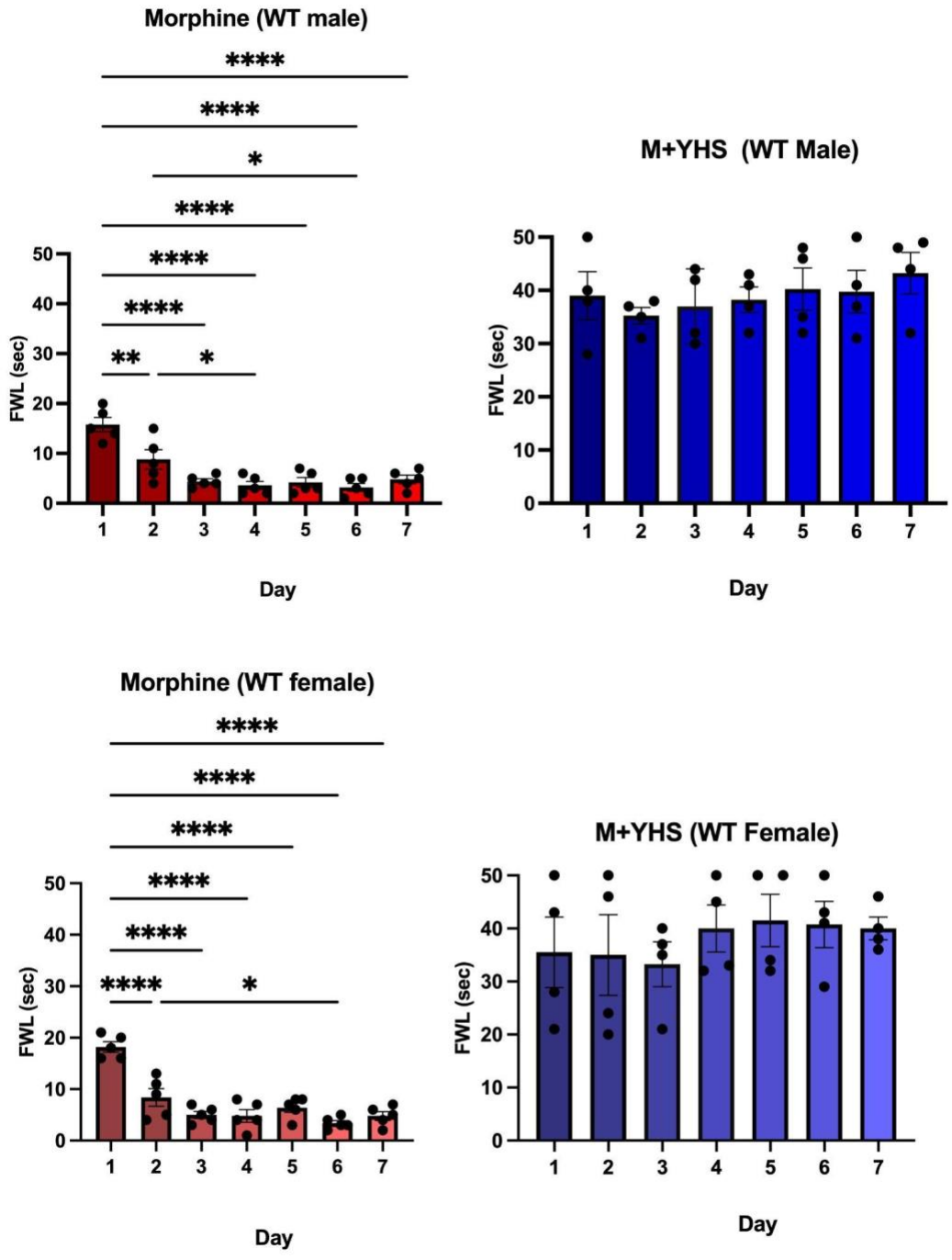
Morphine (WT male)
****
****
*
****
****
****
**
*
FWL (sec)
Day
M+YHS (WT Male)
FWL (sec)
Day
Morphine (WT female)
****
****
****
****
****
****
*
FWL (sec)
Day
M+YHS (WT Female)
FWL (sec)
Day

B

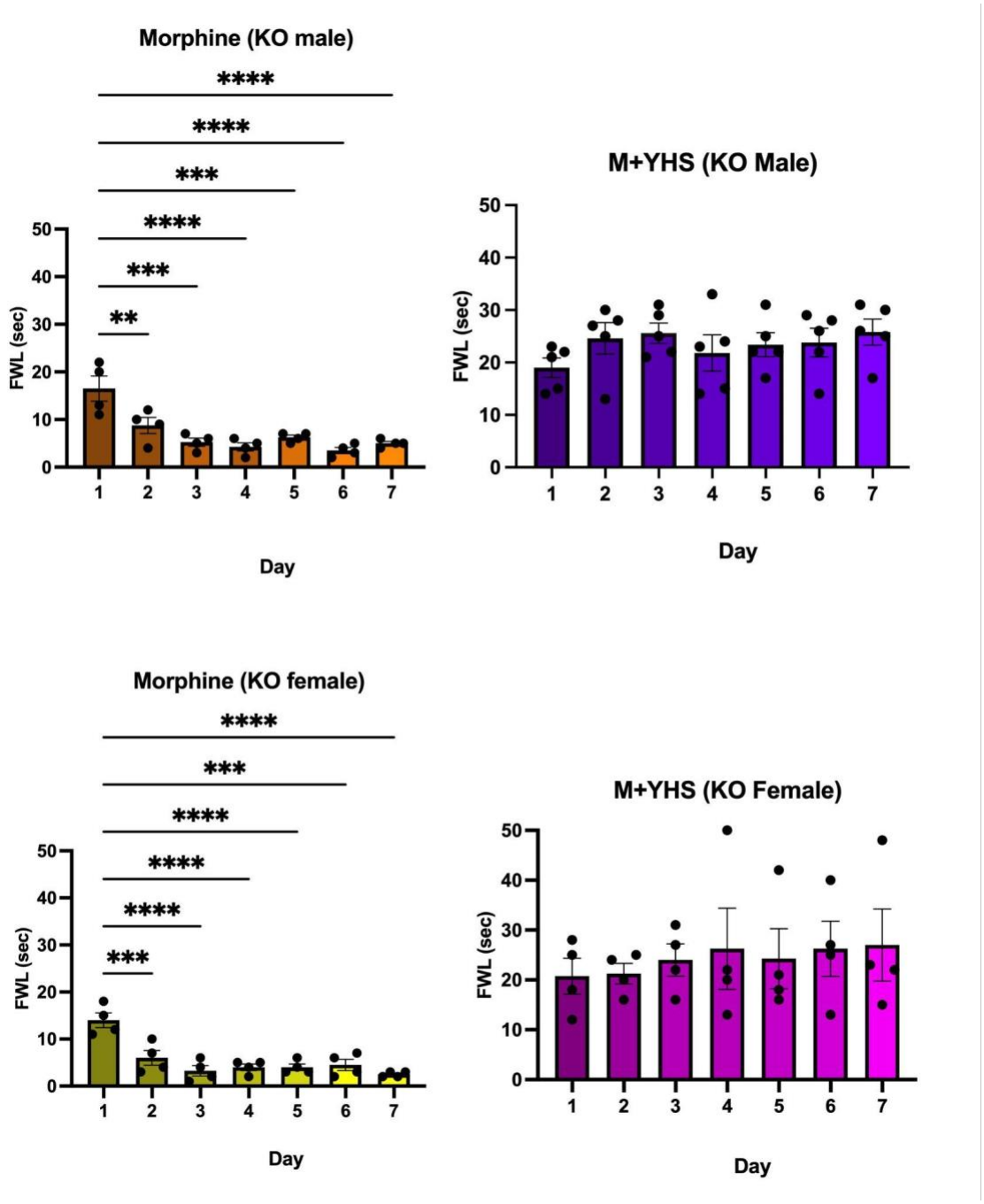

Figure 5.5 YHS-mediated prevention of morphine tolerance in GPR 139 KO mice.

A. Tolerance assays were conducted in GPR 139 WT male and female mice following treatment with morphine (2.5 mg/kg) alone or combined with YHS (100 mg/kg) for 7 days. The Y axis

shows FWL (sec) after 30 min of treatment, and the x axis displays days (D). One-way ANOVA followed by Tukey's multiple comparison test revealed significant drug effects after 7 days of morphine treatment in WT male mice, F=15.99, ****p<0.0001 compared with D1, D3, D4, D5, D6, D7, **p<0.01 compared with D1 and D2, and *p<0.05 compared with D2, D4, and D6. One-way ANOVA followed by Tukey's multiple comparison test revealed significant drug effects after 7 days of morphine treatment in WT female mice, F=22.72, ****p<0.0001 D1-D7, *p<0.05 compared with D2 and D6. **B.** Tolerance assays were conducted in GPR 139 KO male and female mice following treatment with morphine (2.5 mg/kg) alone or combined with YHS (100 mg/kg) for 7 days. One-way ANOVA followed by Tukey's multiple comparison test revealed significant drug effects after 7 days of morphine treatment in KO male mice, F= 11.50, ****p<0.0001 compared with D1, D4, D6, and D7, ***p<0.001 compared with D1, D3, and D5, and **p<0.01 compared with D1 and D2. One-way ANOVA followed by Tukey's multiple comparison test revealed significant drug effects after 7 days of morphine treatment in KO female mice, F=12.30,****p<0.0001compared with D1, D3, D4, D5, and D7, and ***p<0.001 compared with D1, D2, and D6.

Discussion

Unveiling Novel Analgesic Properties of JNJ-63533054

The present study brings forth significant revelations concerning the analgesic properties of JNJ-63533054 and YHS, challenging existing paradigms and shedding light on potential alternative mechanisms. In a recent investigation focusing on JNJ-63533054, an unexpected discovery emerged, indicating its promise in altering morphine analgesia [67]. Intriguingly, administration of JNJ-63533054 resulted in a substantial reduction in morphine-induced analgesia, challenging traditional assumptions about the pharmacological interactions between JNJ-63533054 and morphine [67]. Notably, this study observed that JNJ-63533054 did not exhibit independent analgesic effects in the absence of morphine, adding a layer of complexity to its role in pain modulation.

Our exploration commenced with JNJ-63533054, a compound traditionally not linked to analgesia. Surprisingly, our results revealed pronounced analgesic effects in the hotplate assay, a novel finding not previously reported. This analgesic response was consistent at the selected dose of 3 mg/kg in both male and female GPR 139 wild-type (WT) mice, highlighting the compound's efficacy in diverse contexts. Crucially, the investigation extended to GPR 139 knockout (KO) mice, revealing a marked contrast in analgesic responses. As anticipated, the same dose of JNJ-63533054 exhibited no analgesic effects in GPR 139 KO mice, reaffirming the specificity of its action through the GPR 139 receptor. The intriguing interplay between gender and genotype emphasizes the intricate modulation of analgesic efficacy, underscoring the pivotal role of GPR 139 in mediating JNJ-63533054's analgesic response. This unprecedented finding prompts a reconsideration of JNJ-63533054's pharmacological profile, inviting further investigations into its

mechanisms of action and the selective activation of GPR 139, which, in turn, nuances neural circuits associated with pain processing.

YHS exhibits analgesic and tolerance effects independent of GPR 139 receptor modulation

The colocalization of the dopamine D2 receptor (D2R) and GPR139 has been a subject of interest in neurobiological studies [66]. Existing knowledge suggests their coexpression in specific brain circuits associated with motivated behaviors, movement control, nociception, and cognition. Studies propose a functional interaction between GPR139 and D2R, influencing neuromodulatory processes [66]. Despite our plant extract being identified as a D2 antagonist, our interest extended to observing its analgesic properties and potential interaction with the GPR 139 receptor.

Contrary to our initial hypothesis, YHS's analgesic effects were observed in both GPR 139 WT and KO mice, challenging the notion of GPR 139 mediation. This unexpected outcome directs our attention towards alternative mechanisms underlying YHS's analgesic properties. Intriguingly, YHS also demonstrated efficacy in preventing morphine tolerance, deviating from the anticipated GPR 139-dependent mechanism. While morphine + YHS prevented tolerance development in both GPR 139 WT and KO mice, the overall analgesic responses in KO mice were notably diminished. This observation suggests a potential modulatory role of GPR 139 in the analgesic efficacy of YHS, warranting detailed exploration into the complex interactions between YHS, GPR 139, and morphine tolerance.

Our findings challenge existing paradigms and offer novel insights into the analgesic properties of JNJ-63533054 and YHS. The selectivity of JNJ-63533054 for GPR 139 opens new avenues for drug development, while the unexpected actions of YHS beckon further exploration into its alternative mechanisms and potential modulatory roles of GPR 139. These revelations not

only contribute to our understanding of analgesic pharmacology but also pave the way for future research exploring the intricate interplay between compounds, receptors, and pain modulation.

Conclusions

In conclusion, our study has unveiled unforeseen analgesic properties of JNJ-63533054 and YHS, challenging existing paradigms and sparking inquiries into alternative mechanisms. The unexpected reduction in morphine-induced analgesia by JNJ-63533054 prompts a reevaluation of its pharmacological profile and emphasizes the intricate interplay with morphine. The distinct analgesic responses observed in GPR 139 KO mice underscore the critical role of GPR 139 in mediating JNJ-63533054's effects, opening avenues for future investigations into its specific mechanisms of action and the modulation of neural circuits associated with pain processing. On the other hand, YHS's analgesic efficacy, independent of GPR 139, signifies the existence of alternative pathways, urging further exploration into the intricate network of receptors and signaling cascades involved. The observed modulation of morphine tolerance by YHS in the absence of GPR 139 suggests complex interactions, meriting comprehensive investigation. Future research should delve into elucidating the precise molecular mechanisms underlying JNJ-63533054's analgesic response and unraveling the alternative pathways through which YHS exerts its analgesic effects. Additionally, exploring the broader implications of these findings in the development of novel analgesic strategies and their potential translation to clinical applications holds promise for advancing our understanding of pain modulation and treatment.

References

1. Garland EL. Pain processing in the human nervous system: a selective review of nociceptive and biobehavioral pathways. Prim Care. 2012 Sep;39(3):561-71
2. Yam MF, Loh YC, Tan CS, Khadijah Adam S, Abdul Manan N, Basir R. General Pathways of Pain Sensation and the Major Neurotransmitters Involved in Pain Regulation. Int J Mol Sci. 2018 Jul 24;19(8):2164.
3. Omoigui S. The biochemical origin of pain: the origin of all pain is inflammation and the inflammatory response. Part 2 of 3 - inflammatory profile of pain syndromes. Med Hypotheses. 2007;69(6):1169-78.
4. Mills EP, Keay KA, Henderson LA. Brainstem Pain-Modulation Circuitry and Its Plasticity in Neuropathic Pain: Insights From Human Brain Imaging Investigations. Front Pain Res (Lausanne). 2021 Jul 30;2:705345.
5. Browne TJ, Hughes DI, Dayas CV, Callister RJ, Graham BA. Projection Neuron Axon Collaterals in the Dorsal Horn: Placing a New Player in Spinal Cord Pain Processing. Front Physiol. 2020 Dec 21;11:560802.
6. Hall J.E. *Guyton and Hall Textbook of Medical Physiology e-Book.* Elsevier Health Sciences; Philadelphia, PA, USA: 2010.
7. Dubin A.E., Patapoutian A. Nociceptors: The sensors of the pain pathway. *J. Clin. Investig.* 2010;120:3760–3772.
8. Narahashi T., Moore J.W., Scott W.R. Tetrodotoxin blockage of sodium conductance increase in lobster giant axons. *J. Gen. Physiol.* 1964;47:965–974.
9. Rasband MN, Peles E. The Nodes of Ranvier: Molecular Assembly and Maintenance. Cold Spring Harb Perspect Biol. 2015 Sep 9;8(3):a020495.
10. De Ridder D, Adhia D, Vanneste S. The anatomy of pain and suffering in the brain and its clinical implications. Neurosci Biobehav Rev. 2021 Nov;130:125-146.
11. Basbaum AI, Bautista DM, Scherrer G, Julius D. Cellular and molecular mechanisms of pain. Cell. 2009 Oct 16;139(2):267-84.
12. Yang S, Chang MC. Chronic Pain: Structural and Functional Changes in Brain Structures and Associated Negative Affective States. Int J Mol Sci. 2019 Jun 26;20(13):3130.
13. Afridi B, Khan H, Akkol EK, Aschner M. Pain Perception and Management: Where do We Stand? Curr Mol Pharmacol. 2021;14(5):678-688.
14. Dueñas M, Ojeda B, Salazar A, Mico JA, Failde I. A review of chronic pain impact on patients, their social environment and the health care system. J Pain Res. 2016 Jun 28;9:457-67.
15. Mills SEE, Nicolson KP, Smith BH. Chronic pain: a review of its epidemiology and associated factors in population-based studies. Br J Anaesth. 2019 Aug;123(2):e273-e283.

16. Willis WD, Westlund KN. Neuroanatomy of the pain system and of the pathways that modulate pain. J Clin Neurophysiol. 1997 Jan;14(1):2-31.
17. Lopes PSS, Campos ACP, Fonoff ET, Britto LRG, Pagano RL. Motor cortex and pain control: exploring the descending relay analgesic pathways and spinal nociceptive neurons in healthy conscious rats. Behav Brain Funct. 2019 Mar 25;15(1):5.
18. Costigan M, Scholz J, Woolf CJ. Neuropathic pain: a maladaptive response of the nervous system to damage. Annu Rev Neurosci. 2009;32:1-32.
19. Latremoliere A, Woolf CJ. Central sensitization: a generator of pain hypersensitivity by central neural plasticity. J Pain. 2009 Sep;10(9):895-926.
20. Ossipov MH, Morimura K, Porreca F. Descending pain modulation and chronification of pain. Curr Opin Support Palliat Care. 2014 Jun;8(2):143-51.
21. Colloca L, Ludman T, Bouhassira D, Baron R, Dickenson AH, Yarnitsky D, Freeman R, Truini A, Attal N, Finnerup NB, Eccleston C, Kalso E, Bennett DL, Dworkin RH, Raja SN. Neuropathic pain. Nat Rev Dis Primers. 2017 Feb 16;3:17002.
22. Chen L, Deng H, Cui H, Fang J, Zuo Z, Deng J, Li Y, Wang X, Zhao L. Inflammatory responses and inflammation-associated diseases in organs. Oncotarget. 2017 Dec 14;9(6):7204-7218.
23. Matsuda M, Huh Y, Ji RR. Roles of inflammation, neurogenic inflammation, and neuroinflammation in pain. J Anesth. 2019 Feb;33(1):131-139.
24. Miller RJ, Jung H, Bhangoo SK, White FA. Cytokine and chemokine regulation of sensory neuron function. Handb Exp Pharmacol. 2009;(194):417-49.
25. Jones MR, Viswanath O, Peck J, Kaye AD, Gill JS, Simopoulos TT. A Brief History of the Opioid Epidemic and Strategies for Pain Medicine. Pain Ther. 2018 Jun;7(1):13-21.
26. Kolodny A, Courtwright DT, Hwang CS, Kreiner P, Eadie JL, Clark TW, Alexander GC. The prescription opioid and heroin crisis: A public health approach to an epidemic of addiction. Annual Review of Public Health. 2015;36:559–574.
27. Chenaf, C. *et al.* Prescription opioid analgesic use in France: Trends and impact on morbidity–mortality. *Eur. J. Pain* 23, 124–134.
28. Ahmed S, Sarfraz Z, Sarfraz A. Editorial: A Changing Epidemic and the Rise of Opioid-Stimulant Co-Use. Front Psychiatry. 2022 Jul 6;13:918197.
29. Volkow ND, Frieden TR, Hyde PS, Cha SS. Medication-assisted therapies—Tackling the opioid-overdose epidemic. New England Journal of Medicine. 2014;370(22):2063–2066.
30. Han B, Compton WM, Blanco C, Crane E, Lee J, Jones CM. Prescription opioid use, misuse, and use disorders in U.S. adults: 2015 National Survey on Drug Use and Health. Annals of Internal Medicine. 2017;167(5):293–301.

31. Axeen S. Trends in opioid use and prescribing in Medicare, 2006–2012. Health Services Research. 2018;53(5):3309–3328.
32. Jalali MS, Botticelli M, Hwang RC, Koh HK, McHugh RK. The opioid crisis: a contextual, social-ecological framework. Health Res Policy Syst. 2020 Aug 6;18(1):87.
33. Dart RC, Surratt HL, Cicero TJ, Parrino MW, Severtson SG, Bucher-Bartelson B, Green JL. Trends in opioid analgesic abuse and mortality in the United States. New England Journal of Medicine. 2015;372(3):241–248.
34. Rudd RA, Seth P, David F, Scholl L. Increases in drug and opioid-involved overdose deaths—United States, 2010–2015. Morbidity and Mortality Weekly Report. 2016;65:1445–1452.
35. Pathan H, Williams J. Basic opioid pharmacology: an update. Br J Pain. 2012 Feb;6(1):11-6.
36. Le Merrer J, Becker JA, Befort K, Kieffer BL. Reward processing by the opioid system in the brain. Physiol Rev. 2009 Oct;89(4):1379-412.
37. Wiffen PJ, Wee B, Moore RA. Oral morphine for cancer pain. Cochrane Database Syst Rev. 2016 Apr 22;4(4):CD003868.
38. Morgan MM, Christie MJ. Analysis of opioid efficacy, tolerance, addiction and dependence from cell culture to human. Br J Pharmacol. 2011 Oct;164(4):1322-34.
39. Compton WM, Jones CM. Epidemiology of the U.S. opioid crisis: the importance of the vector. Ann N Y Acad Sci. 2019 Sep;1451(1):130-143.
40. King NB, Fraser V, Boikos C, Richardson R, Harper S. Determinants of increased opioid-related mortality in the United States and Canada, 1990-2013: a systematic review. Am J Public Health. 2014 Aug;104(8):e32-42.
41. Fernandes ES, Ferro ES, Simão G, Alves de Góis G, Arbiser J, Pereira Costa SK. Editorial: Current challenges in inflammation and pain biology: The role of natural and synthetic compounds. Front Physiol. 2022 Sep 7;13:1008538.
42. Bindu S, Mazumder S, Bandyopadhyay U. Non-steroidal anti-inflammatory drugs (NSAIDs) and organ damage: A current perspective. Biochem Pharmacol. 2020 Oct;180:114147.
43. Maroon JC, Bost JW, Maroon A. Natural anti-inflammatory agents for pain relief. Surg Neurol Int. 2010 Dec 13;1:80.
44. Abramson SB, Weaver AL. Current state of therapy for pain and inflammation. Arthritis Res Ther. 2005;7 Suppl 4(Suppl 4):S1-6.
45. Sohail R, Mathew M, Patel KK, Reddy SA, Haider Z, Naria M, Habib A, Abdin ZU, Razzaq Chaudhry W, Akbar A. Effects of Non-steroidal Anti-inflammatory Drugs (NSAIDs) and Gastroprotective NSAIDs on the Gastrointestinal Tract: A Narrative Review. Cureus. 2023 Apr 3;15(4):e37080.
46. Singh G. Recent considerations in nonsteroidal anti-inflammatory drug gastropathy. Am J Med. 1998 Jul 27;105(1B):31S-38S.

47. Fries JF, Murtagh KN, Bennett M, Zatarain E, Lingala B, Bruce B. The rise and decline of nonsteroidal antiinflammatory drug-associated gastropathy in rheumatoid arthritis. Arthritis Rheum. 2004 Aug;50(8):2433-40.
48. Borer JS, Simon LS. Cardiovascular and gastrointestinal effects of COX-2 inhibitors and NSAIDs: achieving a balance. Arthritis Res Ther. 2005;7 Suppl 4(Suppl 4):S14-22.
49. Tai FWD, McAlindon ME. Non-steroidal anti-inflammatory drugs and the gastrointestinal tract. Clin Med (Lond). 2021 Mar;21(2):131-134.
50. Rahme E, Nedjar H. Risks and benefits of COX-2 inhibitors vs non-selective NSAIDs: does their cardiovascular risk exceed their gastrointestinal benefit? A retrospective cohort study. Rheumatology (Oxford). 2007 Mar;46(3):435-8.
51. Knaul FM, Farmer PE, Krakauer EL, De Lima L, Bhadelia A, Jiang Kwete X, Arreola-Ornelas H, Gómez-Dantés O, Rodriguez NM, Alleyne GAO, Connor SR, Hunter DJ, Lohman D, Radbruch L, Del Rocío Sáenz Madrigal M, Atun R, Foley KM, Frenk J, Jamison DT, Rajagopal MR; Lancet Commission on Palliative Care and Pain Relief Study Group. Alleviating the access abyss in palliative care and pain relief-an imperative of universal health coverage: the Lancet Commission report. Lancet. 2018 Apr 7;391(10128):1391-1454.
52. Al-Hasani R, Bruchas MR. Molecular mechanisms of opioid receptor-dependent signaling and behavior. Anesthesiology. 2011 Dec;115(6):1363-81.
53. Pasternak GW, Pan YX. Mu opioids and their receptors: evolution of a concept. Pharmacol Rev. 2013 Sep 27;65(4):1257-317.
54. Christie MJ. Cellular neuroadaptations to chronic opioids: tolerance, withdrawal and addiction. Br J Pharmacol. 2008 May;154(2):384-96.
55. Yuan L, Luo L, Ma X, Wang W, Yu K, Shi H, Chen J, Chen D, Xu T. Chronic morphine induces cyclic adenosine monophosphate formation and hyperpolarization-activated cyclic nucleotide-gated channel expression in the spinal cord of mice. Neuropharmacology. 2020 Oct 1;176:108222.
56. Lane-Ladd SB, Pineda J, Boundy VA, Pfeuffer T, Krupinski J, Aghajanian GK, Nestler EJ. CREB (cAMP response element-binding protein) in the locus coeruleus: biochemical, physiological, and behavioral evidence for a role in opiate dependence. J Neurosci. 1997 Oct 15;17(20):7890-901.
57. Muntean BS, Dao MT, Martemyanov KA. Allostatic Changes in the cAMP System Drive Opioid-Induced Adaptation in Striatal Dopamine Signaling. Cell Rep. 2019 Oct 22;29(4):946-960.e2.
58. Raehal KM, Bohn LM. β-arrestins: regulatory role and therapeutic potential in opioid and cannabinoid receptor-mediated analgesia. Handb Exp Pharmacol. 2014;219:427-43.
59. Valentino RJ, Volkow ND. Untangling the complexity of opioid receptor function. Neuropsychopharmacology. 2018 Dec;43(13):2514-2520.

60. Melief EJ, Miyatake M, Bruchas MR, Chavkin C. Ligand-directed c-Jun N-terminal kinase activation disrupts opioid receptor signaling. Proc Natl Acad Sci U S A. 2010 Jun 22;107(25):11608-13.
61. Terman GW, Jin W, Cheong YP, Lowe J, Caron MG, Lefkowitz RJ, Chavkin C. G-protein receptor kinase 3 (GRK3) influences opioid analgesic tolerance but not opioid withdrawal. Br J Pharmacol. 2004 Jan;141(1):55-64.
62. Zhang Y, Wang C, Wang L, Parks GS, Zhang X, Guo Z, Ke Y, Li KW, Kim MK, Vo B, Borrelli E, Ge G, Yang L, Wang Z, Garcia-Fuster MJ, Luo ZD, Liang X, Civelli O. A novel analgesic isolated from a traditional Chinese medicine. Curr Biol. 2014 Jan 20;24(2):117-123.
63. Alhassen L, Dabbous T, Ha A, Dang LHL, Civelli O. The Analgesic Properties of *Corydalis yanhusuo*. Molecules. 2021 Dec 10;26(24):7498.
64. Wang L, Zhang Y, Wang Z, Gong N, Kweon TD, Vo B, Wang C, Zhang X, Chung JY, Alachkar A, Liang X, Luo DZ, Civelli O. The Antinociceptive Properties of the Corydalis yanhusuo Extract. PLoS One. 2016 Sep 13;11(9):e0162875
65. Liu C, Bonaventure P, Lee G, Nepomuceno D, Kuei C, Wu J, Li Q, Joseph V, Sutton SW, Eckert W, Yao X, Yieh L, Dvorak C, Carruthers N, Coate H, Yun S, Dugovic C, Harrington A, Lovenberg TW. GPR139, an Orphan Receptor Highly Enriched in the Habenula and Septum, Is Activated by the Essential Amino Acids L-Tryptophan and L-Phenylalanine. Mol Pharmacol. 2015 Nov;88(5):911-25.
66. Wang L, Lee G, Kuei C, Yao X, Harrington A, Bonaventure P, Lovenberg TW, Liu C. GPR139 and Dopamine D2 Receptor Co-express in the Same Cells of the Brain and May Functionally Interact. Front Neurosci. 2019 Mar 26;13:281.
67. Wang D, Stoveken HM, Zucca S, Dao M, Orlandi C, Song C, Masuho I, Johnston C, Opperman KJ, Giles AC, Gill MS, Lundquist EA, Grill B, Martemyanov KA. Genetic behavioral screen identifies an orphan anti-opioid system. Science. 2019 Sep 20;365(6459):1267-1273.
68. Wang J., Zhu L. Y., Liu Q., Hentzer M., Smith G. P., and Wang M. W. (2015) High-throughput screening of antagonists for the orphan G-protein coupled receptor GPR139. *Acta Pharmacol. Sin*. 36, 874–878
69. Zhang L, Zhang JT, Hang L, Liu T. Mu Opioid Receptor Heterodimers Emerge as Novel Therapeutic Targets: Recent Progress and Future Perspective. Front Pharmacol. 2020 Jul 15;11:1078.
70. Stoveken HM, Zucca S, Masuho I, Grill B, Martemyanov KA. The orphan receptor GPR139 signals via Gq/11 to oppose opioid effects. J Biol Chem. 2020 Jul 31;295(31):10822-10830.
71. Alavi M. S., Shamsizadeh A., Azhdari-Zarmehri H., and Roohbakhsh A. (2018) Orphan G protein-coupled receptors: the role in CNS disorders. *Biomed. Pharmacother*. 98, 222–232

72. Nepomuceno D., Kuei C., Dvorak C., Lovenberg T., Liu C., and Bonaventure P. (2018) Re-evaluation of adrenocorticotropic hormone and melanocyte stimulating hormone activation of GPR139 *in vitro*. *Front. Pharmacol*. 9, 157
73. Rich, R.L.C., Jr. Prescribing Opioids for Chronic Pain: Unintended Consequences of the 2016 CDC Guideline. *Am. Fam Phys.* 2020, *101*, 458–459.
74. Dowell, D.; Haegerich, M.; Chou, R. CDC Guideline for Prescribing Opioids for Chronic Pain—United States, 2016. *JAMA* 2016, *315*, 1624–1645.
75. McNicol, E.; Strassels, S.; Goudas, L.; Lau, J.; Carr, D. Nonsteroidal anti-inflammatory drugs, alone or combined with opioids, for cancer pain: A systematic review. *J. Clin. Oncol.* 2004, *22*, 1975–1992.
76. McNicol, E.; Strassels, S.; Goudas, L.; Lau, J.; Carr, D. Nonsteroidal anti-inflammatory drugs, alone or combined with opioids, for cancer pain: A systematic review. *J. Clin. Oncol.* 2004, *22*, 1975–1992.
77. Kosten, T.R.; George, T.P. The neurobiology of opioid dependence: Implications for treatment. *Sci. Pract. Perspect.* 2002, *1*, 13–20.
78. Küpeli, E.; Koşar, M.; Yeşilada, E.; Hüsnü, K.; Başer, C. A comparative study on the anti-inflammatory, antinociceptive and antipyretic effects of isoquinoline alkaloids from the roots of Turkish Berberis species. *Life Sci.* 2002, *72*, 645–657.
79. Tian, B.; Tian, M.; Shu-Ming, H. Advances in phytochemical and modern pharmacological research of Rhizoma Corydalis. *Pharm. Biol.* 2020, *58*, 265–275
80. Cruz, H.G.; Berton, F.; Sollini, M.; Blanchet, C.; Pravetoni, M.; Wickman, K.; Lüscher, C. Absence and rescue of morphine withdrawal in GIRK/Kir3 knock-out mice. *J. Neurosci.* 2008, *28*, 4069–4077.
81. Cobacho, N.; Luis de la Calle, J.; Luis Paíno, C. Dopaminergic modulation of neuropathic pain: Analgesia in rats by a D2-type receptor agonist. *Brain Res. Bull.* 2014, *106*, 62–71
82. Hodgson, S.R.; Hofford, R.; Wellman, P.; Eitan, S. Different affective response to opioid withdrawal in adolescent and adult mice. *Life Sci.* 2009, *84*, 52–60.
83. Volkow, N.D.; Jones, E.B.; Einstein, E.B.; Wargo, E.M. Prevention and Treatment of Opioid Misuse and Addiction: A Review. *JAMA Psychiatry* 2019, *76*, 208–216.
84. Taylor, B.K.; Joshi, C.; Uppal, H. Stimulation of dopamine D2 receptors in the nucleus accumbens inhibits inflammatory pain. *Brain Res.* 2003, *987*, 135–143.
85. Viisanen, H.; Ansah, O.B.; Pertovaara, A. The role of the dopamine D2 receptor in descending control of pain induced by motor cortex stimulation in the neuropathic rat. *Brain Res. Bull.* 2012, *89*, 133–143.
86. Wood, P.B. Role of central dopamine in pain and analgesia. *Expert Rev. Neurother.* 2008, *8*, 781–797.

87. Cunningham, C.L.; Gremel, C.M.; Groblewski, P.A. Drug-induced conditioned place preference and aversion in mice. *Nat. Protoc.* 2006, *1*, 1662–1670

88. Roughan, J.V.; Coulter, C.A.; Flecknell, P.A.; Thomas, H.D.; Sufka, K.J. The conditioned place preference test for assessing welfare consequences and potential refinements in a mouse bladder cancer model. *PLoS ONE* 2014, *9*, e103362.

89. Sun, Y.; Chen, G.; Zhou, K.; Zhu, Y. A Conditioned Place Preference Protocol for Measuring Incubation of Craving in Rats. *J. Vis. Exp*. 2018, *141*, e58384.

90. O'Connor, A.B.; Dworkin, R.H. Treatment of neuropathic pain: An overview of recent guidelines. *Am. J. Med.* 2009, *122*, S22–S32.

91. Li, J.X. Combining opioids and non-opioids for pain management: Current status. *Neuropharmacology* 2019, *158*, 107619.

92. Eisenberg, E.; Berkey, C.S.; Carr, D.B.; Mosteller, F.; Chalmers, T.C. Efficacy and safety of nonsteroidal antiinflammatory drugs for cancer pain: A meta-analysis. *J. Clin. Oncol.* 2012, *2756*, 1994–2765.

93. Ong, C.K.S.; Lirk, P.; Tan, C.H.; Seymour, R.A. An evidence-based update on nonsteroidal anti-inflammatory drugs. *Clin. Med. Res.* 2007, *5*, 19–34.

94. Zhang, Y.; Wang, C.; Wang, L.; Parks, G.S.; Zhang, X.; Guo, Z.; Ke, Y.; Li, K.W.; Kim, M.K.; Vo, B.; et al. A novel analgesic isolated from a traditional Chinese medicine. *Curr. Biol.* 2014, *24*, 117–123.

95. Jang, J.H.; Park, J.Y.; Oh, J.Y.; Bae, S.J.; Jang, H.; Jeon, S.; Kim, J.; Park, H.J. Novel analgesic effects of melanin-concentrating hormone on persistent neuropathic and inflammatory pain in mice. *Sci. Rep.* 2018, *8*, 707.

96. Wang, L.; Zhang, Y.; Wang, Z.; Gong, N.; Kweon, T.D.; Vo, B.; Wang, C.; Zhang, X.; Chung, J.Y.; Alachkar, A.; et al. The Antinociceptive Properties of the Corydalis yanhusuo Extract. *PLoS ONE* 2016, *11*, e0162875.

97. Crofford, L.J. Adverse effects of chronic opioid therapy for chronic musculoskeletal pain. *Nat. Rev. Rheumatol.* 2010, *6*, 191–197

98. Robinson, T.E.; Berridge, K.C. The psychology and neurobiology of addiction: An incentive-sensitization view. *Addiction* 2000, *95*, S91–S117.

99. Zhang, Y.; Wang, Z.; Cox, P.D.; Civelli, O. Study on the activation of the opioid receptors by a set of morphine derivatives in a well-defined assay system. *Neurochem. Res.* 2012, *37*, 410–416

100. Ding, B.; Zhou, T.; Fan, G.; Hong, Z.; Wu, Y. Qualitative and quantitative determination of ten alkaloids in traditional Chinese medicine Corydalis yanhusuo W.T. Wang by LC-MS/MS and LC-DAD. *J. Pharm. Biomed. Anal.* 2007, *45*, 219–226.

101. Dunham, N.W.; Miya, T.S. A note on a simple apparatus for detecting neurological deficit in rats and mice. *J. Am. Pharm Assoc. Am. Pharm Assoc.* 1957, *46*, 208–209.

102. Mansikka, H.; Erbs, E.; Borrelli, E.; Pertovaara, A. Influence of the dopamine D2 receptor knockout on pain-related behavior in the mouse. *Brain Res.* 2005, *1052*, 82–87.

103. Ortiz, M.I.; Molina, M.; Arai, Y.; Luca Romanò, C. Analgesic drugs combinations in the treatment of different types of pain. *Pain Res. Treat.* 2012, *2012*, 612519.

104. Angst, M.S.; Phillips, N.G.; Drover, D.R.; Tingle, M.; Ray, A.; Swan, G.E.; Lazzeroni, L.C.; Clark, D.J. Pain sensitivity and opioid analgesia: A pharmacogenomic twin study. *Pain* 2012, *153*, 1397–1409.

105. Liu, Z.; Wang, R.; He, H.; Jiang, X.; Ye, J.; Zeng, S.; Hu, J. Water-soluble non-alkaloid chemical constituents contained in Corydalis yanhusuo by trimethylsilyl derivatization GC-MS. *Zhongguo Zhong Yao Za Zhi* 2012, *37*, 2108–2112

106. Wan, L.; Zhao, Y.; Zhang, Q.; Gao, G.; Zhang, S.; Gao, Y.; Chen, X.; Qian, X. Alkaloid extract of Corydalis yanhusuo inhibits angiogenesis via targeting vascular endothelial growth factor receptor signaling. *BMC Complement. Altern. Med.* 2019, *19*, 359.

107. Kaserer, T.; Steinacher, T.; Kainhofer, R.; Erli, F.; Sturm, S.; Waltenberger, B.; Schuster, D.; Spetea, M. Identification and characterization of plant-derived alkaloids, corydine and corydaline, as novel mu opioid receptor agonists. *Sci. Rep.* 2020, *10*, 13804.

108. Xiao, H.T.; Peng, J.; Liang, Y.; Yang, J.; Bai, X.; Hao, X.Y.; Yang, F.M.; Sun, Q.Y. Acetylcholinesterase inhibitors from Corydalis yanhusuo. *Nat. Prod. Res.* 2011, *25*, 1418–1422.

109. Xi, Z.X.; Yang, Z.; Li, S.J.; Li, X.; Dillon, C.; Peng, X.Q.; Spiller, K.; Gardner, E.L. Levo-tetrahydropalmatine inhibits cocaine's rewarding effects: Experiments with self-administration and brain-stimulation reward in rats. *Neuropharmacology* 2007, *53*, 771–782.

110. Yang, Z.; Shao, Y.C.; Li, S.J.; Qi, J.L.; Zhang, M.J.; Hao, W.; Jin, G.Z. Medication of l-tetrahydropalmatine significantly ameliorates opiate craving and increases the abstinence rate in heroin users: A pilot study. *Acta Pharmacol. Sin.* 2008, *29*, 781–788.

111. Wang, C.; Wang, S.; Fan, G.; Zou, H. Screening of antinociceptive components in Corydalis yanhusuo W.T. Wang by comprehensive two-dimensional liquid chromatography/tandem mass spectrometry. *Anal. Bioanal. Chem.* 2010, *396*, 1731–1740.

112. Pathan H, Williams J. Basic opioid pharmacology: an update. Br J Pain. 2012 Feb;6(1):11-6.
113. Blakemore PR, White JD. Morphine, the Proteus of organic molecules. *Chem Commun* 2002; 1159–1168.
114. Dhawan BN, Cesselin F, Raghubir R, et al. International Union of Pharmacology. XII. Classification of opioid receptors. *Pharmacol Rev* 1996; 48: 567–592.
115. Drolet G, Dumont EC, Gosselin I, Kinkead R, Laforest S, Trottier JF: Role of endogenous opioid system in the regulation of the stress response. *Prog Neuropsychopharmacol Biol Psychiatry* 2001, 25(4):729-741.
116. Zhang J, Muller JF, McDonald AJ: Mu opioid receptor localization in the basolateral amygdala: An ultrastructural analysis. *Neuroscience* 2015, 303:352-363.
117. Mansour A, Khachaturian H, Lewis ME, Akil H, Watson SJ: Autoradiographic differentiation of mu, delta, and kappa opioid receptors in the rat forebrain and midbrain. *J Neurosci* 1987, 7(8):2445-2464.
118. Yam MF, Loh YC, Tan CS, Khadijah Adam S, Abdul Manan N, Basir R: General Pathways of Pain Sensation and the Major Neurotransmitters Involved in Pain Regulation. *Int J Mol Sci* 2018, 19(8).
119. Meier IM, van Honk J, Bos PA, Terburg D: A mu-opioid feedback model of human social behavior. *Neurosci Biobehav Rev* 2021, 121:250-258.
120. Klenowski P, Morgan M, Bartlett SE: The role of delta-opioid receptors in learning and memory underlying the development of addiction. *Br J Pharmacol* 2015, 172(2):297-310.
121. Koob GF, Volkow ND: Neurobiology of addiction: a neurocircuitry analysis. *Lancet Psychiatry* 2016, 3(8):760-773.
122. Goldstein RZ, Volkow ND: Dysfunction of the prefrontal cortex in addiction: neuroimaging findings and clinical implications. *Nat Rev Neurosci* 2011, 12(11):652-669.
123. Le Merrer J, Becker JA, Befort K, Kieffer BL: Reward processing by the opioid system in the brain. *Physiol Rev* 2009, 89(4):1379-1412.
124. Li L, Chen J, Li YQ: The Downregulation of Opioid Receptors and Neuropathic Pain. *Int J Mol Sci* 2023, 24(6).
125. Al-Hasani R, Bruchas MR: Molecular mechanisms of opioid receptor-dependent signaling and behavior. *Anesthesiology* 2011, 115(6):1363-1381.
126. Alhassen L, Nuseir K, Ha A, Phan W, Marmouzi I, Shah S, Civelli O. The Extract of *Corydalis yanhusuo* Prevents Morphine Tolerance and Dependence. Pharmaceuticals (Basel). 2021 Oct 12;14(10):1034.
127. Rizzi-Wise CA, Wang DV. Putting Together Pieces of the Lateral Septum: Multifaceted Functions and Its Neural Pathways. eNeuro. 2021 Dec 3;8(6):ENEURO.0315-21.2021.

128. Ong WY, Stohler CS, Herr DR. Role of the Prefrontal Cortex in Pain Processing. Mol Neurobiol. 2019 Feb;56(2):1137-1166.
129. Sun G, McCartin M, Liu W, Zhang Q, Kenefati G, Chen ZS, Wang J. Temporal pain processing in the primary somatosensory cortex and anterior cingulate cortex. Mol Brain. 2023 Jan 5;16(1):3.
130. Zamfir M, Sharif B, Locke S, Ehrlich AT, Ochandarena NE, Scherrer G, Ribeiro-da-Silva A, Kieffer BL, Séguéla P. Distinct and sex-specific expression of mu opioid receptors in anterior cingulate and somatosensory S1 cortical areas. Pain. 2023 Apr 1;164(4):703-716.
131. He L, Kim JA, Whistler JL. Biomarkers of morphine tolerance and dependence are prevented by morphine-induced endocytosis of a mutant mu-opioid receptor. FASEB J. 2009 Dec;23(12):4327-34.
132. Šimić G, Tkalčić M, Vukić V, Mulc D, Španić E, Šagud M, Olucha-Bordonau FE, Vukšić M, R Hof P. Understanding Emotions: Origins and Roles of the Amygdala. Biomolecules. 2021 May 31;11(6):823.
133. Yang S, Chang MC. Chronic Pain: Structural and Functional Changes in Brain Structures and Associated Negative Affective States. Int J Mol Sci. 2019 Jun 26;20(13):3130.
134. Ab Aziz CB, Ahmad AH. The role of the thalamus in modulating pain. Malays J Med Sci. 2006 Jul;13(2):11-8. PMID: 22589599; PMCID: PMC3349479.
135. Brunton J, Charpak S. mu-Opioid peptides inhibit thalamic neurons. J Neurosci. 1998 Mar 1;18(5):1671-8.
136. Eacret D, Manduchi E, Noreck J, Tyner E, Fenik P, Dunn AD, Schug J, Veasey SC, Blendy JA. Mu-opioid receptor-expressing neurons in the paraventricular thalamus modulate chronic morphine-induced wake alterations. Transl Psychiatry. 2023 Mar 3;13(1):78.
137. Veinante P, Yalcin I, Barrot M. The amygdala between sensation and affect: a role in pain. J Mol Psychiatry. 2013 Jun 5;1(1):9.
138. Gregoriou GC, Patel SD, Pyne S, Winters BL, Bagley EE. Opioid Withdrawal Abruptly Disrupts Amygdala Circuit Function by Reducing Peptide Actions. J Neurosci. 2023 Mar 8;43(10):1668-1681.
139. Mayer DJ, Mao J, Holt J, Price DD. Cellular mechanisms of neuropathic pain, morphine tolerance, and their interactions. Proc Natl Acad Sci U S A. 1999 Jul 6;96(14):7731-6. doi: 10.1073/pnas.96.14.7731. PMID: 10393889; PMCID: PMC33610.
140. Ling W, Mooney L, Hillhouse M. Prescription opioid abuse, pain and addiction: clinical issues and implications. Drug Alcohol Rev. 2011 May;30(3):300-5. doi: 10.1111/j.1465-3362.2010.00271.x. PMID: 21545561; PMCID: PMC4170948.

141. Lu Z, Sun W, Duan X, Yang Z, Liu Y, Tu P. [Chemical constituents from Corydalis yanhusuo]. Zhongguo Zhong Yao Za Zhi. 2012 Jan;37(2):235-7. Chinese. PMID: 22737858.
142. Xiao HT, Peng J, Liang Y, Yang J, Bai X, Hao XY, Yang FM, Sun QY. Acetylcholinesterase inhibitors from Corydalis yanhusuo. Nat Prod Res. 2011 Sep;25(15):1418-22. doi: 10.1080/14786410802496911. Epub 2011 Jul 8. PMID: 20234973.
143. Hashemzaei M, Rezaee R. A review on pain-relieving activity of berberine. Phytother Res. 2021 Jun;35(6):2846-2853. doi: 10.1002/ptr.6984. Epub 2020 Dec 19. PMID: 33340158.
144. Chen C., Lu M., Pan Q., Fichna J., Zheng L., Wang K., Yu Z., Li Y., Li K., Song A., et al. Berberine Improves Intestinal Motility and Visceral Pain in the Mouse Models Mimicking Diarrhea-Predominant Irritable Bowel Syndrome (IBS-D) Symptoms in an Opioid-Receptor Dependent Manner. *PLoS ONE.* 2015;10:e0145556. doi: 10.1371/journal.pone.0145556.
145. Long J., Song J., Zhong L., Liao Y., Liu L., Li X. Palmatine: A review of its pharmacology, toxicity and pharmacokinetics. *Biochimie.* 2019;162:176–184. doi: 10.1016/j.biochi.2019.04.008.
146. Yan B., Wang D., Dong S., Cheng Z., Na L., Sang M., Yang H., Yang Z., Zhang S., Yan Z. Palmatine inhibits TRIF-dependent NF-κB pathway against inflammation induced by LPS in goat endometrial epithelial cell. *Int. Immunopharmacol.* 2017;45:194–200. doi: 10.1016/j.intimp.2017.02.004.
147. Xu T., Kuang T., Du H., Li Q., Feng T., Zhang Y., Fan G. Magnoflorine: A review of its pharmacology, pharmacokinetics and toxicity. *Pharmacol. Res.* 2020;152:104632. doi: 10.1016/j.phrs.2020.104632.
148. Li C., Wang M.-H. Potential Biological Activities of Magnoflorine: A Compound from Aristolochia debilis Sieb. et Zucc. *Korean J. Plant Res.* 2014;27:223–228. doi: 10.7732/kjpr.2014.27.3.223.
149. Han Y, Zhang W, Tang Y, Bai W, Yang F, Xie L, Li X, Zhou S, Pan S, Chen Q, Ferro A, Ji Y. l-Tetrahydropalmatine, an active component of Corydalis yanhusuo W.T. Wang, protects against myocardial ischaemia-reperfusion injury in rats. PLoS One. 2012;7(6):e38627.
150. Tian B, Tian M, Huang SM. Advances in phytochemical and modern pharmacological research of *Rhizoma Corydalis*. Pharm Biol. 2020 Dec;58(1):265-275.
151. Mantsch JR, Li SJ, Risinger R, Awad S, Katz E, Baker DA, Yang Z. Levo-tetrahydropalmatine attenuates cocaine self-administration and cocaine-induced reinstatement in rats. Psychopharmacology (Berl). 2007 Jul;192(4):581-91.
152. Xi ZX, Yang Z, Li SJ, Li X, Dillon C, Peng XQ, Spiller K, Gardner EL. Levo-tetrahydropalmatine inhibits cocaine's rewarding effects: experiments with self-

administration and brain-stimulation reward in rats. Neuropharmacology. 2007 Nov;53(6):771-82.

153. Yue K., Ma B., Ru Q., Chen L., Gan Y., Wang D., Jin G., Li C. The Dopamine Receptor Antagonist Levo-Tetrahydropalmatine Attenuates Heroin Self-Administration and Heroin-Induced Reinstatement in Rats. *Pharmacol. Biochem. Behav.* 2012;102:1–5.

154. Jiang W.-N., Jing X., Li M., Deng H., Jiang T., Xiong K.-Z., Chen Y., Wang X.-F., Wang Q.-J. Corydaline and L-Tetrahydropalmatine Attenuate Morphine-Induced Conditioned Place Preference and the Changes in Dopamine D2 and GluA1 AMPA Receptor Expression in Rats. *Eur. J. Pharmacol.* 2020;884:173397.

155. Civelli O. Orphan GPCRs and neuromodulation. Neuron. 2012 Oct 4;76(1):12-21. doi: 10.1016/j.neuron.2012.09.009. PMID: 23040803; PMCID: PMC3474844.

156. Dao M, Stoveken HM, Cao Y, Martemyanov KA. The role of orphan receptor GPR139 in neuropsychiatric behavior. Neuropsychopharmacology. 2022 Mar;47(4):902-913. doi: 10.1038/s41386-021-00962-2. Epub 2021 Jan 21. PMID: 33479510; PMCID: PMC8882194.

157. Wang L, Dugovic C, Yun S, White A, Lord B, Dvorak C, Liu C, Lovenberg T, Bonaventure P. Putative role of GPR139 on sleep modulation using pharmacological and genetic rodent models. Eur J Pharmacol. 2020 Sep 5;882:173256.

158. Shoblock JR, Welty N, Fraser I, Wyatt R, Lord B, Lovenberg T, Liu C, Bonaventure P. *In vivo* Characterization of a Selective, Orally Available, and Brain Penetrant Small Molecule GPR139 Agonist. Front Pharmacol. 2019 Mar 21;10:273.

159. Wang L, Alachkar A, Sanathara N, Belluzzi JD, Wang Z, Civelli O. A Methionine-Induced Animal Model of Schizophrenia: Face and Predictive Validity. Int J Neuropsychopharmacol. 2015 May 19;18(12):pyv054.